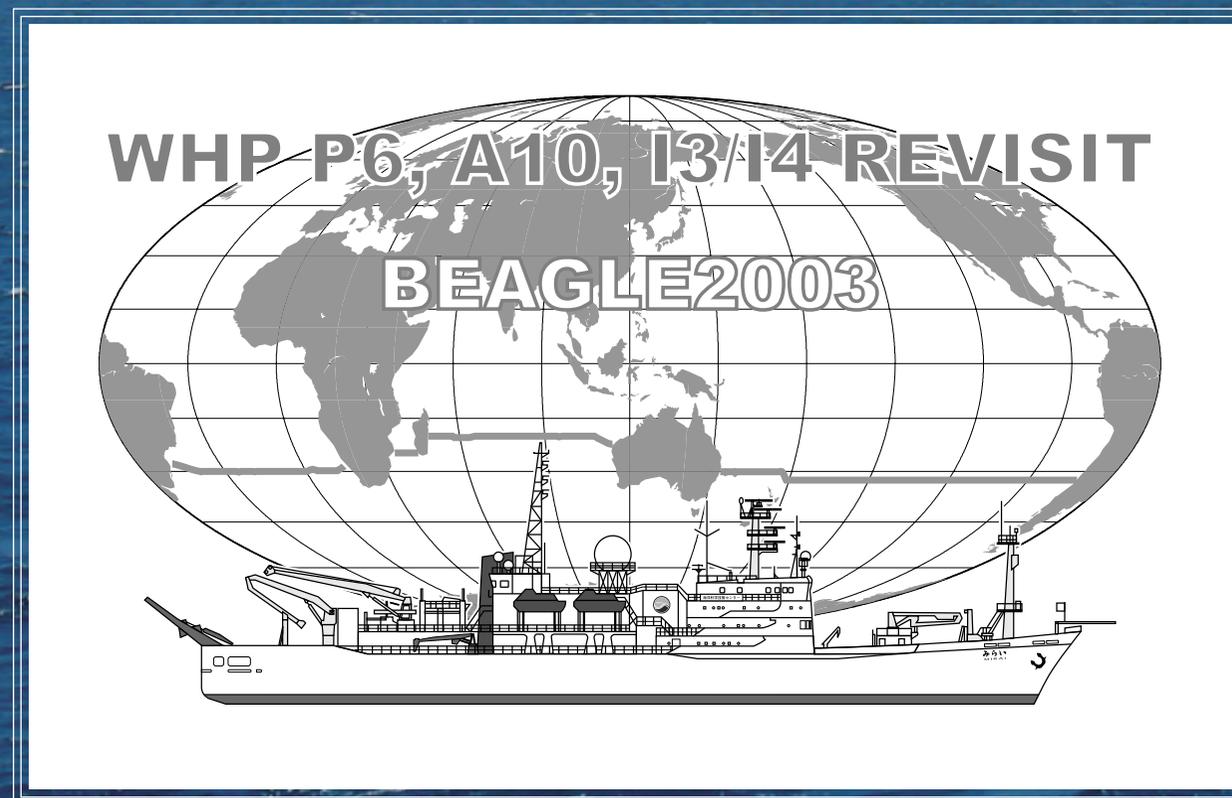


WHP P6, A10, I3/I4 REVISIT DATA BOOK

Blue Earth Global Expedition 2003 (BEAGLE2003)

Volume 3

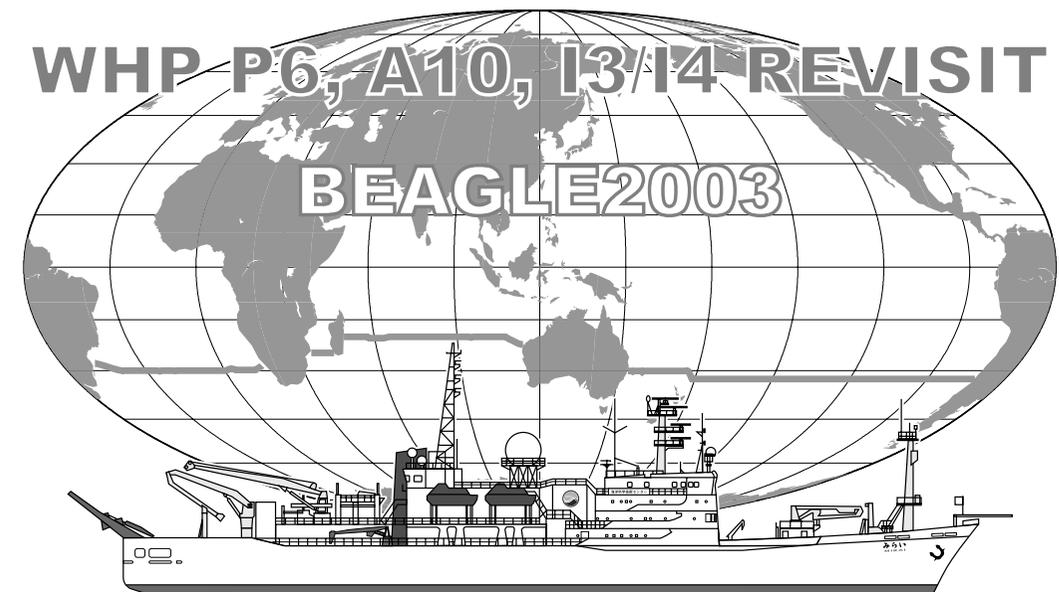


WHP P6, A10, I3/I4 REVISIT DATA BOOK
Blue Earth Global Expedition 2003 (BEAGLE2003)

Volume 3



Edited by
Yuichiro Kumamoto (JAMSTEC),
Shuichi Watanabe (JAMSTEC)



WHP P06, A10, I3/I4 REVISIT DATA BOOK

Blue Earth Global Expedition 2003 (BEAGLE2003)

Volume 3

24 March, 2007 Published

Edited by Yuichiro Kumamoto (JAMSTEC) and Shuichi Watanabe (JAMSTEC)

Published by © JAMSTEC, Yokosuka, Kanagawa, 2007

Japan Agency for Marine-Earth Science and Technology

2-15 Natsushima, Yokosuka, Kanagawa 237-0061, Japan

Phone +81-46-867-9505, Fax +81-46-867-9455

Printed by Ryoin Co. Ltd.

12 Nishiki-cho, Naka-ku, Yokohama, Kanagawa 231-8715, Japan

Contents (Volume 3)

Documents

3. Hydrographic Measurement Techniques and Calibrations (continued from Volume 2)

3.9	Chlorofluorocarbons (CFCs)	1
	<i>K. Sasaki (JAMSTEC), Y. W. Watanabe (Hokkaido University), S. Watanabe (JAMSTEC), M. Wakita (JAMSTEC), S. TANAKA (Hokkaido University), K. Sagishima (MWJ), Y. Sonoyama (MWJ), H. Yamamoto (MWJ), and K. Wataki (MWJ).</i>	
3.10	$\delta^{13}\text{C}$ and $\Delta^{14}\text{C}$ of dissolved inorganic carbon	5
	<i>Y. Kumamoto (JAMSTEC)</i>	
3.11	Artificial radionuclides	23
3.11.1	General information	23
	<i>M. Aoyama (MRI), A. Takeuchi (KANSO), S. Lee (IAEA-MEL), B. Oregioni (IAEA-MEL), and J. Gasutaud (IAEA-MEL)</i>	
3.11.2	Analyses at Meteorological Research Institute (MRI) and Low Level Radioactivity Laboratory, Kanazawa University (LLRL) in Japan	25
	<i>M. Aoyama (MRI), K. Hirose (MRI, LLRL), K. Komura (LLRL), and Y. Hamajima (LLRL)</i>	
3.11.3	Analyses at Marine Environmental Laboratories (IAEA-MEL) in Monaco, Comenius University of Bratislava in Slovakia, and Risoe National Laboratory (RNL) in Denmark	27
	<i>J. A. Sanchez-Cabeza (IAEA-MEL), P. P. Povinec (Comenius Univ. of Bratislava), P. Ross (RNL), J. Gastaud (IAEA-MEL), M. Eriksson (IAEA-MEL), I. Levy-Palomo (IAEA-MEL), S. Rezzoug (IAEA-MEL), and I. Sykora (Comenius Univ. of Bratislava)</i>	
3.11.4	Analyses at Korean Institute of Nuclear Safety (KINS) in South Korea	36
	<i>C.S. Kim (KINS)</i>	

3.11.5	Preliminary results of ^{137}Cs and Pu isotopes in the surface layers	40
	<i>M. Aoyama (MRI), M. Eriksson (IAEA-MEL), J. Gastaud (IAEA-MEL), K. Hirose (MRI, LLRL), Y. Hamajima (LLRL), C. S. Kim (KINS), K. Komura (LLRL), I. Levy-Palomo (IAEA-MEL), P. P. Povinec (Comenius Univ. of Bratislava), S. Rezzoug (IAEA-MEL), P. Ross (RNL), J. A. Sanchez-Cabeza (IAEA-MEL), and I. Sykora (Comenius Univ. of Bratislava)</i>	

4. Errata and Updated Data of the Data Books Volume 1 and 2

4.1	Errata in the documents	44
4.2	Mistakes in the figures	44
4.3	Updates in the data files	44
4.4	Planned updates	44

Figures

Figure captions	45
Figure 1: Observation lines (Same as Figure 1 in Volume 1 and 2)	47
Figure 2: Station locations (Same as Figure 2 in Volume 1 and 2)	48
Figure 3: Cross-section of CFC-11	50
Figure 4: Cross-section of CFC-12	52
Figure 5: Cross-section of $\Delta^{14}\text{C}$	54
Figure 6: Cross-section of $\delta^{13}\text{C}$	56

Updated .sea files and other data (CD-ROM on the back cover)

3. Hydrographic Measurement Techniques and Calibrations (continued from Volume 2)

3.9 Chlorofluorocarbons (CFCs)

7 December 2006

(1) Personnel

Ken'ichi Sasaki: Mutsu Institute of Oceanography, Japan Agency of Marine Science and Technology

(MIO, JAMSTEC)

Yutaka W. Watanabe: Hokkaido University

Shuichi Watanabe: MIO, JAMSTEC

Masahide Wakita: MIO, JAMSTEC

Shinichi Tanaka: Hokkaido University

Katsunori Sagishima: Marine Works Japan LTD (MWJ)

Yuichi Sonoyama: MWJ

Hideki Yamamoto: MWJ

Keisuke Wataki: MWJ

(2) Introduction

Chlorofluorocarbons (CFCs) are completely man-made gasses that are chemically and biologically stable gasses in the environment. The CFCs have been accumulated in the atmosphere since 1930's (Walker et al., 2000) and the atmospheric CFCs can slightly dissolve in sea surface water. The dissolved CFC concentrations in sea surface water should have changed year by year and then penetrated into the ocean interior by water circulation. Three chemical species of CFCs, namely CFC-11 (CCl_3F), CFC-12 (CCl_2F_2) and CFC-113 ($\text{C}_2\text{Cl}_3\text{F}_3$), dissolved in seawater are useful transient tracers for the ocean circulation with time scale on the order of decades.

In this cruise, we determined the concentrations of these CFCs in seawater on board.

(3) Apparatus

Dissolved CFCs were measured by a method modified from the original design of Bullister and Weiss (1988). Two systems were used for CFCs measurement. A custom made purging and trapping system was attached to gas chromatograph (GC-14B; Shimadzu Ltd) having an electron capture detector (ECD-14; Shimadzu Ltd). Porapak T $\text{\textcircled{R}}$ filler was packed in a 1/8" stainless steel trap column. PoraPlot Q-HT capillary columns [i.d.: 0.53mm, length: 2m, film layer thickness: 20 μm] was used as a pre-column. PoraPlot Q-HT capillary columns [i.d.: 0.53mm, length: 20m, film layer thickness: 20 μm] was used as a main analytical column in leg 1 and 2. The main analytical column was replaced by PoraBond Q capillary columns [i.d.: 0.53mm, length: 25m, film layer thickness: 10 μm] in legs 4 and 5.

The change in main analytical columns has been due to serious problems found in the columns used in legs 1 and 2. The main columns used in legs 1 and 2 were clogged by particles peeled from column wall and carrier gas could not flow sufficiently. This problem affected to separation of compounds and analytical time.

(4) Shipboard measurement

Sampling

Seawater sub-samples for CFCs measurement were collected from 12 liter Niskin bottles to 300ml sub-sampling glass bottles which were developed for CFCs analyses in JAMSTEC. The sub-sampling bottles have stainless steel union altered from original design of Swagelok $\text{\textcircled{R}}$ on the top. A 1/4" ϕ stainless steel tube goes through the union into the bottle interior and reaches to near the bottom of bottle. A small plastic stop valve was on the upper tip of stainless steel tube. The bottles were filled by nitrogen gas before sampling. The valve was connected to Niskin bottle. The sub-sampling bottles were filled by seawater sample from the bottom. Two times of the bottle volumes of seawater sample were overflowed from vent valve put on side of the union and then the all valves closed from downstream. The bottles filled by seawater sample were kept in water bathes roughly controlled on sample temperature. The CFC concentrations were determined as soon as possible after sampling. These procedures were needed in order to minimize contamination from atmospheric CFCs.

Analysis

The CFCs analytical system is modified from the original design of Bullister and Weiss (1988). Constant volume of sample water is taken into the purging & trapping system. The volume of sample was 150 ml in legs 1 and 2 and 100 ml in legs 4 and 5. Dissolved CFCs are de-gassed by N₂ gas purge and concentrated in a 1/8" SUS packed trap column (Porapak T) cooled to -40 degree centigrade. The CFCs are desorbed by electrically heating the trap column to 130 °C, and lead into the pre-column. CFCs and other compounds are roughly separated in the pre-column and the compounds having earlier retention time than CFC-113 are sent to main analytical column. And then the pre-column is flushed back by counter flow of pure nitrogen gas (Back flush system). The back flush system is prevent to enter any compounds that have higher retention time than CFC-113 into main analytical column and permits short time analysis. CFCs which are sent into main column are separated further and detected by an electron capture detector (ECD).

In legs 1 and 2, temperature rising analysis has been used because of too long of retention times of CFCs to use temperature constant analysis. The long retention time was due to problems on main analytical column mentioned above.

In legs 4 and 5, we can use temperature constant analysis due to applying new column for main analytical column. Analytical conditions are listed in Table 3.9.1.

Gas loops that the volumes were around 1, 3 and 10 ml were used for introducing standard gases into the analytical system.

Table 3.9.1. Analytical conditions of dissolved CFCs in seawater.

Leg 1

Temperature

Analytical Column:	70 or 100 °C constant for 10 minutes followed by temperature changing stage in 10 °C/min of the rate to 140 °C.
Detector (ECD):	200 or 250 °C
Trap column:	-45 °C (at adsorbing) & 130 °C (at desorbing)

Mass flow rate of nitrogen gas (99.9999%)

Carrier gas:	3 - 7 ml/min
Detector make-up gas:	17 ml/min
Back flush gas:	>10 ml/min
Sample purge gas:	100 ml/min

Leg 2

Temperature

Analytical Column:	75 °C constant for 5 minutes followed by temperature changing stage in 20°C/min of the rate to 130 °C.
Detector (ECD):	270 or 290 °C
Trap column:	-45 °C (at adsorbing) & 130 °C (at desorbing)

Mass flow rate of nitrogen gas (99.9999%)

Carrier gas:	8 - 9 ml/min
Detector make-up gas:	16 - 21 ml/min

Table 3.9.1. continued

Back flush gas:	4 - 7 ml/min
Sample purge gas:	200 ml/min
<i>Legs 4 and 5</i>	
Temperature	
Analytical Column:	95 °C constant.
Detector (ECD):	290 °C
Trap column:	-45 °C (at adsorbing) & 130 °C (at desorbing)
Mass flow rate of nitrogen gas (99.9999%)	
Carrier gas:	27 ml/min
Detector make-up gas:	28 ml/min
Back flush gas:	>15 ml/min
Sample purge gas:	300 ml/min
Standard gas (Taiyo Toyo Sanso co. ltd.) in all legs	
Base gas:	Nitrogen
CFC-11:	850 ppt (v/v)
CFC-12:	500 ppt (v/v)
CFC-113:	90 ppt (v/v)

(5) Quality control

Analytical conditions of CFCs have been changed among legs. Data qualities are mentioned for each leg.

Legs 1

One of two analytical systems had serious problem in cold trap heating system. We needed considerable time for repairing the problem and we could not obtain CFCs data in around half of planned stations. Another system also had some problems in the analytical columns. It was closed by the resins and considerable high pressure of carrier gas had been needed to obtain the mass flow rate of 5 ml/min. Additionally, the column cannot separate CFC-11 peak from unknown interference peaks. Almost all CFC-11 data was bad in the quality and flag was "4". Considerable numbers of CFC-12 and -113 data were also not good in quality due to unstable condition of analytical systems and were given flag of "4".

Legs 2

Before starting leg 2, analytical conditions have been coordinated again. The peaks of CFC-11 and -113 cannot separate from unknown interference peaks. Separation of CFC-12 peak was better than that in leg 1. Most CFC-12 data was good in quality and given flag of "2". The analytical precision was estimated from replicate sample analysis of CFC-12. The precision was estimated from average of absolute difference to be 0.009 ± 0.011 pmol/kg (n = 24).

Legs 4

We got new analytical columns at before Leg 3 that did not have plan for CFCs analyses. During Leg 3, we have tested the columns and successfully decided the analytical condition for CFC-11 and 12. CFC-113 however had been interfered by unknown large peak. We tried to calculate CFC-113 peak by post analyses of the chromatogram and gave the data flag "4". In the case of that the CFC-113 peak had completely been covered by interference peaks, we could not calculate the area of peak and given the data flag "5". The analytical precisions

are estimated from replicate sample analyses for CFC-11 and -12. The precisions were estimated from average of absolute difference to be 0.012 ± 0.013 (n = 98) and 0.007 ± 0.008 pmol/kg (n = 98) for CFC-11 and -12, respectively.

Legs 5

Analytical conditions were same as that in leg 4. In the one of the analytical systems, serious problem has been found in several stations of this leg. The problem was considerable high blank for CFC-12 chromatogram peak. We could not find the causes of the problems by end of this leg. The problems interfered in determination of CFC-12. This problem was remarkable in 5 stations namely stations of I03-557, I03-480, I03-455, I03-451 and I03-447. Although we tried to correct the blank, quality of the data is not good. CFC-12 data in these stations had been given flag of "4". In CFC-113 analyses, there are same problems as that of leg 4 and almost all quality flags were "4". The precisions were estimated from average of absolute difference to be 0.009 ± 0.010 pmol/kg (n = 131) and 0.006 ± 0.006 pmol/kg (n = 122) for CFC-11 and -12, respectively.

Standard Gasses

Standard gasses used in this cruise have been made by Taiyo Nissan Co. Ltd. CFC mixing ratios of the standard gases have been determined by the maker using gravimetric method. The standard gases used in this cruise have not been calibrated to SIO scale standard gases yet because SIO scale standard gasses is hard to obtain due to legal difficulties for CFCs import into Japan. The data will be corrected as soon as possible when we will obtain the standard gasses.

Blank correction

CFCs concentrations in deep water which was one of oldest water masses of the ocean were low but not zero for CFC-11 and -12. In leg 2, Average concentrations of CFC-12 in water samples collected from density range of 27.5 - 27.8 sigma-theta were 0.009 ± 0.004 (n = 226). Average concentrations of CFC-11 and -12 in water samples

collected from density range of sigma-theta > 27.8 and sigma-4 < 45.87 were 0.029 ± 0.005 (n = 195), 0.011 ± 0.003 (n = 195) in leg 4 except data from western region where relatively new deep water mass could come by western boundary current (on Santos Plateau and Vema Channel). Average concentrations of CFC-11 and -12 in water samples collected from density range of sigma-theta > 27.76 and sigma-4 < 45.87 were 0.021 ± 0.006 (n = 251), 0.011 ± 0.003 (n = 243) in leg 5 except data from I04 section where relatively new deep water mass could come (on Mozambique Basin). These values would be sampling blanks which was contaminations from Niskin bottle and/or during sub-sampling and were subtracted from all measurements.

(6) References

- Walker, S.J., Weiss, R.F. and Salameh, P.K., Reconstructed histories of the annual mean atmospheric mole fractions for the halocarbons CFC-11, CFC-12, CFC-113 and Carbon Tetrachloride, *Journal of Geophysical Research*, 105, 14,285-14,296, (2000).
- Bullister, J.L and Weiss, R.F. Determination of CCl_3F and CCl_2F_2 in seawater and air. *Deep Sea Research*, 35, 839-853 (1988).

3.10 $\delta^{13}\text{C}$ and $\Delta^{14}\text{C}$ of Dissolved Inorganic Carbon

25 December 2006

(1) Personnel

Yuichiro Kumamoto: Institute of Observational Research for Global Change, Japan Agency for Marine-Earth Science and Technology (IORGC, JAMSTEC)

(2) Introduction

Stable and radioactive carbon isotopic ratios ($\delta^{13}\text{C}$ and $\Delta^{14}\text{C}$) of dissolved inorganic carbon (DIC) are good tracers for the anthropogenic carbon in the ocean. During MR03-K04 cruise, named BEAGLE2003, we collected seawater samples for $\delta^{13}\text{C}$ and $\Delta^{14}\text{C}$ analyses at stations along the WOCE-P6 (Leg-1&2), WOCE-A10 (Leg-4), and WOCE-I3&I4 (Leg-5) lines in the southern hemisphere. Here we report the final results of $\delta^{13}\text{C}$ and $\Delta^{14}\text{C}$ of DIC. Our preliminary reports of $\delta^{13}\text{C}$ and $\Delta^{14}\text{C}$ measurements are replaced by this final report. General information and other hydrographic data of BEAGLE2003 cruise have already published in our previous data books of BEAGLE2003 (Uchida and Fukasawa, 2005a,b)

(3) Sample collection

The sampling stations are summarized in Figure 3.10.1 and Table 3.10.1-4. A total of 3,060 seawater samples, including 233 replicate samples, were collected between surface (about 10 m depth) and near bottom at 97 stations using 12-liter X-Niskin bottles. The seawater in the X-Niskin bottle was siphoned into a 250 cm³ glass bottle with enough seawater to fill the glass bottle 2 times. Immediately after sampling, 10 cm³ of seawater was removed from the bottle and poisoned by 50 μl of saturated HgCl_2 solution. Then the bottle was sealed by a glass stopper with Apiezon M grease and stored in a cool and dark space on board. These procedures on board basically follow the methods described in WOCE Operation Manual (McNichol and Jones, 1991).

(4) Sample preparation

In our laboratory, DIC in the seawater samples were stripped cryogenically and split into three aliquots: Accelerator Mass Spectrometry (AMS) ^{14}C measurement (about 200 μmol), ^{13}C measurement (about 100 μmol), and archive (about 200 μmol). Efficiency of the CO_2 stripping from seawater sample was more than 95 % that was calculated from concentration of DIC in the seawater samples. The stripped CO_2 gas for ^{14}C was then converted to graphite catalytically on iron powder with pure hydrogen gas. Yield of graphite powder from CO_2 gas was estimated to be 73 ± 9 % in average by weighing of sample graphite powder. Details of these preparation procedures were described by Kumamoto et al. (2000).

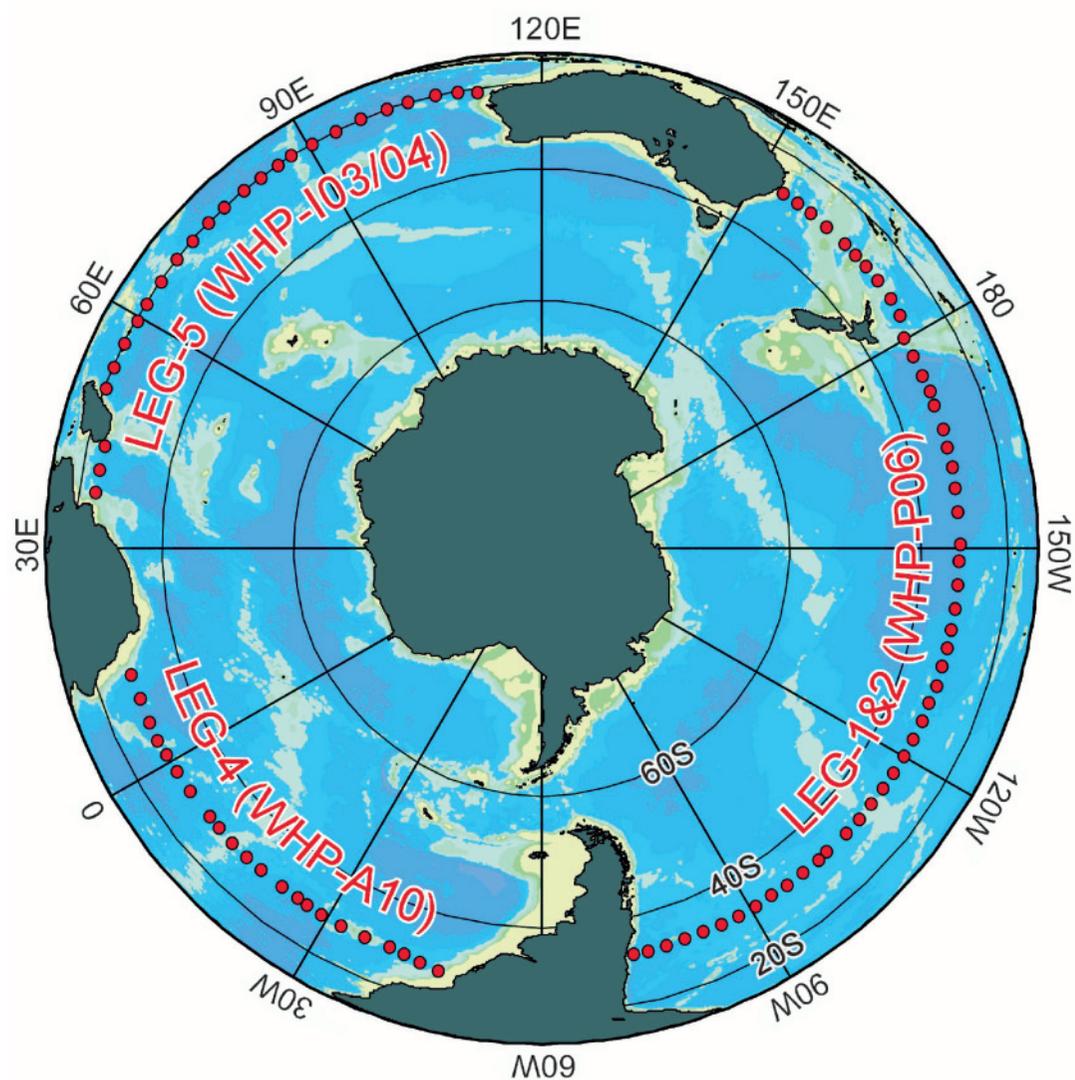


Figure 3.10.1. Sampling stations for $\delta^{13}\text{C}$ and $\Delta^{14}\text{C}$ of dissolved inorganic carbon during BEAGLE2003 Leg-1 (August-September, 2003), Leg-2 (September-October, 2003), Leg-4 (November-December, 2003), and Leg-5 (December, 2003-January, 2004).

Table 3.10.1. The sampling dates, locations, number of samples, and maximum sampling pressure for carbon isotopes in DIC during BEAGLE2003 Leg-1.

Station	Date (UTC)	Latitude	Longitude	Number of samples	Number of replicates	Max. pressure /db
P06W-239	04/Aug/2003	30.087 S	154.165 E	31	3	4,680
P06W-234	05/Aug/2003	30.081 S	156.533 E	32	3	4,898
P06W-227	06/Aug/2003	30.079 S	158.682 E	24	3	3,235
P06W-221	07/Aug/2003	30.086 S	161.500 E	15	1	1,185
P06W-215	08/Aug/2003	30.086 S	164.834 E	26	2	3,419
P06W-211	10/Aug/2003	30.084 S	166.999 E	23	2	2,873
P06W-207	11/Aug/2003	30.084 S	168.999 E	25	3	3,153
P06W-201	12/Aug/2003	30.089 S	171.501 E	20	2	2,264
P06W-195	13/Aug/2003	30.083 S	174.497 E	27	3	3,689
P06W-191	14/Aug/2003	30.582 S	177.000 E	30	3	4,353
P06C-182	15/Aug/2003	32.501 S	179.917 E	24	3	2,872
P06C-174	18/Aug/2003	32.502 S	177.251 W	36	3	6,503
P06C-168	20/Aug/2003	32.497 S	174.330 W	36	3	5,958
P06C-162	21/Aug/2003	32.500 S	171.909 W	29	3	4,200
P06C-X15	22/Aug/2003	32.504 S	170.001 W	34	3	5,610
P06C-150	24/Aug/2003	32.497 S	166.500 W	33	3	5,357
P06C-146	26/Aug/2003	32.491 S	163.832 W	34	3	5,630
P06C-142	27/Aug/2003	32.500 S	161.164 W	33	3	5,221
P06C-137	28/Aug/2003	32.500 S	158.166 W	35	3	5,781
P06C-133	29/Aug/2003	32.504 S	154.847 W	32	3	5,076
P06C-X16	31/Aug/2003	32.499 S	150.499 W	33	3	5,234
P06C-125	01/Sep/2003	32.501 S	148.160 W	30	3	4,626
P06C-121	02/Sep/2003	32.508 S	144.831 W	33	3	5,354
Total				675	64	

Table 3.10.2. As same as Table 3.10.1 but for Leg-2.

Station	Date (UTC)	Latitude	Longitude	Number of samples	Number of replicates	Max. pressure /db
P06C-117	14/Sep/2003	32.497 S	141.494 W	31	3	4,762
P06C-113	15/Sep/2003	32.501 S	138.665 W	31	3	4,640
P06C-109	16/Sep/2003	32.499 S	136.003 W	31	3	4,456
P06C-105	17/Sep/2003	32.502 S	133.344 W	29	3	4,306
P06C-101	18/Sep/2003	32.494 S	130.660 W	27	3	3,650
P06C-097	19/Sep/2003	32.494 S	127.997 W	28	3	3,988
P06C-093	21/Sep/2003	32.509 S	125.336 W	20	2	2,183
P06C-089	21/Sep/2003	32.492 S	122.658 W	22	2	2,625
P06C-085	22/Sep/2003	32.501 S	119.992 W	24	3	3,089
P06C-081	23/Sep/2003	32.499 S	117.320 W	26	3	3,352
P06C-077	24/Sep/2003	32.500 S	114.668 W	24	2	2,970
P06E-071	25/Sep/2003	32.499 S	111.999 W	23	2	2,722
P06E-067	26/Sep/2003	32.500 S	109.343 W	30	3	4,496
P06E-063	27/Sep/2003	32.501 S	106.674 W	26	3	3,343
P06E-X18	28/Sep/2003	32.500 S	103.000 W	27	3	3,617
P06E-055	29/Sep/2003	32.503 S	101.332 W	27	3	3,622
P06E-051	01/Oct/2003	32.501 S	98.667 W	28	3	3,847
P06E-047	02/Oct/2003	32.498 S	96.000 W	28	3	4,012
P06E-043	02/Oct/2003	32.501 S	93.338 W	23	2	2,691
P06E-039	03/Oct/2003	32.500 S	90.682 W	27	3	3,741
P06E-X19	04/Oct/2003	32.503 S	87.994 W	27	3	3,774
P06E-031	05/Oct/2003	32.497 S	85.334 W	28	3	4,054
P06E-027	06/Oct/2003	32.501 S	82.664 W	28	3	3,934
P06E-023	08/Oct/2003	32.502 S	79.997 W	23	2	2,811
P06E-019	09/Oct/2003	32.495 S	77.328 W	26	3	3,608
P06E-015	10/Oct/2003	32.497 S	74.673 W	28	3	3,886
P06E-011	11/Oct/2003	32.495 S	72.716 W	36	3	6,054
Total				728	75	

Table 3.10.3. As same as Table 3.10.1 but for Leg-4.

Station	Date (UTC)	Latitude	Longitude	Number of samples	Number of replicates	Max. pressure /db
A10-629	08/Nov/2003	28.044 S	46.127 W	22	2	2,429
A10-003	09/Nov/2003	28.832 S	43.593 W	28	3	3,935
A10-007	10/Nov/2003	29.613 S	41.161 W	28	3	3,835
A10-X17	11/Nov/2003	30.098 S	39.037 W	30	2	4,249
A10-021	12/Nov/2003	30.001 S	35.488 W	22	1	2,328
A10-029	14/Nov/2003	30.000 S	32.007 W	28	2	3,862
A10-035	16/Nov/2003	29.998 S	29.003 W	26	2	3,199
A10-038	17/Nov/2003	29.999 S	26.716 W	35	2	5,368
A10-X16	17/Nov/2003	30.220 S	25.049 W	31	2	4,411
A10-043	18/Nov/2003	30.000 S	22.482 W	32	2	4,660
A10-X15	19/Nov/2003	30.109 S	19.007 W	31	2	4,671
A10-051	20/Nov/2003	30.002 S	16.334 W	28	2	3,741
A10-055	21/Nov/2003	30.003 S	13.665 W	22	2	2,317
A10-059	22/Nov/2003	30.000 S	11.001 W	28	2	3,767
A10-X14	22/Nov/2003	30.003 S	8.999 W	29	2	3,981
A10-067	24/Nov/2003	30.000 S	4.829 W	31	2	4,302
A10-071	26/Nov/2003	30.001 S	1.505 W	32	2	4,789
A10-075	27/Nov/2003	29.732 S	1.122 E	28	2	3,747
A10-079	27/Nov/2003	29.467 S	3.302 E	32	2	4,816
A10-083	29/Nov/2003	29.746 S	5.931 E	34	2	5,204
A10-087	30/Nov/2003	29.745 S	9.288 E	34	2	5,067
A10-093	01/Dec/2003	29.372 S	12.790 E	28	3	3,250
Total				639	46	

Table 3.10.4. As same as Table 3.10.1 but for Leg-5.

Station	Date (UTC)	Latitude	Longitude	Number of samples	Number of replicates	Max. pressure /db
I04-601	14/Dec/2003	24.673 S	36.991 E	25	2	3,084
I04-595	15/Dec/2003	24.661 S	39.996 E	27	2	3,578
I04-589	16/Dec/2003	24.665 S	42.997 E	28	2	3,725
I03-557	21/Dec/2003	19.997 S	50.060 E	31	2	4,401
I03-551	22/Dec/2003	19.985 S	52.777 E	34	1	5,002
I03-545	23/Dec/2003	19.999 S	56.092 E	31	2	4,441
I03-535	25/Dec/2003	20.380 S	59.228 E	33	2	4,823
I03-531	28/Dec/2003	20.368 S	61.631 E	28	2	3,650
I03-525	29/Dec/2003	20.089 S	64.934 E	27	1	2,935
I03-519	30/Dec/2003	19.998 S	68.213 E	23	1	2,541
I03-513	01/Jan/2004	19.997 S	71.256 E	30	1	4,240
I03-507	02/Jan/2004	20.000 S	74.167 E	33	2	5,032
I03-503	03/Jan/2004	19.987 S	76.908 E	34	2	5,168
I03-X08	05/Jan/2004	19.996 S	79.998 E	34	2	4,928
I03-495	06/Jan/2004	19.996 S	82.736 E	34	2	5,305
I03-491	07/Jan/2004	19.990 S	85.304 E	33	2	4,951
I03-487	09/Jan/2004	20.000 S	87.333 E	20	1	2,022
I03-480	10/Jan/2004	19.992 S	90.288 E	35	2	5,251
I03-474	11/Jan/2004	19.991 S	93.533 E	35	2	5,410
I03-470	13/Jan/2004	19.991 S	96.953 E	35	2	5,419
I03-466	14/Jan/2004	19.990 S	100.466 E	36	2	6,067
I03-463	16/Jan/2004	19.992 S	103.129 E	36	2	5,751
I03-459	17/Jan/2004	19.996 S	106.625 E	36	3	5,617
I03-455	18/Jan/2004	20.932 S	109.445 E	34	3	5,140
I03-451	20/Jan/2004	21.825 S	111.902 E	33	3	5,019
Total				785	48	

(5) Sample measurements

$\delta^{13}\text{C}$ of the sample CO_2 gas was measured using Finnigan MAT252 mass spectrometer. The $\delta^{13}\text{C}$ value was calculated by a following equation:

$$\delta^{13}\text{C} (\text{‰}) = (R_{\text{sample}} / R_{\text{standard}} - 1) \times 1000, \quad (1)$$

where R_{sample} and R_{standard} denote $^{13}\text{C} / ^{12}\text{C}$ ratios of the sample CO_2 gas and the standard CO_2 gas, respectively. The working standard gas was purchased from Oztech Gas Co. with assigned $\delta^{13}\text{C}$ value of -3.64‰ versus VPDB (Lot No. SHO-873C). The gas has been calibrated relative to the appropriate internationally accepted IAEA primary standards. $\Delta^{14}\text{C}$ in the graphite sample was measured in AMS facilities of Institute of Accelerator Analysis Ltd in Shirakawa (Pelletron 9SDH-2, NEC) and Paleo Labo Co. Ltd in Kiryu (Compact-AMS, NEC), Japan. The $\Delta^{14}\text{C}$ value was calculated by:

$$\delta^{14}\text{C} (\text{‰}) = (R_{\text{sample}} / R_{\text{standard}} - 1) \times 1000, \quad (2)$$

$$\Delta^{14}\text{C} (\text{‰}) = \delta^{14}\text{C} - 2(\delta^{13}\text{C} + 25)(1 + \delta^{14}\text{C} / 1000), \quad (3)$$

where R_{sample} and R_{standard} denote, respectively, $^{14}\text{C} / ^{12}\text{C}$ ratios of the sample and the international standard, NIST Oxalic Acid SRM4990-C (HOxII). R_{standard} was corrected for decay since A.D. 1950 (Stuiver and Polach, 1977; Stuiver, 1983). Equation 3 is normalization for isotopic fractionation. When quality of $\delta^{13}\text{C}$ data was not "good", $\Delta^{14}\text{C}$ was calculated by interpolated $\delta^{13}\text{C}$ value derived from data at just above and below layers. Finally $\Delta^{14}\text{C}$ value was corrected for radiocarbon decay between the sampling and the measurement dates. Individual errors of $\delta^{13}\text{C}$ were given by standard deviation of repeat measurements. Errors of $\Delta^{14}\text{C}$ were derived from larger of the standard deviation of repeat measurements and the counting error. Means of the $\delta^{13}\text{C}$ and $\Delta^{14}\text{C}$ errors were calculated to be 0.004‰ and 3.6‰ that probably correspond to "repeatabilities" of our $\delta^{13}\text{C}$ and $\Delta^{14}\text{C}$ measurements. It should be noted that these errors did not include error due to sample preparation.

(6) Replicate measurements

Replicate samples were taken at all the 97 stations. Results of 233 pairs of the replicate samples are shown in Table 3.10.5. The standard deviations of the $\delta^{13}\text{C}$ and $\Delta^{14}\text{C}$ replicate analyses were calculated to be 0.020 ‰ (n = 217) and 3.9 ‰ (n = 214), respectively. The standard deviations of $\delta^{13}\text{C}$ replicate analyses during Leg-1, Leg-2, Leg-4, and Leg-5 were 0.021 (n = 58), 0.019 (n = 74), 0.020 (n = 42), and 0.019 ‰ (n = 43), respectively. The standard deviation of $\Delta^{14}\text{C}$ replicate analyses during Leg-1, Leg-2, Leg-4, and Leg-5 were 3.6 (n = 62), 3.7 (n = 68), 4.4 (n = 37), and 3.9 ‰ (n = 47), respectively.

Table 3.10.5. Summary of replicate analyses.

Station	Btl	$\delta^{13}\text{C} / \text{‰}$				$\Delta^{14}\text{C} / \text{‰}$			
		$\delta^{13}\text{C}$	Error ^a	E.W.Mean ^b	Uncertainty ^c	$\Delta^{14}\text{C}$	Error ^d	E.W.Mean ^b	Uncertainty ^c
P06W-239	32	0.949	0.002	0.930	0.028	79.5	3.8	78.0	3.0
		0.910	0.002			75.7	4.8		
P06W-239	21	0.484	0.003	0.483	0.003	-170.4	3.3	-171.0	2.3
		0.482	0.003			-171.4	3.1		
P06W-239	13	0.437	0.005	0.408	0.028	-165.5	3.2	-167.7	3.0
		0.397	0.003			-169.8	3.2		
P06W-234	32	1.135	0.004	1.124	0.012	83.6	3.8	81.9	2.7
		1.118	0.003			80.1	3.8		
P06W-234	21	0.608	0.003	0.615	0.009	-147.3	3.2	-146.1	2.3
		0.621	0.003			-144.9	3.2		
P06W-234	13	0.385	0.004	0.471	0.064	-155.8	4.4	-159.2	4.7
		0.476	0.001			-162.5	4.4		
P06W-227	32	0.918	0.002	0.914	0.006	92.8	5.4	91.1	3.7
		0.910	0.002			89.5	5.2		
P06W-227	21	0.542	0.002	0.540	0.007	-166.9	4.4	-165.6	3.1
		0.532	0.004			-164.2	4.4		
P06W-227	13	0.440	0.003	0.394	0.036	-165.9	4.4	-164.9	3.1
		0.389	0.001			-163.9	4.4		
P06W-221	32	0.956	0.004	0.941	0.022	-	-	-	-
		0.925	0.004			-	-		
P06W-215	32	0.979	0.003	0.963	0.023	-	-	-	-
		0.947	0.003			-	-		
P06W-215	21	0.530	0.002	0.531	0.002	-142.7	4.2	-140.1	3.7
		0.533	0.003			-137.4	4.3		
P06W-211	32	0.994	0.002	0.975	0.043	88.6	4.0	91.1	3.5
		0.933	0.003			93.6	4.0		
P06W-211	21	0.546	0.006	0.542	0.004	-158.5	3.3	-161.4	3.7
		0.541	0.003			-163.7	2.9		
P06W-207	32	1.086	0.003	1.091	0.005	85.3	4.0	83.2	3.1
		1.093	0.002			80.9	4.1		

Table 3.10.5. continued.

Station	Btl	$\delta^{13}\text{C} / \text{‰}$				$\Delta^{14}\text{C} / \text{‰}$			
		$\delta^{13}\text{C}$	Error ^a	E.W.Mean ^b	Uncertainty ^c	$\Delta^{14}\text{C}$	Error ^d	E.W.Mean ^b	Uncertainty ^c
P06W-207	21	0.615	0.005	0.594	0.025	-148.3	3.4	-153.7	7.6
		0.580	0.004			-159.1	3.4		
P06W-207	13	0.197	0.003	0.182	0.022	-208.4	3.1	-207.4	2.2
		0.166	0.003			-206.3	3.1		
P06W-201	32	-	-	-	-	80.7	3.8	80.8	2.7
		-	-			80.9	3.7		
P06W-201	21	0.548	0.002	0.579	0.044	-149.4	3.3	-151.6	4.5
		0.610	0.002			-155.8	4.5		
P06W-195	32	0.984	0.002	0.985	0.005	86.9	6.1	89.9	3.1
		0.991	0.005			90.9	3.6		
P06W-195	21	0.533	0.003	0.547	0.020	-163.2	3.2	-163.1	2.3
		0.561	0.003			-162.9	3.2		
P06W-195	13	-	-	-	-	-202.6	3.1	-206.8	5.9
		-	-			-211.0	3.1		
P06W-191	32	0.987	0.004	0.988	0.002	77.3	3.7	74.6	4.0
		0.988	0.003			71.7	3.8		
P06W-191	21	0.540	0.002	0.539	0.003	-173.5	3.1	-171.9	2.3
		0.536	0.004			-170.3	3.1		
P06W-191	13	0.190	0.003	0.173	0.017	-209.3	3.0	-212.1	4.2
		0.166	0.002			-215.2	3.2		
P06C-182	32	1.039	0.004	1.033	0.009	73.3	4.0	71.9	3.1
		1.026	0.004			69.5	5.0		
P06C-182	21	0.653	0.005	0.645	0.013	-143.8	3.4	-148.5	6.2
		0.634	0.006			-152.5	3.1		
P06C-182	13	0.294	0.003	0.297	0.006	-197.8	3.2	-201.3	4.8
		0.303	0.004			-204.6	3.1		
P06C-174	32	1.043	0.002	1.047	0.009	73.4	4.2	74.6	3.0
		1.056	0.003			75.7	4.3		
P06C-174	21	0.664	0.005	0.657	0.006	-147.0	3.4	-150.9	5.4
		0.656	0.002			-154.6	3.3		

Table 3.10.5. continued.

Station	Btl	$\delta^{13}\text{C} / \text{‰}$				$\Delta^{14}\text{C} / \text{‰}$			
		$\delta^{13}\text{C}$	Error ^a	E.W.Mean ^b	Uncertainty ^c	$\Delta^{14}\text{C}$	Error ^d	E.W.Mean ^b	Uncertainty ^c
P06C-174	13	-	-	-	-	-177.3	3.1	-180.1	4.3
		-	-			-183.4	3.4		
P06C-168	32	1.067	0.002	1.070	0.013	75.1	4.5	75.4	3.0
		1.086	0.005			75.6	4.1		
P06C-168	21	0.619	0.004	0.636	0.015	-150.4	3.4	-153.2	4.1
		0.640	0.002			-156.2	3.5		
P06C-168	13	0.202	0.005	0.215	0.013	-219.0	3.1	-218.7	2.3
		0.220	0.003			-218.3	3.3		
P06C-162	32	1.077	0.005	1.077	0.002	71.6	4.5	73.4	3.1
		1.077	0.002			75.0	4.4		
P06C-162	21	0.639	0.002	0.636	0.018	-143.0	3.6	-144.7	2.6
		0.614	0.005			-146.6	3.7		
P06C-162	13	0.255	0.005	0.263	0.008	-204.1	3.4	-207.2	4.4
		0.266	0.003			-210.3	3.4		
P06C-X15	32	1.106	0.003	1.098	0.021	69.7	3.7	69.1	2.7
		1.077	0.005			68.4	4.0		
P06C-X15	21	0.595	0.003	0.615	0.021	-146.2	3.2	-152.2	8.8
		0.624	0.002			-158.7	3.3		
P06C-X15	13	0.228	0.004	0.226	0.001	-210.4	3.1	-208.4	3.0
		0.226	0.001			-206.2	3.2		
P06C-150	32	1.138	0.004	1.126	0.017	78.6	3.8	77.1	2.7
		1.114	0.004			75.5	3.7		
P06C-150	21	0.659	0.005	0.657	0.004	-151.7	3.4	-148.8	4.0
		0.654	0.005			-146.1	3.3		
P06C-150	13	0.212	0.001	0.210	0.011	-214.2	3.2	-214.9	2.2
		0.196	0.003			-215.5	3.1		
P06C-146	32	1.178	0.004	1.152	0.037	81.2	4.2	80.4	2.9
		1.126	0.004			79.6	4.1		
P06C-146	21	-	-	-	-	-142.7	3.5	-143.5	2.5
		-	-			-144.3	3.5		

Table 3.10.5. continued.

Station	Btl	$\delta^{13}\text{C} / \text{‰}$				$\Delta^{14}\text{C} / \text{‰}$			
		$\delta^{13}\text{C}$	Error ^a	E.W.Mean ^b	Uncertainty ^c	$\Delta^{14}\text{C}$	Error ^d	E.W.Mean ^b	Uncertainty ^c
P06C-146	13	0.168	0.004	0.191	0.033	-222.9	3.3	-220.6	3.4
		0.214	0.004			-218.1	3.4		
P06C-142	32	1.163	0.003	1.151	0.018	76.4	3.8	71.3	7.7
		1.138	0.003			65.5	4.1		
P06C-142	21	0.671	0.004	0.654	0.015	-144.7	3.4	-142.4	3.2
		0.650	0.002			-140.2	3.4		
P06C-142	13	0.182	0.005	0.185	0.005	-212.2	2.9	-213.3	2.1
		0.189	0.006			-214.7	3.1		
P06C-137	32	1.131	0.003	1.120	0.029	84.7	3.6	82.9	2.5
		1.090	0.005			81.2	3.5		
P06C-137	21	0.597	0.003	0.600	0.005	-145.7	3.0	-142.0	5.2
		0.604	0.004			-138.3	3.0		
P06C-137	13	0.210	0.003	0.227	0.023	-209.3	3.0	-213.1	5.6
		0.243	0.003			-217.2	3.1		
P06C-133	32	-	-	-	-	86.7	4.3	89.8	4.3
		-	-			92.8	4.2		
P06C-133	21	0.639	0.004	0.615	0.034	-146.7	3.6	-144.9	2.5
		0.591	0.004			-143.1	3.6		
P06C-133	13	0.232	0.002	0.234	0.008	-214.9	3.5	-212.7	3.0
		0.244	0.005			-210.7	3.4		
P06C-X16	32	1.230	0.004	1.222	0.008	99.8	3.7	100.9	2.7
		1.218	0.003			102.0	3.8		
P06C-X16	21	0.573	0.004	0.596	0.032	-145.1	3.2	-147.7	3.6
		0.618	0.004			-150.2	3.2		
P06C-X16	13	0.198	0.003	0.228	0.031	-210.8	3.2	-211.8	2.2
		0.242	0.002			-212.7	3.0		
P06C-125	32	1.282	0.002	1.278	0.006	83.6	3.8	83.0	2.7
		1.274	0.002			82.5	3.7		
P06C-125	21	0.607	0.004	0.619	0.009	-155.4	3.1	-158.9	5.4
		0.620	0.001			-163.0	3.3		

Table 3.10.5. continued.

Station	Btl	$\delta^{13}\text{C} / \text{‰}$				$\Delta^{14}\text{C} / \text{‰}$			
		$\delta^{13}\text{C}$	Error ^a	E.W.Mean ^b	Uncertainty ^c	$\Delta^{14}\text{C}$	Error ^d	E.W.Mean ^b	Uncertainty ^c
P06C-125	13	0.245	0.007	0.263	0.017	-214.7	3.0	-212.5	3.0
		0.269	0.004			-210.5	2.9		
P06C-121	32	-	-	-	-	79.9	3.8	80.3	2.7
		-	-			80.7	3.8		
P06C-121	21	0.571	0.003	0.587	0.016	-154.9	4.2	-151.0	4.4
		0.594	0.002			-148.7	3.2		
P06C-121	13	0.258	0.002	0.262	0.013	-211.2	3.0	-208.9	3.4
		0.277	0.004			-206.4	3.1		
P06C-117	32	1.236	0.004	1.249	0.023	-	-	-	-
		1.269	0.005			-	-		
P06C-117	21	0.592	0.003	0.571	0.021	-148.1	3.3	-153.5	7.6
		0.562	0.002			-158.8	3.3		
P06C-117	13	0.261	0.005	0.260	0.003	-205.8	3.0	-206.9	2.1
		0.260	0.003			-207.8	2.9		
P06C-113	32	1.257	0.004	1.221	0.040	92.5	3.7	91.6	2.6
		1.201	0.003			90.6	3.7		
P06C-113	21	0.585	0.005	0.630	0.033	-145.1	3.2	-145.6	2.3
		0.632	0.001			-146.2	3.3		
P06C-113	13	0.262	0.002	0.266	0.013	-213.1	3.0	-210.3	4.2
		0.280	0.004			-207.2	3.2		
P06C-109	32	1.323	0.004	1.276	0.052	91.1	3.8	86.1	7.4
		1.250	0.003			80.7	4.0		
P06C-109	21	0.532	0.003	0.542	0.013	-160.6	3.4	-156.2	6.2
		0.551	0.003			-151.9	3.4		
P06C-109	13	0.293	0.002	0.295	0.004	-213.6	3.2	-213.9	2.3
		0.299	0.003			-214.2	3.3		
P06C-105	32	1.359	0.002	1.348	0.025	88.4	3.9	84.6	5.4
		1.323	0.003			80.7	4.0		
P06C-105	21	0.552	0.005	0.569	0.016	-158.2	3.3	-157.0	2.3
		0.575	0.003			-156.0	3.2		

Table 3.10.5. continued.

Station	Btl	$\delta^{13}\text{C} / \text{‰}$				$\Delta^{14}\text{C} / \text{‰}$			
		$\delta^{13}\text{C}$	Error ^a	E.W.Mean ^b	Uncertainty ^c	$\Delta^{14}\text{C}$	Error ^d	E.W.Mean ^b	Uncertainty ^c
P06C-105	13	0.276	0.005	0.328	0.038	-208.5	3.1	-210.8	3.3
		0.330	0.001			-213.2	3.1		
P06C-101	32	1.231	0.004	1.244	0.014	95.0	3.8	92.5	6.6
		1.251	0.003			85.7	6.3		
P06C-101	21	0.555	0.006	0.562	0.005	-145.8	3.2	-147.4	2.3
		0.562	0.001			-149.0	3.2		
P06C-101	13	0.297	0.005	0.259	0.044	-208.6	2.9	-207.3	2.1
		0.235	0.004			-206.0	3.0		
P06C-097	32	-	-	-	-	100.4	3.8	105.7	7.6
		-	-			111.2	3.9		
P06C-097	21	0.617	0.005	0.577	0.033	-138.7	3.1	-138.8	2.2
		0.571	0.002			-138.8	3.0		
P06C-097	13	0.303	0.003	0.297	0.009	-198.7	2.9	-201.7	4.0
		0.290	0.003			-204.4	2.8		
P06C-093	32	1.208	0.001	1.209	0.007	83.7	3.6	87.5	5.4
		1.218	0.003			91.4	3.7		
P06C-093	21	0.515	0.004	0.517	0.002	-155.6	3.1	-156.8	2.2
		0.518	0.003			-157.8	3.0		
P06C-089	32	1.267	0.007	1.251	0.013	90.6	3.7	89.5	2.6
		1.248	0.003			88.4	3.7		
P06C-089	21	0.578	0.003	0.562	0.042	-157.9	3.1	-156.8	2.2
		0.519	0.005			-155.6	3.2		
P06C-085	32	1.374	0.002	1.375	0.004	90.4	3.5	91.7	2.5
		1.379	0.006			93.1	3.7		
P06C-085	21	0.543	0.003	0.548	0.005	-151.6	2.9	-153.7	3.1
		0.550	0.002			-156.0	3.0		
P06C-085	13	0.283	0.004	0.282	0.002	-204.5	2.9	-206.8	3.3
		0.282	0.003			-209.2	3.0		
P06C-081	32	1.275	0.005	1.271	0.004	87.4	3.5	83.2	6.4
		1.270	0.003			78.4	3.7		

Table 3.10.5. continued.

Station	Btl	$\delta^{13}\text{C} / \text{‰}$				$\Delta^{14}\text{C} / \text{‰}$			
		$\delta^{13}\text{C}$	Error ^a	E.W.Mean ^b	Uncertainty ^c	$\Delta^{14}\text{C}$	Error ^d	E.W.Mean ^b	Uncertainty ^c
P06C-081	21	0.565	0.003	0.565	0.003	-155.3	4.2	-146.6	9.3
		0.565	0.005			-142.2	3.0		
P06C-081	13	0.287	0.004	0.286	0.002	-204.0	2.9	-203.5	2.1
		0.286	0.002			-202.9	3.0		
P06C-077	32	1.450	0.004	1.444	0.018	69.9	3.7	70.2	2.6
		1.425	0.007			70.4	3.7		
P06C-077	21	0.473	0.004	0.496	0.032	-150.5	3.1	-150.3	2.1
		0.518	0.004			-150.1	2.9		
P06E-071	32	1.294	0.004	1.290	0.006	90.6	4.0	91.0	2.8
		1.286	0.004			91.4	4.0		
P06E-071	21	0.477	0.004	0.481	0.006	-153.8	3.4	-157.2	4.7
		0.486	0.005			-160.4	3.3		
P06E-067	32	1.296	0.004	1.293	0.003	89.5	4.0	92.2	3.6
		1.292	0.002			94.6	3.8		
P06E-067	21	0.383	0.002	0.375	0.007	-173.5	3.2	-174.8	2.3
		0.373	0.001			-176.3	3.4		
P06E-067	13	0.322	0.004	0.300	0.031	-202.9	3.2	-201.6	2.3
		0.278	0.004			-200.3	3.2		
P06E-063	32	1.356	0.002	1.358	0.008	98.1	3.9	97.5	2.8
		1.368	0.004			96.7	4.0		
P06E-063	21	0.337	0.005	0.352	0.018	-175.2	3.3	-174.7	2.8
		0.362	0.004			-173.2	5.6		
P06E-063	13	0.329	0.003	0.331	0.004	-197.9	3.3	-195.8	3.0
		0.334	0.004			-193.6	3.3		
P06E-X18	21	0.353	0.001	0.352	0.023	-182.0	3.0	-179.1	4.1
		0.320	0.005			-176.2	3.0		
P06E-X18	13	0.314	0.002	0.319	0.018	-198.1	2.9	-194.6	5.2
		0.340	0.004			-190.7	3.0		
P06E-X18	1	1.417	0.004	1.407	0.008	88.3	3.6	87.5	2.5
		1.405	0.002			86.7	3.6		

Table 3.10.5. continued.

Station	Btl	$\delta^{13}\text{C} / \text{‰}$				$\Delta^{14}\text{C} / \text{‰}$			
		$\delta^{13}\text{C}$	Error ^a	E.W.Mean ^b	Uncertainty ^c	$\Delta^{14}\text{C}$	Error ^d	E.W.Mean ^b	Uncertainty ^c
P06E-055	32	1.393	0.007	1.366	0.023	93.0	3.7	89.1	5.4
		1.361	0.003			85.3	3.6		
P06E-055	21	0.310	0.004	0.310	0.002	-185.6	3.2	-186.0	2.2
		0.310	0.003			-186.3	3.1		
P06E-055	13	0.319	0.006	0.321	0.003	-	-	-	-
		0.322	0.004			-	-		
P06E-051	32	1.330	0.001	1.332	0.011	85.9	3.6	88.9	4.5
		1.346	0.003			92.2	3.8		
P06E-051	21	0.297	0.004	0.303	0.013	-187.3	3.0	-183.7	5.0
		0.315	0.006			-180.2	2.9		
P06E-051	13	0.304	0.001	0.308	0.013	-196.6	2.9	-195.5	2.1
		0.322	0.002			-194.3	3.0		
P06E-047	32	1.456	0.004	1.466	0.008	75.3	3.6	76.2	2.9
		1.468	0.002			77.8	5.0		
P06E-047	21	0.313	0.003	0.326	0.025	-186.7	3.0	-183.9	4.1
		0.348	0.004			-180.9	3.1		
P06E-047	13	0.305	0.003	0.316	0.021	-190.8	2.9	-188.5	3.3
		0.335	0.004			-186.1	2.9		
P06E-043	32	1.389	0.004	1.401	0.021	85.8	3.5	87.1	2.9
		1.419	0.005			89.7	5.0		
P06E-043	21	0.272	0.002	0.275	0.011	-	-	-	-
		0.288	0.004			-	-		
P06E-039	32	1.326	0.007	1.365	0.030	83.1	2.5	82.2	1.8
		1.368	0.002			81.4	2.6		
P06E-039	21	0.298	0.004	0.288	0.018	-191.1	2.3	-192.4	1.7
		0.273	0.005			-193.5	2.2		
P06E-039	13	0.286	0.002	0.277	0.020	-196.8	2.2	-195.0	2.3
		0.258	0.003			-193.5	2.0		
P06E-X19	32	1.515	0.003	1.521	0.011	83.8	3.6	84.0	2.5
		1.531	0.004			84.3	3.6		

Table 3.10.5. continued.

Station	Btl	$\delta^{13}\text{C} / \text{‰}$				$\Delta^{14}\text{C} / \text{‰}$			
		$\delta^{13}\text{C}$	Error ^a	E.W.Mean ^b	Uncertainty ^c	$\Delta^{14}\text{C}$	Error ^d	E.W.Mean ^b	Uncertainty ^c
P06E-X19	21	0.266	0.004	0.270	0.004	-184.8	3.0	-184.4	2.1
		0.272	0.003			-184.1	2.9		
P06E-X19	13	0.304	0.003	0.305	0.003	-	-	-	-
		0.306	0.005			-	-		
P06E-031	32	1.402	0.004	1.430	0.030	80.2	4.1	82.4	2.9
		1.445	0.003			84.4	4.0		
P06E-031	21	0.244	0.003	0.274	0.031	-190.7	3.3	-194.6	5.5
		0.288	0.002			-198.5	3.3		
P06E-031	13	0.276	0.002	0.290	0.032	-198.4	3.3	-201.8	4.8
		0.321	0.003			-205.2	3.3		
P06E-027	32	1.357	0.004	1.352	0.008	54.4	4.0	50.8	5.3
		1.345	0.005			46.9	4.1		
P06E-027	21	0.227	0.002	0.234	0.009	-212.8	3.5	-210.2	3.5
		0.240	0.002			-207.8	3.4		
P06E-027	13	0.229	0.003	0.233	0.008	-215.2	3.3	-218.6	4.7
		0.240	0.004			-221.8	3.2		
P06E-023	32	1.310	0.005	1.316	0.006	-	-	-	-
		1.318	0.003			-	-		
P06E-023	21	0.204	0.003	0.204	0.003	-189.3	3.2	-188.9	2.3
		0.203	0.005			-188.4	3.2		
P06E-019	32	0.474	0.003	0.461	0.025	21.7	3.5	22.8	2.5
		0.438	0.004			24.0	3.6		
P06E-019	21	0.211	0.004	0.214	0.004	-193.5	3.1	-195.8	3.1
		0.216	0.004			-197.9	3.0		
P06E-019	13	0.206	0.004	0.210	0.006	-224.3	3.0	-219.8	6.4
		0.215	0.005			-215.3	3.0		
P06E-015	32	0.084	0.004	0.076	0.011	-6.9	3.5	-7.4	2.5
		0.068	0.004			-8.0	3.5		
P06E-015	21	0.177	0.005	0.184	0.013	-207.2	3.2	-206.3	2.2
		0.195	0.006			-205.4	3.0		

Table 3.10.5. continued.

Station	Btl	$\delta^{13}\text{C} / \text{‰}$				$\Delta^{14}\text{C} / \text{‰}$			
		$\delta^{13}\text{C}$	Error ^a	E.W.Mean ^b	Uncertainty ^c	$\Delta^{14}\text{C}$	Error ^d	E.W.Mean ^b	Uncertainty ^c
P06E-015	13	0.249	0.004	0.246	0.009	-215.0	2.9	-217.7	3.9
		0.236	0.007			-220.5	3.0		
P06E-011	32	-0.082	0.003	-0.078	0.010	-	-	-	-
		-0.068	0.005			-	-		
P06E-011	21	0.208	0.003	0.203	0.014	-200.1	3.1	-199.5	2.1
		0.188	0.005			-198.9	2.9		
P06E-011	13	0.211	0.003	0.202	0.013	-	-	-	-
		0.193	0.003			-	-		
A10-629	32	1.098	0.003	1.091	0.010	-	-	-	-
		1.084	0.003			-	-		
A10-629	1	-	-	-	-	-114.9	3.5	-113.7	2.5
		-	-			-112.5	3.5		
A10-003	32	1.251	0.005	1.250	0.003	103.0	4.1	102.3	3.0
		1.250	0.003			101.6	4.3		
A10-003	21	0.655	0.003	0.670	0.030	-118.6	3.3	-117.3	3.7
		0.697	0.004			-113.3	5.9		
A10-003	13	1.043	0.004	1.009	0.030	-99.7	3.3	-100.0	2.8
		1.000	0.002			-100.6	5.1		
A10-007	32	1.174	0.003	1.180	0.015	83.9	4.0	81.3	3.7
		1.195	0.005			78.6	4.0		
A10-007	21	0.677	0.001	0.677	0.006	-128.1	3.5	-131.8	5.0
		0.668	0.005			-135.2	3.4		
A10-007	13	0.992	0.005	1.002	0.021	-104.6	3.7	-103.9	2.6
		1.022	0.007			-103.2	3.6		
A10-X17	21	0.694	0.003	0.686	0.012	-119.3	3.3	-121.7	3.5
		0.677	0.003			-124.2	3.3		
A10-X17	1	1.028	0.004	1.046	0.033	-	-	-	-
		1.074	0.005			-	-		
A10-021	32	1.238	0.002	1.237	0.002	83.9	4.0	83.0	2.8
		1.235	0.004			82.1	4.0		

Table 3.10.5. continued.

Station	Btl	$\delta^{13}\text{C} / \text{‰}$				$\Delta^{14}\text{C} / \text{‰}$			
		$\delta^{13}\text{C}$	Error ^a	E.W.Mean ^b	Uncertainty ^c	$\Delta^{14}\text{C}$	Error ^d	E.W.Mean ^b	Uncertainty ^c
A10-029	32	1.217	0.002	1.213	0.026	88.9	4.1	90.2	3.7
		1.180	0.006			94.1	7.1		
A10-029	21	0.670	0.003	0.995	0.004	-	-	-	-
		0.681	0.003			-	-		
A10-035	21	0.671	0.003	0.660	0.016	-120.0	3.3	-117.3	3.8
		0.648	0.003			-114.6	3.4		
A10-035	13	-	-	-	-	-107.0	3.3	-103.4	5.1
		-	-			-99.8	3.3		
A10-038	32	1.173	0.004	1.171	0.004	-	-	-	-
		1.168	0.004			-	-		
A10-038	21	0.678	0.004	0.661	0.019	-123.7	3.3	-120.7	4.2
		0.651	0.003			-117.7	3.3		
A10-X16	32	1.204	0.002	1.203	0.006	74.4	6.0	77.6	3.3
		1.195	0.005			79.0	4.0		
A10-X16	13	0.983	0.006	0.935	0.037	-99.1	3.4	-98.5	2.4
		0.930	0.002			-97.9	3.4		
A10-043	21	0.648	0.004	0.654	0.008	-130.0	3.3	-126.9	4.5
		0.660	0.004			-123.7	3.4		
A10-043	13	0.954	0.004	0.935	0.021	-98.2	3.3	-103.9	8.6
		0.924	0.003			-110.4	3.5		
A10-X15	32	1.233	0.002	1.209	0.034	88.3	3.9	83.9	6.4
		1.185	0.002			79.3	4.0		
A10-X15	13	0.927	0.004	0.950	0.032	-113.1	3.6	-113.7	2.5
		0.972	0.004			-114.3	3.4		
A10-051	32	1.092	0.004	1.123	0.034	70.3	3.9	70.3	2.8
		1.140	0.003			70.3	3.9		
A10-051	21	0.576	0.002	0.581	0.025	-127.9	3.2	-123.2	7.0
		0.612	0.005			-118.0	3.4		
A10-055	21	0.600	0.003	0.574	0.037	-121.2	3.6	-119.5	2.5
		0.548	0.003			-117.8	3.6		

Table 3.10.5. continued.

Station	Btl	$\delta^{13}\text{C} / \text{‰}$				$\Delta^{14}\text{C} / \text{‰}$			
		$\delta^{13}\text{C}$	Error ^a	E.W.Mean ^b	Uncertainty ^c	$\Delta^{14}\text{C}$	Error ^d	E.W.Mean ^b	Uncertainty ^c
A10-059	32	1.191	0.002	1.190	0.002	71.6	3.8	74.4	6.6
		1.188	0.003			80.9	5.8		
A10-059	13	0.880	0.003	0.871	0.009	-111.2	3.4	-112.2	2.9
		0.867	0.002			-114.9	5.4		
A10-X14	32	1.219	0.005	1.215	0.004	-	-	-	-
		1.214	0.003			-	-		
A10-X14	21	0.623	0.003	0.580	0.044	-120.9	3.5	-116.7	5.7
		0.561	0.002			-112.8	3.4		
A10-067	21	0.618	0.003	0.595	0.033	-129.4	3.4	-125.1	5.5
		0.571	0.003			-121.6	3.1		
A10-067	13	0.904	0.002	0.893	0.016	-115.7	3.4	-117.1	2.4
		0.882	0.002			-118.5	3.4		
A10-071	32	0.917	0.003	0.925	0.011	89.6	3.7	88.2	2.7
		0.933	0.003			86.7	3.8		
A10-071	13	0.874	0.004	0.872	0.002	-118.4	3.5	-112.6	7.4
		0.872	0.002			-107.9	3.2		
A10-075	32	1.030	0.003	1.034	0.006	94.3	3.8	93.4	2.7
		1.038	0.003			92.5	3.7		
A10-075	21	0.661	0.007	0.649	0.010	-122.3	3.3	-122.1	2.3
		0.647	0.003			-121.9	3.3		
A10-079	21	0.653	0.002	0.655	0.010	-	-	-	-
		0.667	0.005			-	-		
A10-079	13	0.846	0.004	0.850	0.005	-128.8	3.4	-123.8	6.8
		0.853	0.004			-119.2	3.3		
A10-083	32	1.042	0.002	1.035	0.016	-	-	-	-
		1.020	0.003			-	-		
A10-083	13	0.852	0.002	0.850	0.004	-117.2	3.3	-114.4	4.2
		0.847	0.003			-111.3	3.5		
A10-087	32	1.034	0.005	1.027	0.006	-	-	-	-
		1.026	0.002			-	-		

Table 3.10.5. continued.

Station	Btl	$\delta^{13}\text{C} / \text{‰}$				$\Delta^{14}\text{C} / \text{‰}$			
		$\delta^{13}\text{C}$	Error ^a	E.W.Mean ^b	Uncertainty ^c	$\Delta^{14}\text{C}$	Error ^d	E.W.Mean ^b	Uncertainty ^c
A10-087	1	0.593	0.004	0.591	0.004	-126.1	3.4	-123.5	3.6
		0.587	0.005			-121.0	3.4		
A10-093	32	1.032	0.005	1.026	0.007	74.6	4.0	81.1	9.5
		1.022	0.004			88.0	4.1		
A10-093	21	-	-	-	-	-124.2	5.3	-119.7	4.5
		-	-			-117.8	3.5		
A10-093	13	0.877	0.003	0.882	0.007	-114.5	3.7	-113.8	2.5
		0.887	0.003			-113.3	3.5		
I04-601	21	0.683	0.005	0.683	0.004	-141.4	3.1	-141.2	2.3
		0.683	0.007			-140.8	3.3		
I04-601	13	0.681	0.003	0.696	0.015	-144.0	3.3	-147.0	4.2
		0.702	0.002			-150.0	3.3		
I04-595	32	0.671	0.006	0.632	0.047	67.4	3.8	64.9	3.6
		0.605	0.005			62.3	3.9		
I04-595	13	0.723	0.005	0.705	0.018	-142.6	3.2	-144.3	2.3
		0.698	0.003			-145.8	3.1		
I04-589	32	-	-	-	-	80.2	3.7	81.7	2.7
		-	-			83.3	3.8		
I04-589	21	0.377	0.002	0.378	0.004	-153.3	4.3	-150.4	3.2
		0.382	0.004			-148.7	3.3		
I03-557	21	0.467	0.003	0.469	0.008	-165.7	3.0	-163.9	2.5
		0.479	0.006			-162.2	3.0		
I03-557	13	0.293	0.004	0.288	0.008	-184.3	3.0	-184.9	2.2
		0.281	0.005			-185.7	3.2		
I03-551	13	0.339	0.003	0.333	0.012	-190.5	3.0	-189.7	2.2
		0.322	0.004			-188.9	3.1		
I03-545	32	0.512	0.006	0.502	0.010	51.4	3.5	49.5	2.8
		0.498	0.004			47.4	3.6		
I03-545	21	0.416	0.001	0.418	0.008	-153.9	3.0	-156.4	3.7
		0.427	0.002			-159.2	3.1		

Table 3.10.5. continued.

Station	Btl	$\delta^{13}\text{C} / \text{‰}$				$\Delta^{14}\text{C} / \text{‰}$			
		$\delta^{13}\text{C}$	Error ^a	E.W.Mean ^b	Uncertainty ^c	$\Delta^{14}\text{C}$	Error ^d	E.W.Mean ^b	Uncertainty ^c
I03-535	21	0.384	0.003	0.383	0.003	-172.6	3.1	-168.4	6.0
		0.380	0.004			-164.1	3.2		
I03-535	13	0.378	0.003	0.379	0.003	-186.1	3.3	-185.9	2.3
		0.382	0.004			-185.7	3.3		
I03-531	32	0.735	0.006	0.679	0.044	67.3	3.9	64.1	4.5
		0.673	0.002			61.0	3.8		
I03-531	13	0.380	0.004	0.379	0.003	-172.9	3.2	-171.8	2.3
		0.377	0.005			-170.8	3.3		
I03-525	32	0.860	0.005	0.870	0.013	68.9	3.7	63.9	6.9
		0.879	0.005			59.2	3.6		
I03-519	21	-	-	-	-	-167.6	3.1	-172.1	6.2
		-	-			-176.4	3.0		
I03-513	32	0.736	0.003	0.712	0.035	-	-	-	-
		0.687	0.003			-	-		
I03-513	21	0.274	0.004	0.244	0.026	-170.2	2.9	-167.6	3.7
		0.237	0.002			-165.0	2.9		
I03-507	21	0.234	0.003	0.222	0.017	-163.5	3.1	-168.8	7.6
		0.210	0.003			-174.3	3.2		
I03-507	13	0.435	0.003	0.432	0.003	-175.9	3.3	-179.2	4.5
		0.431	0.002			-182.2	3.2		
I03-503	32	0.825	0.002	0.823	0.004	75.0	3.6	75.9	2.6
		0.819	0.003			76.8	3.8		
I03-503	13	0.415	0.005	0.433	0.021	-184.7	3.0	-183.5	2.1
		0.445	0.004			-182.3	3.0		
I03-X08	32	0.869	0.004	0.846	0.017	61.8	3.5	61.6	2.5
		0.845	0.001			61.3	3.5		
I03-X08	21	0.255	0.001	0.255	0.006	-175.6	3.1	-176.1	2.2
		0.264	0.005			-176.6	3.1		
I03-495	21	0.308	0.005	0.307	0.003	-174.6	3.0	-177.9	4.6
		0.306	0.004			-181.1	3.0		

Table 3.10.5. continued.

Station	Btl	$\delta^{13}\text{C} / \text{‰}$				$\Delta^{14}\text{C} / \text{‰}$			
		$\delta^{13}\text{C}$	Error ^a	E.W.Mean ^b	Uncertainty ^c	$\Delta^{14}\text{C}$	Error ^d	E.W.Mean ^b	Uncertainty ^c
I03-495	13	-	-	-	-	-186.1	3.0	-183.0	4.5
		-	-			-179.8	3.0		
I03-491	32	0.856	0.003	0.854	0.002	68.4	3.7	70.2	2.6
		0.853	0.002			72.0	3.6		
I03-491	13	0.415	0.002	0.414	0.003	-184.2	3.1	-182.7	2.3
		0.411	0.003			-181.0	3.2		
I03-487	1	0.304	0.005	0.324	0.019	-179.1	3.3	-180.6	2.3
		0.331	0.003			-181.8	3.1		
I03-480	32	0.934	0.008	0.926	0.007	65.7	3.7	66.4	2.6
		0.924	0.004			67.1	3.6		
I03-480	21	0.287	0.004	0.291	0.006	-180.8	3.1	-179.6	2.2
		0.295	0.004			-178.3	3.2		
I03-474	32	0.845	0.003	0.852	0.014	63.5	3.6	66.4	4.1
		0.865	0.004			69.3	3.6		
I03-474	13	0.362	0.003	0.351	0.008	-190.3	2.8	-193.1	4.1
		0.350	0.001			-196.1	2.9		
I03-470	32	0.785	0.007	0.764	0.018	77.6	3.4	78.4	2.4
		0.760	0.003			79.3	3.3		
I03-470	21	0.290	0.003	0.293	0.008	-171.4	2.9	-170.9	2.1
		0.302	0.005			-170.4	2.9		
I03-466	21	0.255	0.005	0.257	0.003	-177.6	3.1	-175.8	2.6
		0.259	0.004			-173.9	3.1		
I03-466	13	0.326	0.006	0.352	0.027	-196.7	2.9	-194.5	3.3
		0.364	0.004			-192.0	3.0		
I03-463	32	0.717	0.005	0.695	0.016	71.4	3.5	73.0	2.5
		0.694	0.001			74.7	3.5		
I03-463	1	0.318	0.004	0.325	0.013	-183.9	3.1	-183.6	2.2
		0.337	0.005			-183.3	3.0		
I03-459	32	0.788	0.004	0.775	0.015	57.3	3.7	62.6	7.2
		0.767	0.003			67.5	3.6		

Table 3.10.5. continued.

Station	Btl	$\delta^{13}\text{C} / \text{‰}$				$\Delta^{14}\text{C} / \text{‰}$			
		$\delta^{13}\text{C}$	Error ^a	E.W.Mean ^b	Uncertainty ^c	$\Delta^{14}\text{C}$	Error ^d	E.W.Mean ^b	Uncertainty ^c
I03-459	21	0.277	0.004	0.280	0.004	-187.8	3.1	-180.5	10.3
		0.282	0.003			-173.2	3.1		
I03-459	13	0.397	0.003	0.374	0.045	-190.3	3.1	-188.8	2.7
		0.334	0.004			-186.5	3.9		
I03-455	32	-	-	-	-	38.0	3.7	43.0	7.2
		-	-			48.2	3.8		
I03-455	21	0.284	0.005	0.269	0.022	-192.9	3.1	-188.3	6.5
		0.253	0.005			-183.7	3.1		
I03-455	13	0.349	0.001	0.343	0.042	-186.1	3.1	-186.5	2.2
		0.290	0.003			-187.0	3.2		
I03-451	32	0.826	0.004	0.825	0.003	-	-	-	-
		0.824	0.006			-	-		
I03-451	21	-	-	-	-	-177.7	3.2	-177.0	2.3
		-	-			-176.4	3.2		
I03-451	13	-	-	-	-	-189.5	3.2	-192.5	4.3
		-	-			-195.6	3.2		

a. Standard deviation of repeat measurements.

b. Error weighted mean of the replicate pair.

c. Larger of the standard deviation and the error weighted standard deviation of the replicate pair.

d. Larger of the standard deviation of repeat measurements and the counting errors.

(7) Duplicate measurements

At 48 stations, seawater samples were taken from two X-Niskin bottles that were collected at same depth (duplicate sampling). Most of the duplicate samples were collected in deep layers below 1,000 dbar. Results of the duplicate pair analyses are shown in Table 3.10.6. The standard deviations of the $\delta^{13}\text{C}$ and $\Delta^{14}\text{C}$ duplicate analyses in good measurement were calculated to be 0.014 ‰ (n = 39) and 3.7 ‰ (n = 40), respectively. These deviations are almost same as those obtained by the replicate analyses (0.020 ‰ for $\delta^{13}\text{C}$ and 3.9 ‰ for $\Delta^{14}\text{C}$). The results of replicate and duplicate measurements suggested that "reproducibilities" of our $\delta^{13}\text{C}$ and $\Delta^{14}\text{C}$ measurements including errors due to the sample preparation were less than 0.02 ‰ and 4 ‰, respectively.

Table 3.10.6. Summary of duplicate analyses.

Station	Btl	$\delta^{13}\text{C} / \text{‰}$				$\Delta^{14}\text{C} / \text{‰}$			
		$\delta^{13}\text{C}$	Error ^a	E.W.Mean ^b	Uncertainty ^c	$\Delta^{14}\text{C}$	Error ^d	E.W.Mean ^b	Uncertainty ^c
P06W-201	35	1.206	0.002	1.201	0.024	91.5	3.9	87.7	5.4
	16	1.172	0.005			83.9	3.9		
P06E-039	22	0.321	0.001	0.320	0.006	-196.6	2.5	-193.6	3.7
	11	0.313	0.003			-191.3	2.2		
P06E-X19	20	0.274	0.002	0.278	0.006	-190.4	3.0	-191.2	2.1
	11	0.282	0.002			-191.9	3.0		
P06E-027	16	0.274	0.006	0.256	0.016	-208.7	3.2	-210.7	2.9
	10	0.252	0.003			-212.8	3.3		
P06E-023	14	0.201	0.004	0.200	0.002	-210.0	3.1	-213.7	5.2
	1	0.199	0.003			-217.3	3.1		
P06E-019	12	0.250	0.004	0.236	0.016	-218.0	3.0	-217.2	2.1
	1	0.228	0.003			-216.4	2.9		
A10-629	21	1.035	0.003	1.026	0.018	-	-	-	-
	17	1.010	0.004			-	-		
A10-007	16	1.014	0.004	0.994	0.018	-99.6	3.6	-101.2	2.5
	15	0.989	0.002			-102.9	3.6		
A10-X17	13	0.727	0.006	0.729	0.004	-136.5	3.3	-136.5	2.3
	9	0.730	0.006			-136.6	3.3		
A10-021	17	0.882	0.004	0.876	0.011	-126.8	3.4	-125.2	2.4
	8	0.866	0.005			-123.6	3.5		
A10-035	23	0.974	0.005	0.967	0.006	-	-	-	-
	13	0.965	0.003			-	-		
A10-038	22	0.639	0.002	0.634	0.011	-	-	-	-
	4	0.623	0.003			-	-		
A10-X16	21	0.664	0.005	0.651	0.013	-	-	-	-
	8	0.646	0.003			-	-		
A10-043	20	0.650	0.003	0.668	0.018	-145.2	3.5	-146.6	2.4
	7	0.676	0.002			-147.9	3.4		
A10-X15	18	0.794	0.003	0.805	0.016	-124.5	3.4	-122.8	2.4
	9	0.816	0.003			-121.3	3.3		
A10-051	16	0.880	0.005	0.869	0.016	-117.3	3.4	-116.1	2.5
	11	0.858	0.005			-114.9	3.6		

Table 3.10.6. continued.

Station	Btl	$\delta^{13}\text{C} / \text{‰}$				$\Delta^{14}\text{C} / \text{‰}$			
		$\delta^{13}\text{C}$	Error ^a	E.W.Mean ^b	Uncertainty ^c	$\Delta^{14}\text{C}$	Error ^d	E.W.Mean ^b	Uncertainty ^c
A10-055	17	0.796	0.002	0.801	0.007	-	-	-	-
	14	0.806	0.002			-	-		
A10-059	12	-	-	-	-	-105.9	3.5	-106.5	2.5
	11	-	-			-107.3	3.6		
A10-X14	10	0.844	0.002	0.885	0.036	-105.0	3.5	-107.9	4.2
	1	0.895	0.001			-110.9	3.5		
A10-067	9	0.884	0.004	0.867	0.025	-111.8	3.3	-113.0	2.3
	8	0.849	0.004			-114.3	3.2		
A10-071	7	0.788	0.004	0.793	0.006	-121.3	3.4	-117.9	4.7
	6	0.797	0.004			-114.7	3.3		
A10-075	11	0.842	0.001	0.846	0.013	-125.9	3.5	-121.7	5.6
	4	0.860	0.002			-118.0	3.3		
A10-079	7	-	-	-	-	-148.5	3.4	-150.9	3.4
	2	-	-			-153.3	3.3		
A10-083	23	0.554	0.005	0.546	0.009	-	-	-	-
	5	0.541	0.004			-	-		
A10-087	21	0.576	0.002	0.553	0.021	-	-	-	-
	5	0.547	0.001			-	-		
A10-093	12	0.855	0.003	0.835	0.021	-	-	-	-
	8	0.826	0.002			-	-		
I04-601	21	0.683	0.004	0.684	0.002	-141.2	2.3	-141.1	1.8
	14	0.684	0.002			-141.0	3.2		
I04-595	18	0.668	0.003	0.676	0.016	-137.5	3.3	-142.8	7.1
	12	0.690	0.004			-147.6	3.2		
I04-589	15	-	-	-	-	-142.7	3.1	-142.8	2.2
	11	-	-			-142.9	3.1		
I03-557	10	0.474	0.002	0.480	0.015	-174.8	3.1	-170.7	5.6
	8	0.495	0.003			-166.9	3.0		
I03-551	7	0.502	0.008	0.490	0.010	-161.3	3.1	-160.2	2.3
	6	0.488	0.003			-159.0	3.3		
I03-545	8	-	-	-	-	-170.5	3.2	-168.7	2.5
	4	-	-			-166.9	3.2		

Table 3.10.6. continued.

Station	Btl	$\delta^{13}\text{C} / \text{‰}$				$\Delta^{14}\text{C} / \text{‰}$			
		$\delta^{13}\text{C}$	Error ^a	E.W.Mean ^b	Uncertainty ^c	$\Delta^{14}\text{C}$	Error ^d	E.W.Mean ^b	Uncertainty ^c
I03-535	22	0.444	0.004	0.424	0.015	-167.0	3.1	-171.0	5.7
	7	0.423	0.001			-175.1	3.1		
I03-535	23	0.622	0.005	0.637	0.021	-125.8	3.4	-123.7	3.0
	3	0.652	0.005			-121.6	3.4		
I03-525	17	-	-	-	-	-177.9	3.0	-176.8	2.2
	14	-	-			-175.8	3.1		
I03-519	16	0.445	0.002	0.446	0.004	-162.9	3.0	-165.1	3.0
	14	0.451	0.004			-167.2	3.0		
I03-513	11	-	-	-	-	-177.1	3.0	-176.6	2.1
	9	-	-			-176.2	2.9		
I03-507	8	-	-	-	-	-193.3	3.1	-189.1	6.1
	6	-	-			-184.6	3.2		
I03-503	6	0.411	0.003	0.396	0.022	-189.7	2.9	-189.4	2.1
	1	0.380	0.003			-189.0	2.9		
I03-X08	6	0.357	0.003	0.364	0.009	-191.3	2.9	-189.2	3.3
	4	0.370	0.003			-186.7	3.1		
I03-495	5	-	-	-	-	-187.6	3.0	-186.8	2.1
	2	-	-			-186.0	3.0		
I03-491	23	0.381	0.002	0.384	0.003	-193.5	3.0	-191.5	2.9
	6	0.385	0.001			-189.4	3.1		
I03-487	21	0.321	0.003	0.322	0.002	-189.4	3.1	-188.9	2.2
	19	0.322	0.003			-188.4	3.1		
I03-480	18	0.484	0.004	0.481	0.004	-179.2	3.2	-175.7	5.1
	4	0.478	0.004			-172.0	3.3		
I03-474	16	-	-	-	-	-163.7	2.8	-170.0	9.3
	6	-	-			-176.8	2.9		
I03-470	14	0.451	0.002	0.453	0.006	-161.8	2.9	-162.6	2.0
	4	0.459	0.003			-163.4	2.8		
I03-463	13	0.430	0.004	0.434	0.004	-170.1	2.9	-166.9	5.1
	3	0.436	0.003			-162.9	3.2		
I03-455	10	0.437	0.004	0.436	0.003	-176.2	3.2	-173.8	3.3
	5	0.434	0.004			-171.6	3.1		

- a. Standard deviation of repeat measurements.
- b. Error weighted mean of the replicate pair.
- c. Larger of the standard deviation and the error weighted standard deviation of the replicate pair.
- d. Larger of the standard deviation of repeat measurements and the counting errors.

(8) Reference seawater measurements

During the sample measurements period from May 2004 to October 2006, we synchronously carried out $\delta^{13}\text{C}$ and $\Delta^{14}\text{C}$ measurements of reference seawaters. The reference seawater was prepared from a large volume of surface seawater collected in open ocean. The surface seawater was filtered, exposed to ultraviolet irradiation, poisoned by HgCl_2 , and then dispensed in 250 cm^3 glass bottles. The $\delta^{13}\text{C}$ and $\Delta^{14}\text{C}$ of the reference seawater was measured at every 40 samples analyses approximately. The results are shown in Figure 3.10.2 and Table 3.10.7. The standard deviations of $\delta^{13}\text{C}$ and $\Delta^{14}\text{C}$ were 0.027 ‰ and 5.8 ‰, respectively. These deviations were slightly larger than those obtained by the replicate and duplicate measurements (0.02 ‰ for $\delta^{13}\text{C}$ and 4 ‰ for $\Delta^{14}\text{C}$). Finally we concluded that "precisions" of our $\delta^{13}\text{C}$ and $\Delta^{14}\text{C}$ analyses including error due to the sample preparation and storage were about 0.03 ‰ and 6 ‰, respectively.

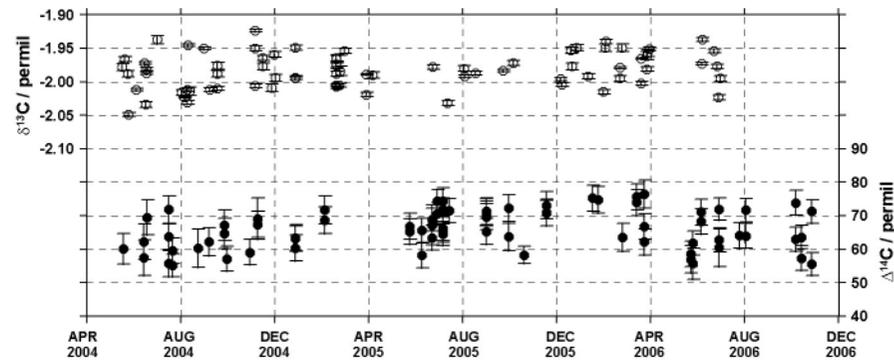


Figure 3.10.2. $\delta^{13}\text{C}$ (open circles) and $\Delta^{14}\text{C}$ (closed circles) measurements of the reference seawaters.

Table 3.10.7. Summary of reference seawaters measurements.

No.	RS No.	$\delta^{13}\text{C} / \text{‰}$			$\Delta^{14}\text{C}^a / \text{‰}$		
		Measurement date	$\delta^{13}\text{C}$	Error ^b	Measurement date	$\Delta^{14}\text{C}$	Error ^c
1	RM0204-026	17-May-04	-1.978	0.005	18-May-04	60.2	4.6
2	RM0204-156	20-May-04	-1.966	0.004	14-Jun-04	62.3	5.3
3	RM0204-093	24-May-04	-1.988	0.005	14-Jun-04	57.5	5.3
4	RM0204-103	25-May-04	-2.049	0.003	18-Jun-04	69.5	5.2
5	RM0204-028	04-Jun-04	-2.012	0.002	16-Jul-04	71.9	4.1
6	RM0204-148	15-Jun-04	-1.972	0.002	16-Jul-04	55.7	3.9
7	RM0204-022	16-Jun-04	-2.034	0.004	16-Jul-04	63.8	3.8
8	RM0204-152	17-Jun-04	-1.987	0.002	21-Jul-04	55.2	3.5
9	RM0204-064	01-Jul-04	-1.937	0.006	21-Jul-04	59.6	3.8
10	RM0204-076	02-Aug-04	-2.016	0.004	23-Aug-04	60.3	5.7
11	RM0204-115	05-Aug-04	-2.023	0.001	06-Sep-04	62.2	4.2
12	RM0204-092	10-Aug-04	-1.945	0.002	26-Sep-04	67.2	4.6
13	RM0204-027	12-Aug-04	-2.014	0.006	26-Sep-04	64.7	4.5
14	RM0204-018	31-Aug-04	-1.950	0.002	29-Sep-04	57.1	3.7
15	RM0204-169	17-Jun-04	-1.981	0.002	29-Oct-04	59.2	3.8
16	RM0204-062	12-Jul-05	-2.032	0.004	08-Nov-04	69.2	6.2
17	RM0204-048	09-Aug-04	-2.031	0.003	08-Nov-04	67.5	3.9
18	RM0204-004	15-Nov-04	-1.977	0.005	27-Dec-04	60.5	3.9
19	RM0204-119	26-Nov-04	-2.009	0.006	27-Dec-04	63.5	3.9
20	RM0204-108	09-Aug-04	-2.012	0.003	27-Dec-04	63.3	3.8
21	RM0204-123	30-Nov-04	-1.959	0.004	03-Feb-05	68.8	4.0
22	RM0204-065	01-Dec-04	-1.994	0.005	03-Feb-05	71.8	4.2
23	RM0204-159	22-Feb-05	-2.005	0.003	24-May-05	65.3	3.8
24	RM0204-055	18-Feb-05	-1.966	0.006	24-May-05	66.9	3.9
25	RM0204-177	23-Feb-05	-1.984	0.007	09-Jun-05	58.3	3.7
26	RM0204-111	01-Mar-05	-1.954	0.004	09-Jun-05	65.7	3.6
27	RM0204-138	07-Sep-04	-2.012	0.003	22-Jun-05	69.0	3.5
28	RM0204-058	17-Sep-04	-2.010	0.003	22-Jun-05	63.5	3.7
29	RM0204-165	17-Sep-04	-1.976	0.005	22-Jun-05	67.3	6.0
30	RM0204-183	17-Sep-04	-1.988	0.005	29-Jun-05	70.7	3.5

Table 3.10.7. continued.

No.	RS No.	$\delta^{13}\text{C} / \text{‰}$			$\Delta^{14}\text{C}^{\text{a}} / \text{‰}$		
		Measurement date	$\delta^{13}\text{C}$	Error ^b	Measurement date	$\Delta^{14}\text{C}$	Error ^c
31	RM0204-135	05-Nov-04	-2.006	0.003	29-Jun-05	74.4	3.6
32	RM0204-070	05-Nov-04	-1.923	0.002	06-Jul-05	65.9	3.8
33	RM0204-081	05-Nov-04	-1.950	0.004	06-Jul-05	71.5	3.8
34	RM0204-179	15-Nov-04	-1.964	0.004	06-Jul-05	74.4	4.0
35	RM0204-016	27-Dec-04	-1.949	0.004	06-Jul-05	72.0	3.5
36	RM0204-075	27-Dec-04	-1.995	0.002	06-Jul-05	66.4	3.7
37	RM0204-133	27-Dec-04	-1.994	0.003	06-Jul-05	64.7	3.6
38	RM0204-098	18-Feb-05	-2.007	0.003	14-Jul-05	71.6	3.6
39	RM0204-087	18-Feb-05	-1.964	0.005	19-Oct-05	58.5	2.5
40	RM0204-014	18-Feb-05	-1.988	0.004	31-Aug-05	71.1	3.5
41	RM0204-182	18-Feb-05	-1.975	0.005	31-Aug-05	71.5	4.1
42	RM0204-145	18-Feb-05	-2.005	0.002	31-Aug-05	69.9	3.9
43	RM0204-106	18-Feb-05	-1.974	0.004	31-Aug-05	65.5	3.9
44	RM0204-035	29-Mar-05	-1.989	0.001	31-Aug-05	71.2	4.1
45	RM0204-147	29-Mar-05	-2.019	0.003	29-Sep-05	63.9	4.1
46	RM0204-061	06-Apr-05	-1.990	0.005	29-Sep-05	72.5	4.0
47	RM0204-132	23-Jun-05	-1.978	0.003	17-Nov-05	71.0	3.8
48	RM0204-044	02-Aug-05	-1.980	0.004	17-Nov-05	73.3	4.1
49	RM0204-176	03-Aug-05	-1.992	0.002	17-Nov-05	71.2	4.0
50	RM0204-053	17-Aug-05	-1.987	0.003	16-Jan-06	75.5	3.9
51	RM0204-097	22-Sep-05	-1.983	0.002	23-Jan-06	75.0	4.0
52	RM0204-160	05-Oct-05	-1.972	0.004	24-Feb-06	63.7	4.2
53	RM0204-034	05-Dec-05	-1.996	0.002	14-Mar-06	75.9	3.9
54	RM0204-141	07-Dec-05	-2.004	0.003	14-Mar-06	74.2	3.9
55	RM0204-188	19-Dec-05	-1.953	0.005	24-Mar-06	62.4	3.9
56	RM0204-083	20-Dec-05	-1.977	0.005	24-Mar-06	67.0	3.8
57	RM0204-010	26-Dec-05	-1.949	0.005	24-Mar-06	76.7	4.1
58	RM0204-173	30-Jan-06	-2.015	0.003	23-May-06	59.0	3.8
59	RM0204-001	01-Feb-06	-1.949	0.006	23-May-06	57.3	4.0
60	RM0204-172	02-Feb-06	-1.940	0.003	26-May-06	62.1	3.6

Table 3.10.7. continued.

No.	RS No.	$\delta^{13}\text{C} / \text{‰}$			$\Delta^{14}\text{C}^{\text{a}} / \text{‰}$		
		Measurement date	$\delta^{13}\text{C}$	Error ^b	Measurement date	$\Delta^{14}\text{C}$	Error ^c
61	RM0204-144	20-Feb-06	-1.979	0.001	26-May-06	56.0	4.6
62	RM0204-080	23-Feb-06	-1.949	0.006	05-Jun-06	71.4	3.9
63	RM0204-146	27-Mar-06	-1.981	0.003	05-Jun-06	68.6	3.8
64	RM0204-126	28-Mar-06	-1.957	0.005	29-Jun-06	63.1	3.6
65	RM0204-021	30-Mar-06	-1.951	0.003	29-Jun-06	72.3	3.4
66	RM0204-039	06-Jun-06	-1.973	0.002	29-Jun-06	72.3	3.8
67	RM0204-105	07-Jun-06	-1.937	0.003	29-Jun-06	60.8	5.6
68	RM0204-178	10-Jan-06	-1.992	0.004	25-Jul-06	64.4	3.8
69	RM0204-029	20-Feb-06	-1.995	0.004	02-Aug-06	72.0	3.5
70	RM0204-167	20-Mar-06	-2.002	0.003	02-Aug-06	64.3	3.7
71	RM0204-117	20-Mar-06	-1.965	0.001	06-Oct-06	63.2	3.6
72	RM0204-024	27-Mar-06	-1.961	0.006	06-Oct-06	74.2	3.7
73	RM0204-067	22-Jun-06	-1.954	0.003	13-Oct-06	57.6	3.7
74	RM0204-107	26-Jun-06	-1.977	0.003	13-Oct-06	63.9	3.5
75	RM0204-153	28-Jun-06	-2.023	0.004	27-Oct-06	71.6	3.5
76	RM0204-051	30-Jun-06	-1.995	0.004	27-Oct-06	55.9	3.5
		mean	-1.983		mean	66.3	
		standard deviation	0.027		standard deviation	5.8	

a. Decay corrected for 01/May/2004.

b. Standard deviation of repeat measurements.

c. Larger of the standard deviation and the counting error.

(9) Quality control flag assignment

Quality flag values were assigned to all $\delta^{13}\text{C}$ and $\Delta^{14}\text{C}$ measurements using the code defined in Table 0.2 of WHP Office Report WHPO 91-1 Rev.2 section 4.5.2 (Joyce et al., 1994). Measurement flags of 2, 3, 4, 5, and 6 have been assigned (Table 3.10.8). For the choice between 2 (good), 3 (questionable) or 4 (bad), we basically followed a flagging procedure in Key et al. (1996) as listed below:

- a. On a station-by-station basis, a datum was plotted against pressure. Any points not lying on a generally smooth trend were noted.
- b. $\delta^{13}\text{C}$ ($\Delta^{14}\text{C}$) was then plotted against dissolved oxygen (silicate) concentration and deviant points noted. If a datum deviated from both the depth and oxygen (silicate) plots, it was flagged 3.
- c. Vertical sections against depth were prepared using the Ocean Data View (Schlitzer, 2006). If a datum was anomalous on the section plots, datum flag was degraded from 2 to 3, or from 3 to 4.

Table 3.10.8. Summary of assigned quality control flags.

Flag	Definition	Number	
		$\delta^{13}\text{C}$	$\Delta^{14}\text{C}$
2	Good	2,486	2,518
3	Questionable	94	80
4	Bad	19	3
5	Not report (missing)	11	12
6	Replicate	217	214
Total		2,827	2,827

(10) Data Summary

Figure 3.10.3 and 3.10.4 show vertical sections of $\delta^{13}\text{C}$ and $\Delta^{14}\text{C}$ against depth, respectively. Maximum of $\delta^{13}\text{C}$ was observed in the mode waters (SAMW: Subantarctic Mode Water) in the Pacific and Indian Oceans. In the Southwest Pacific Basin (180° - 130°W), Madagascan Basin (50°E - 60°E), and West Australian Basin (90°E - 110°E), high $\delta^{13}\text{C}$ waters near bottom well correspond to the Circumpolar Deep Water (CDW). In the South Atlantic Ocean, one can distinguish low- $\delta^{13}\text{C}$ water of the Antarctic Bottom Water (AABW) from high- $\delta^{13}\text{C}$ water of the North Atlantic Deep Water (NADW). Low $\delta^{13}\text{C}$ was found in deep waters in the Indian Ocean (IDW: Indian Deep Water) and in the Pacific Ocean (PDW: Pacific Deep Water) from 1,000 to 4,000 m depth approximately. The global distribution of $\delta^{13}\text{C}$ well agree with that presented in a previous study (Kroopnick, 1985). Temporal increase of the anthropogenic CO_2 inventory can be estimated by comparison the BEAGLE2003 $\delta^{13}\text{C}$ with historical data because atmospheric $\delta^{13}\text{C}$ decrease, named " ^{13}C -Suess Effect", has been imprinted in $\delta^{13}\text{C}$ of DIC in surface ocean.

Higher $\Delta^{14}\text{C}$ values were observed in the thermocline (< about 1,000 m depth) of the three basins because of the bomb-produced radiocarbon penetration. Deep $\Delta^{14}\text{C}$ data clearly indicate the global pattern of thermohaline circulation. Relative higher $\Delta^{14}\text{C}$ was measured in CDW where the high- $\delta^{13}\text{C}$ water was found. In the South Atlantic Ocean, one can distinguish low- $\Delta^{14}\text{C}$ water of AABW from high- $\Delta^{14}\text{C}$ water of NADW. Minimum of $\Delta^{14}\text{C}$ was measured in IDW and PDW where the $\delta^{13}\text{C}$ minimum was found. The global distribution of $\Delta^{14}\text{C}$ in deep and bottom waters supports a previous study (Key et al., 2004). Difference between BEAGLE2003 and historical radiocarbon data will suggest temporal change of bomb radiocarbon in the thermocline.

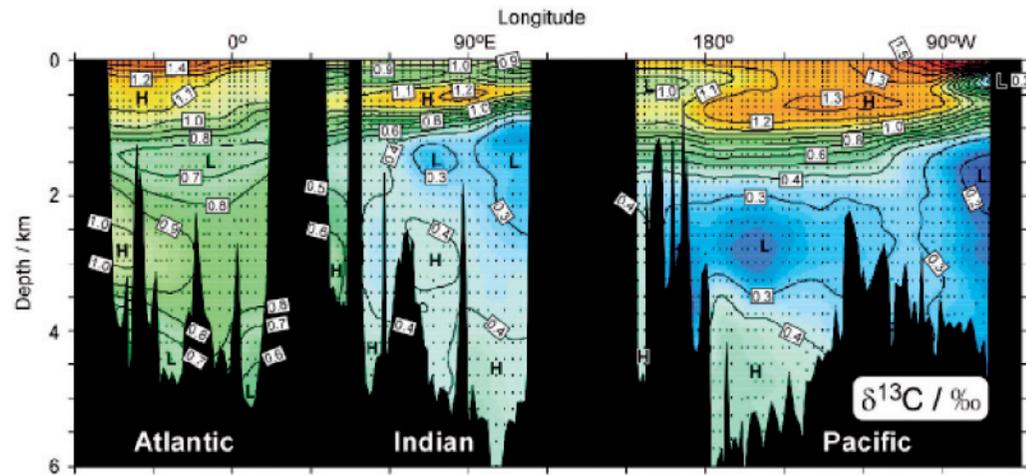


Figure 3.10.3. Vertical sections of $\delta^{13}\text{C}$ against depth during BEAGLE2003 cruise in 2003/2004.

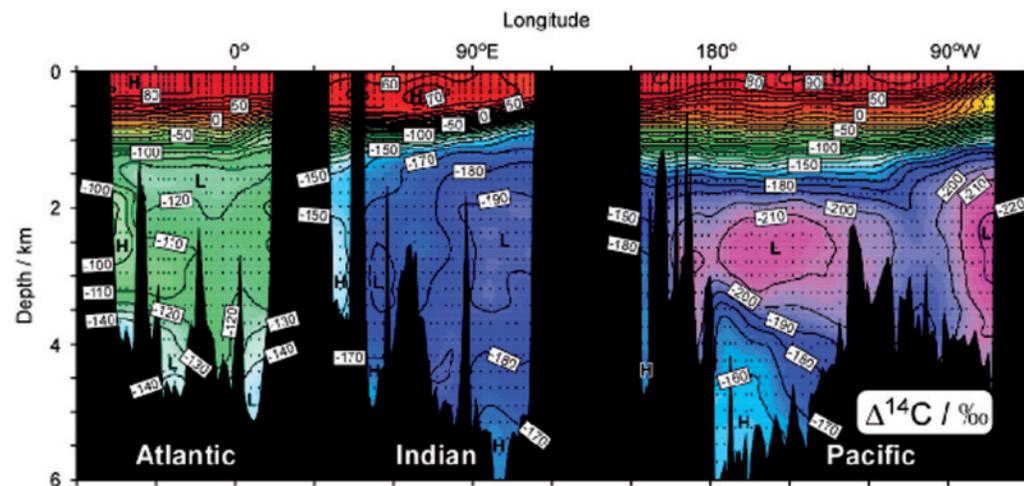


Figure 3.10.4. Vertical sections of $\Delta^{14}\text{C}$ against depth during BEAGLE2003 cruise in 2003/2004.

References

- Joyce, T., and C. Corry, eds., C. Corry, A. Dessier, A. Dickson, T. Joyce, M. Kenny, R. Key, D. Legler, R. Millard, R. Onken, P. Saunders, M. Stalcup, *contrib.*, 1994. Requirements for WOCE Hydrographic Programme Data Reporting, WHP0 Pub. 90-1 Rev. 2, 145pp.
- Key, R.M., A. Kozyr, C.L. Sabine, K. Lee, R. Wanninkhof, J.L. Bullister, R.A. Feely, F.J. Millero, C. Mordy, T.H. Peng, 2004. A global ocean carbon climatology: Results from Global Data Analysis Project (GLODAP), *Global Biogeochemical Cycles*, 18, GB4031, doi:10.1029/2004GB002247.
- Key, R.M., P.D. Quay, G.A. Jones, A.P. McNichol, K.F. von Reden, R.J. Schneider, 1996. WOCE AMS radiocarbon I: Pacific Ocean results (P6, P16, P17), *Radiocarbon* 38, 425-518.
- Kroopnick, P.M., 1985. The distribution of ^{13}C of ΣCO_2 in the world oceans, *Deep-Sea Research*, 32, 57-84.
- Kumamoto, Y., M.C. Honda, A. Murata, N. Harada, M. Kusakabe, K. Hayashi, N. Kisen, M. Katagiri, K. Nakao, and J.R. Southon, 2000. Distribution of radiocarbon in the western North Pacific: preliminary results from MR97-02 cruise in 1997, *Nuclear Instruments and Methods in Physics Research B172*, 495-500.
- McNichol, A.P. and G.A. Jones, 1991. Measuring ^{14}C in seawater CO_2 by accelerator mass spectrometry, WOCE Operations Manual, WOCE Report No.68/91, Woods Hole, MA.
- Schlitzer, R., 2006. Ocean Data View, <http://www.awi-bremerhaven.de/GEO/ODV>.
- Stuiver, M., 1983. International agreements and the use of the new oxalic acid standard, *Radiocarbon*, 25, 793-795.
- Stuiver, M. and H.A. Polach, 1977. Reporting of ^{14}C data. *Radiocarbon* 19, 355-363.
- Uchida, H. and M. Fukasawa, 2005a. WHP P6, A10, I3/I4 Revisit Data Book, Blue Earth Global Expedition 2003 (BEAGLE2003) Volume 1. JAMSTEC. Yokosuka. pp 115.
- Uchida, H. and M. Fukasawa, 2005b. WHP P6, A10, I3/I4 Revisit Data Book, Blue Earth Global Expedition 2003 (BEAGLE2003) Volume 2. JAMSTEC. Yokosuka. pp 129.

3.11 Anthropogenic radionuclides

23 January 2007

3.11.1 General information

M. Aoyama (MRI), A. Takeuchi (KANSO), S. Lee (IAEA-MEL), B. Oregioni (IAEA-MEL), and J. Gasutaud (IAEA-MEL)

(1) Personnel

M. Aoyama: Meteorological Research Institute (MRI)

A. Takeuchi: The General Environmental Technos Co., LTD (KANSO)

S. Lee: International Atomic Energy Agency, Marine Environmental Laboratories (IAEA-MEL)

B. Oregioni: IAEA-MEL

J. Gasutaud: IAEA-MEL

(2) Objectives

1) Geochemical studies of global fallout, anthropogenic radionuclides such as ^{137}Cs , ^{90}Sr and Pu isotopes, including studies on the long term behaviour of ^{137}Cs in the world ocean, and to learn more about the present geographical distribution of ^{137}Cs in the oceans in the southern hemisphere.

2) Use of anthropogenic radionuclides as tracers for oceanographic and climate change studies. Development of the anthropogenic radionuclides database for validation and update of ocean general circulation models.

(3) Target radionuclides

Main target radionuclides are ^{137}Cs , Pu isotopes and tritium. In some samples analysis of ^{90}Sr will be carried out as well.

(4) Sampling procedures

Seawater sampling for analysis of radionuclides in the water column was carried out using adopted procedures. If additional Niskin bottles filled with samples were available, volumes of water column samples varied from 6 L to 20 L. The samples were drawn from Niskin bottles into 20 L cubitainers. The samples were then filtered through 0.45 μm pore size filters and filled into cubitainers or bottles of appropriate sizes. Filters were also archived. Concentrated nitric acid was added to the samples to keep pH at 1.6, except for tritium samples.

Surface water samples were drawn through an intake pump located several meters below the sea surface. Volumes up to 85 L were collected for ^{137}Cs and Pu analysis. For tritium analysis, samples of 1 L were collected.

All samples were stored in a storage room at a stable temperature by the end of the cruise. In March 2004 the samples were loaded on land and transported to MRI at Tsukuba for the analysis of radionuclides on land. In June 2004, selected samples were sent to IAEA-MEL at Monaco for the analysis of radionuclides on land, too.

(5) Samples accomplished during the cruises

A total of 91 samples were collected for surface seawater samples. At the 56 stations, a total of 777 samples were collected for water column samples (Table 3.11.1). The sampling locations and depths are shown in Figure 3.11.1. A total weight of the samples was around 22,000 kg.

Table 3.11.1. Number of stations for each ocean.

	The Pacific Ocean	The Atlantic Ocean	The Indian Ocean	Total
Surface	51	18	22	91
Water column	27	12	17	56

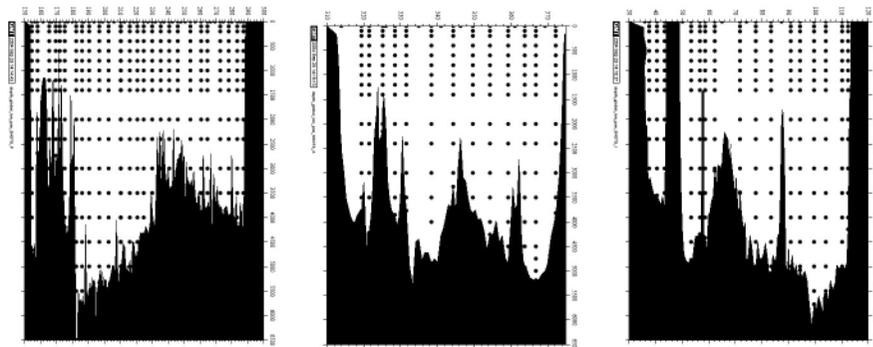


Figure 3.11.1. locations and depths of sampling sites.

(6) Problems during the cruise and solutions

No serious problems occurred during the cruise.

(7) Comparability on the analysis of radionuclides among the laboratories on land

Since the samples were measured by several laboratories on land, we checked the comparability of the measurements. Results are presented in Table 3.11.2, 3.11.3 and 3.11.4.

Table 3.11.2. Results of intercomparison of ^{137}Cs measurements.

	MRI (Bq m^{-3})	MEL (Bq m^{-3})	LLRL (Bq m^{-3})	Comenius Univ. (Bq m^{-3})
P06C-127	1.23 ± 0.00	1.24 ± 0.06		
	1.20 ± 0.04			
I03-507	1.36 ± 0.07			1.32 ± 0.07
	1.19 ± 0.05			
A10-X15	1.23 ± 0.06	1.15 ± 0.03		
	1.20 ± 0.04			
165E-33-800	0.97 ± 0.03		1.14 ± 0.05	
165E-33-900	0.63 ± 0.02		0.78 ± 0.04	
165E-33-1000	0.50 ± 0.05		0.66 ± 0.06	
165E-37-800	0.55 ± 0.03		0.69 ± 0.05	

Table 3.11.3. Results of measurements of ^{137}Cs in IAEA-381 reference material (Irish seawater).

	MRI (Bq kg^{-1})	MEL (Bq kg^{-1})	Certified value (Bq kg^{-1})
IAEA381	0.445 ± 0.002		0.49 ± 0.01

Table 3.11.4. Results of intercomparison of Pu measurements.

	MRI (mBq m^{-3})	MEL (mBq m^{-3})	KINS (mBq m^{-3})
P06C-175	1.1 ± 0.3		1.41 ± 0.24
P06C-124	1.5 ± 0.4		
P06C-127			

3.11.2 Analyses at Meteorological Research Institute (MRI) and Low Level Radioactivity Laboratory , Kanazawa University (LLRL) in Japan

M. Aoyama (MRI), K. Hirose (MRI, LLRL), K. Komura (LLRL), and Y. Hamajima (LLRL)

(1) Personnel

M. Aoyama: MRI

K. Hirose: MRI, Low Level Radioactivity Laboratory, Kanazawa University (LLRL)

K. Komura: LLRL

Y. Hamajima: LLRL

(2) Analytical method of ^{137}Cs analysis in seawater at MRI and LLRL

Cs is one of the alkali metals, which exists in ionic form in natural water, and chemically shows less affinity than other chemicals. Known adsorbents to collect Cs in seawater are ammonium phosphomolybdate (AMP) and hexacyanoferrate compounds (Folsom and Sreekumaran, 1966; La Rosa et al., 2001). The AMP has been an effective ion exchanger of alkali metals (Van R. Smit et al., 1959). Aoyama et al. (2000) re-examined the AMP procedure and their experiments revealed that the stable Cs carrier of the same equivalent amount as AMP is required to form insoluble Cs-AMP compounds in an acidic solution (pH from 1.2 to 2.2). The improved method has achieved high chemical yields of more than 95 % for sample volumes of less than 100 L. Another improvement is a reduction of the amount of AMP from ~10 g to 4 g to adsorb ^{137}Cs from seawater samples. As a result, it has been possible to reduce the sample volumes from ~100 L to less than 20 L, so after final sample treatment high-efficiency well-type Ge-detectors can be used for analysis of ^{137}Cs . These improvements have enabled to apply ^{137}Cs as a chemical tracer for studying oceanographic processes in much larger scales, as has been documented during the BEAGLE cruise.

Recently Komura (Komura, 2004; Komura and Hamajima, 2004) has established an underground facility (Ogoya Underground Laboratory, OUL) to achieve an extremely low background of γ -spectrometers, operating

with Ge detectors of high efficiency. The OUL has been constructed in 1995 by Low Level Radioactivity Laboratory of the Kanazawa University in the tunnel of former Ogoya copper mine (235 m above the sea level, Ishikawa prefecture). The shielding depth of the OUL is 270 m of water equivalent, where contributions of meon are more than four orders of magnitude lower than at the ground level. In order to achieve an extremely low background of γ -spectrometers, high efficiency well type Ge detectors specially designed for low level γ -ray spectrometry were shielded with low background lead prepared from old roof tiles of the Kanazawa Castle. As a result, the background of γ -ray spectrometers in the energy range of ^{137}Cs is two orders of magnitude lower than that in ground-level facilities, as shown in Table 3.11.5. A detection limit of ^{137}Cs at the OUL is 0.18 mBq for a counting time of 10000 minutes (Hirose et al., 2005).

There is a residual problem in low-level γ -spectrometry for ^{137}Cs measurements as AMP adsorbs trace amounts of potassium when Cs is extracted from seawater. Potassium is a major component in seawater, and natural potassium compounds contains 0.0118 % of radioactive potassium (^{40}K) to stable potassium. Therefore even trace amounts of ^{40}K cause elevation of background in the ^{137}Cs energy window due to Compton scattering of gamma-rays from ^{40}K . If ^{40}K can be removed from AMP(Cs) compound samples, a better sensitivity of underground γ -spectrometers for ^{137}Cs measurements can be achieved. To remove ^{40}K from AMP(Cs) compounds, a precipitation method including insoluble platinate salt of Cs was developed for purification of Cs. This method helped to remove trace amounts of ^{40}K from from AMP(Cs) compounds with a chemical yield of around 90 % for ^{137}Cs (Hirose et al., 2007). This method has been applied for seawater samples collected below the 1200 m water depth.

Materials and procedures of chemical separation

All reagents used for ^{137}Cs , ^{90}Sr and Pu assay are special (G.R.) grade for analytical use. All experiments and sample treatments have been carried out at ambient temperatures. It is very important to know background γ -activity of reagents. The ^{137}Cs activity of CsCl and AMP reagents was less than 0.03 mBq g^{-1} and 0.008 mBq g^{-1} , respectively. There has not been any ^{137}Cs contamination observed from other reagents.

An improved AMP procedure of chemical separation of ^{137}Cs from seawater samples for the ground-level γ -spectrometry was as follows:

- 1) Measure the seawater volume (5-100 L) and put the sample into a tank of appropriate size.
- 2) pH should be adjusted to be 1.6-2.0 by adding concentrated HNO_3 (addition of 40 mL conc. HNO_3 for 20 L seawater sample makes pH of seawater sample about 1.6).
- 3) Add CsCl of 0.26 g to form an insoluble compound, and stir at a rate of 25 L per minute for several minutes.
- 4) Weigh AMP of 4 g and pour it into a tank to disperse the AMP with seawater.
- 5) 1 hour stirring at the rate of 25 L air per minute.
- 6) Settle until the supernate becomes clear. A settling time is usually 6 hours to overnight, but no longer than 24 hours.
- 7) Take an aliquot of 50 mL supernate to calculate the amount of the residual caesium in the supernate.
- 8) Loosen the AMP(Cs) compound from the bottom of the tank and transfer into a 1-2 L beaker, if it is necessary do an additional step of decantation.
- 9) Collect the AMP/Cs compound onto 5 B filter by filtration and wash the compound with 1 M HNO_3
- 10) Dry up the AMP(Cs) compound for several days in room temperature
- 11) Weigh the AMP(Cs) compound and determine weight yield
- 12) Transfer the AMP(Cs) compound into a teflon tube of 4 mL volume and analyze in a γ -ray spectrometer.

^{137}Cs measurements were carried out by γ -spectrometry using well-type Ge detectors coupled with multi-channel pulse height analyzers. The performance of the well-type Ge detectors is summarized in Table 3.11.5. The detector energy calibration was done using IPL mixed γ -ray sources, while the geometry calibration was done using an internal reference material of similar density, placed in the same sample tube.

Table 3.11.5. The performance of HPGe coaxial well-type detectors (Hirose et al., 2007).

Institute	Type	Active volume (cm^3)	Absolute efficiency ^a (%)	Background ^b (cpm/1keV)
MRI	ORTEC 6	280	20.5	0.092
	7	80	10.8	0.033
	8	280	16.5	0.109
	9	600	23.7	0.074
Ogoya	Canberra	199	14.5	0.0005
	EYRISYS	315	20	0.0016

a: The absolute efficiencies of HPGE are calculated at 662 keV photo-peak of ^{137}Cs .

b: The background values were calculated as a sum from 660 keV to 664 keV corresponding to 662 keV photo-peak of ^{137}Cs .

For samples collected deeper than 1200 m, an additional treatment using $\text{Cs}_2\text{Pt}(\text{Cl})_6$ precipitate was applied to remove traces of ^{40}K . These samples were analyzed for ^{137}Cs in the underground facility at Ogoya.

- 1) the same procedure from step 1) to step 12).
- 2) Dissolve the AMP(Cs) compound by adding alkali solution.
- 3) pH should be adjusted to 8.1 by adding 2 M HCl and adjust the volume of solution to 70-100 mL.
- 4) Perform precipitation of $\text{Cs}_2\text{Pt}(\text{Cl})_6$ adding chloroplatinic acid (1g/5mL DW) at pH = 8.1 and keep in refrigerator during a half-day.
- 5) Collect the $\text{Cs}_2\text{Pt}(\text{Cl})_6$ precipitate onto a filter by filtration and wash the compound with solution (pH = 8.1).
- 10) Dry up the $\text{Cs}_2\text{Pt}(\text{Cl})_6$ precipitate for several days at room temperature.
- 11) Weigh the $\text{Cs}_2\text{Pt}(\text{Cl})_6$ precipitate and determine weight yield.

12) Transfer the $\text{Cs}_2\text{Pt}(\text{Cl})_6$ precipitate into a teflon tube of 4 mL volume and analyze by underground γ -spectrometry.

(3) Analytical method of $^{239+240}\text{Pu}$ in seawater at MRI

Preconcentration of Pu

Co-precipitation method of Pu with Fe hydroxides was used as a preconcentration method. Seawater sample of 60 L was acidified to pH=2 with 12 M HCl (60 mL). After addition of ferric chloride (0.6 g), a known amount of tracer (^{242}Pu) and $\text{K}_2\text{S}_2\text{O}_8$ (30 g), the solution was stirred for 1 h. In this stage, all Pu species in solution were reduced to Pu(III). Coprecipitation of Pu with ferric hydroxide was formed at pH=10 to adding dilute NaOH solution (0.5-1 M). The formed ferric oxide precipitation contained small amounts of $\text{Ca}(\text{OH})_2$ and $\text{Mg}(\text{OH})_2$.

Radiochemical separation

Precipitates (Fe, Mg, Ca hydroxides) were dissolved with 12 M HCl and added to bring the acid strength to 9 M (three times of the dissolved materials). One drop of 30 % H_2O_2 was added for each 10 mL solution, and the solution was heated just below boiling for 1 h. After the solution had cooled, Pu was isolated by anion exchange techniques (Dowex 1-X2 resin, 100 mesh; a large column (15 mm of diameter and 250 mm long) was used.) The sample solution passed through the column and was washed with 50 ml 9 M HCl. In this stage, Pu, Fe and U were retained onto resin, whereas Am and Th were in effluents. Fe and U fractions were sequentially eluted with 8 M HNO_3 . After elution of U, the column was washed with 5 ml 1.2 M HCl. Finally Pu fraction was eluted with 1.2 M HCl (100 ml) containing 2 ml of 30% H_2O_2 . The solution was dried onto hot plate. The chemical yield was around 70 %.

Electrodeposition

Pu samples for α -spectrometry were electroplated onto stainless steel disks. The diameter of stainless steel disk depends on the active surface area of detectors. The electrodeposition was performed using an electrolysis

apparatus with electrodeposition cell consisting of teflon cylinder, a cathode of platinum electrode and an anode of stainless steel disk.

The purified Pu fraction was dissolved in 1 mL of 2 M HCl and transferred into an electrodeposition cell using 20 mL ethanol. Pu was then electroplated onto a stainless steel disk (30 mm in diameter) at 15 V and 250 mA for 2 hours.

α -spectrometry

The α -spectrometers consist of several vacuum chambers with solid-state detectors, a pulse height analyzer and a computer system. The detector, which is silicone surface barrier type (PIPS, energy resolution: <25 keV (FWHM), counting efficiency: 15 - 25 %), has an active surface area of 450 - 600 mm^2 and a minimum depletion thickness of 100 μm . The vacuum in the chamber is less than 100 mTorr by using a vacuum pump. The counting time was more than 800000 s. Counting uncertainties (1σ) for BEAGLE samples were 10 - 20 %.

3.11.3 Analyses at Marine Environmental Laboratories (IAEA-MEL) in Monaco, Comenius University of Bratislava in Slovakia, and Risoe National Laboratory (RNL) in Denmark

J. A. Sanchez-Cabeza (IAEA-MEL), P. P. Povinec (Comenius Univ. of Bratislava), P. Ross (RNL), J. Gastaud (IAEA-MEL), M. Eriksson (IAEA-MEL), I. Levy-Palomo (IAEA-MEL), S. Rezzoug (IAEA-MEL), and I. Sykora (Comenius Univ. of Bratislava)

(1) Personnel

J. A. Sanchez-Cabeza: International Atomic Energy Agency, Marine Environmental Laboratories (IAEA-MEL)

P. P. Povinec: Comenius University of Bratislava

P. Ross: Risoe National Laboratory (RNL)

J. Gastaud: IAEA-MEL

M. Eriksson: IAEA-MEL

I. Levy-Palomo: IAEA-MEL

S. Rezzoug: IAEA-MEL

I. Sykora: Comenius University of Bratislava

(2) Introduction

IAEA-MEL performed the radiochemical separation of samples from the Atlantic and Indian Oceans. The seawater samples were filtered (0.45 μm) and acidified on board RV Mirai and sent to Monaco. In average, the volumes received were 80 L for surface and 20 L for deeper samples. For all samples, plutonium and caesium were analyzed. Strontium was analyzed all surface samples and 4 profiles. Therefore, 3 separation processes were sequentially performed based on co-precipitation techniques. Also, selected samples were analyzed for tritium.

(3) Sample preparation

When transferring the acidified filtered sea water samples to the precipitation containers, sample volume and weight were determined. After adjusting pH to 1, plutonium tracer (^{242}Pu : 1,022 dpm per sample) and carriers (caesium: 40 to 800 mg, depending on sample volume; strontium: 1 g) were added.

Pre-concentration of plutonium with manganese dioxide

After mixing of the tracer and the carriers to equilibrium, saturated KMnO_4 (0.5 mL per liter of sample) was added to the samples and stirred. To precipitate MnO_2 , 0.5 M MnCl_2 (1 mL per liter of sample) was added to the sample and pH was increased to 9 with 10M NaOH. After precipitation and stirring, the pH was readjusted to 8. The precipitate was allowed to settle overnight. The supernatant was carefully siphoned and transferred to another container for the caesium separation. The MnO_2 (Pu) precipitate was poured into a beaker for further

chemical separation.

Pre-concentration of caesium with ammonium molybdophosphate (AMP)

The supernatant solution was re-acidified to pH 1.5 - 2 with concentrated HCl (1 to 1.5 mL per liter of sample). Addition of a few ml of 30 % H_2O_2 was needed to dissolve a small amount of MnO_2 suspension carried over from the previous step. A slurry of AMP (0.2 g per liter of sample) in water was added and the suspension stirred for 30 minutes. The AMP was let to settle in the tank. For the subsequent precipitation of Ca(Sr) oxalate, the samples were transferred to another container. The AMP(Cs) precipitate was poured into a beaker for further chemical processing.

Pre-concentration of strontium with calcium oxalate

The strontium is co-precipitated with calcium as an insoluble oxalate from solution containing excess oxalic acid and adjusted to pH 5 - 6. As the Sr chemical recovery is estimated by X-Ray fluorescence, an aliquot of the seawater was collected kept before the Ca(Sr) precipitation. The mixed Ca(Sr) oxalate precipitation was carried out by adding an appropriate quantity of oxalic acid dissolved in very hot de-ionized water (10g per liter of sample) to the AMP(Cs) supernatant solution, mixing well and adjusting to a final pH 5 - 6 with 10M NaOH. The Ca(Sr) oxalate precipitate was let to settle overnight. Afterwards, the supernate was pumped out. The Ca(Sr) mixed oxalate precipitate was recovered from the tank bottom and transferred into a beaker for further separation.

The schematic diagram of pre-concentration of radionuclides in seawater is shown in Figure 3.11.2.

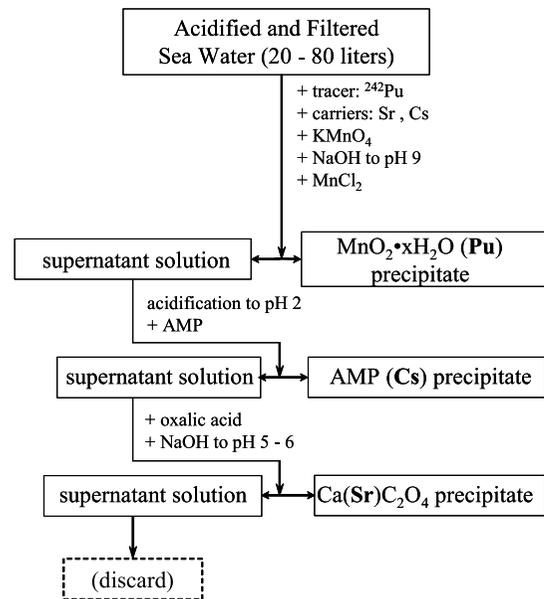


Figure 3.11.2. Pre-concentration of radionuclides in sea water.

(4) Plutonium analysis

Dissolution of manganese dioxide

After the precipitate settled in the beaker, the supernatant was siphoned out. The solution containing the MnO_2 precipitate was acidified to pH 1 and a solution of hydroxylammonium hydrochloride ($NH_2OH \cdot HCl$, 0.1 g/ml) was added in small portions to the hot suspension until all of the manganese dioxide had dissolved by reduction from Mn(IV) dioxide to soluble Mn(II).

Oxidation state adjustment of plutonium

Fifty milligrams of Fe(III) were added. A few mL of $NH_2OH \cdot HCl$ solution were added and the manganese-iron-Pu solution was heated to reduce Fe(III) to Fe(II). The Fe(II) rapidly reduced all soluble Pu species to Pu(III). After the reduction to Fe(II) and Pu(III), 2 g of $NaNO_2$ dissolved in 20 mL of water was added to the hot

solution in order to oxidize the excess $NH_2OH \cdot HCl$ and to convert Fe(II) and Pu(III) to Fe(III) and Pu(IV), respectively.

Iron hydroxide precipitation

NH_4OH was added to the hot solution to make the pH 8 - 9, causing precipitation of $Fe(OH)_3$ and co-precipitation of Pu(IV). The freshly precipitated iron hydroxide was flocculated by heating. After heating, the pH of the suspension was adjusted to 6 - 7 with HCl. At this pH, manganese will stay in solution but the flocculated iron hydroxide and its co-precipitated Pu(IV) remain insoluble.

The iron hydroxide (Pu) was left to settle overnight. The $Fe(OH)_3$ (Pu) was separated from the supernatant solution by siphoning and the precipitate was separated by centrifugation of the suspension left in the precipitating vessel. Hot, concentrated HCl was used to dissolve the separated iron hydroxide, including that on the wall of the precipitating beaker. Concentrated nitric acid additions and evaporations were used to convert this to a nitrate salt residue. (Figure 3.11.3)

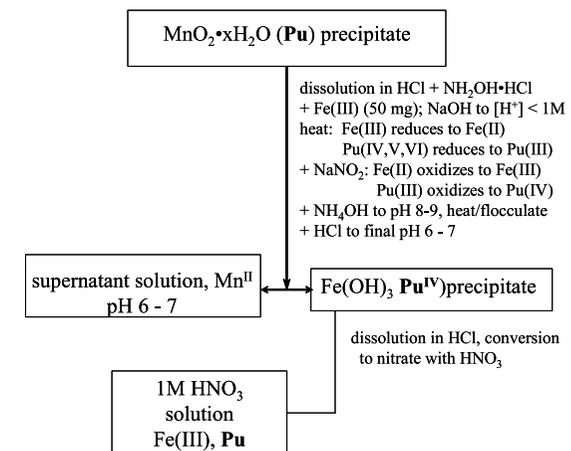


Figure 3.11.3. Dissolution and treatment of $MnO_2 \cdot xH_2O$ (Pu) concentrate.

Preparations for Pu separation by anion exchange

The Fe(Pu) precipitate was dissolved in 1 M HNO₃ and after adding hydrazinium hydrate (1 to 2 mL). The solution was heated to facilitate the reduction of Fe(III) to Fe(II). Successful conversion of the iron to the ferrous state ensures that the dissolved Pu species are brought to their lower oxidation states of III and IV. Excess N₂H₄•H₂O was destroyed by adding 70 % HNO₃ and heating the solution strongly. At this stage, Pu was in the Pu(IV) oxidation state, but this was further assured by adding NaNO₂ to the cooled solution and boiled. Finally, the solution was adjusted to 7 - 8 M HNO₃ with 70 % HNO₃.

Plutonium separation by column chromatography

The anion exchange resin used was analytical grade AG 1-X8, 100 - 200 mesh bead size, supplied in the chloride form from Bio-Rad. A water slurry of the resin (10 mL) was loaded into a 30 cm glass column (1 cm inner diameter). The resin was conditioned from chloride to nitrate form by passing 8 M HNO₃ (50 mL) through the resin bed.

The sample solution (7 - 8 M HNO₃) from the previous step and the rinse solution of the beaker were loaded into the column reservoir. This was followed by 50 ml of 8 M HNO₃ “wash” to rinse the feed solution thoroughly out of the column (removing non-retained species such as Am, Fe, Al, Ca, K). After this wash, 100 mL of 10 M HCl were passed through the column to elute thorium. The plutonium was eluted with freshly prepared 0.1 M NH₄I-9M HCl. The so-called “Pu strip” was collected in a beaker. This solution was evaporated down. Iodine was removed as volatile iodine (I₂) vapour by repeated additions of concentrated HNO₃ with small portions of 30 % H₂O₂. (Figure 3.11.4)

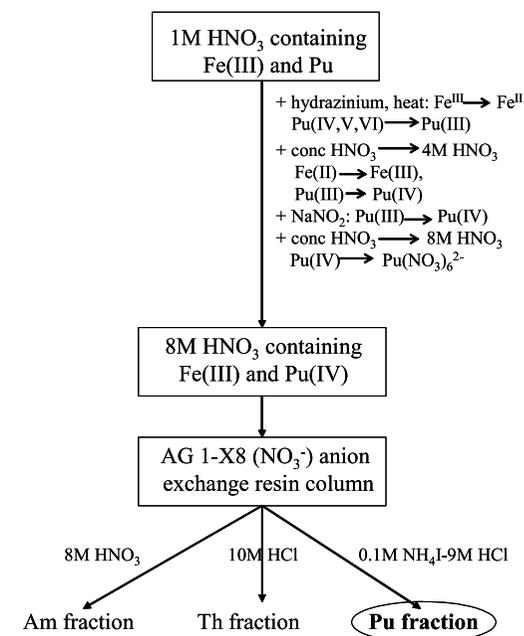


Figure 3.11.4. Separation of Plutonium by oxidation state adjustment and anion exchange chromatography.

Neodymium fluoride precipitate

Considering that Pu was to be measured by ICP-MS, it is important to efficiently remove the uranium with NdF₃ precipitations. The solution residue (Pu) was dissolved in 1 M HNO₃ and transferred to a centrifuge tube with the rinsing solution of the beaker. 10 mg of Nd (from a neodymium oxide solution) was added and a sequence of reduction-oxidation of the Pu was done by adding Mohr's salts followed by 25 % NaNO₂ solution. The Pu was co-precipitated as NdF₃ by adding concentrated HF (5 ml). This precipitate was centrifuged to remove the supernatant. The dissolution of the precipitate was done with 4 M HNO₃-H₃BO₃ (10mg/ml). A second precipitation was carried out in the same conditions. Finally, after dissolution, the precipitate was conditioned in 3 M HNO₃. (Figure 3.11.5)

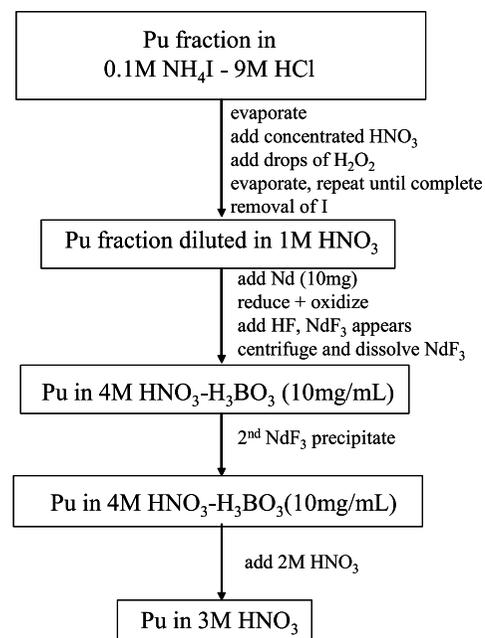


Figure 3.11.5. Separation of Plutonium by NdF_3 precipitation.

Plutonium separation by Eichrom-TEVA column

The purpose is to separate thorium traces in the solution. The pre-packed TEVA column (2 mL) was conditioned in 3 M HNO_3 and the solution was passed through it. The rinsing and following cleaning steps were processed with Ultra-Pure (UP) acids. First, thorium was eluted with 10 M HCL UP. Then Pu was eluted with a 0.1 M HCl-0.1 M HF UP solution in a Teflon beaker. (Figure 3.11.6)

Preparation of samples for ICP-MS measurements

The final solution was evaporated to dryness, treated a few times with concentrated HNO_3 UP and dried. The residue was diluted and the walls of the beaker were rinsed with 1 M HNO_3 UP. The 3 successively small volumes (0.5 mL, 0.5 mL and 0.25 mL) used were transferred to closed plastic tubes for further analysis by ICP-MS.

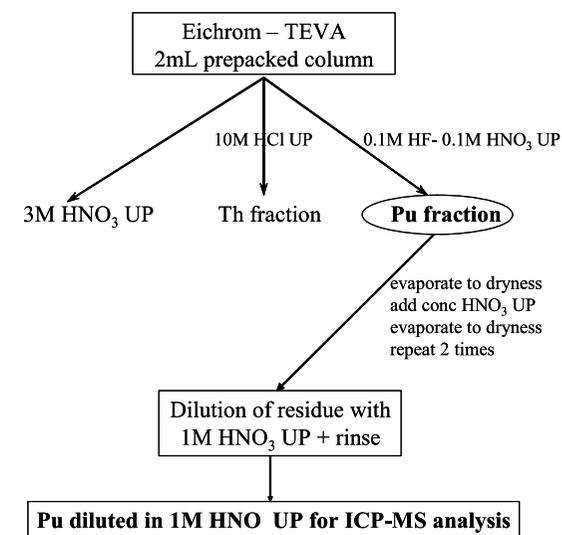


Figure 3.11.6. Plutonium separation by Eichrom-TEVA column and preparation for ICP-MS analysis.

ICP-MS analysis

Samples were analyzed using a high resolution ICP-MS at Risoe National Laboratory. An ultrasonic nebuliser was used for introduction of samples into the spectrometer. The settings of the system were as follow:

Xs- cones with Cetac USN 5000+. Heater 140 °C, cooler 3 °C

Extraction voltage -694 V

Lens 1 -1019 V

Lens 2 -69 V

Auxiliary gas 0.7 lpm

Nebuliser gas 0.92 lpm

RF power 1405 W

Hexapole bias -2 V

Sample uptake rate: 0.5 ml/min

Sensitivity ^{238}U : 4.5 MHz/ppb

Number of points per peak: 1

Dwell time: 50 ms ($^{239\&240}\text{Pu}$), 1ms (^{238}U), 2ms (^{242}Pu)

Number of sweeps: 250

Repetitions per sample: 20

Reagent blanks and reference materials were analyzed together with the seawater samples. An example of the mass spectrum obtained is shown in Figure 3.11.7.

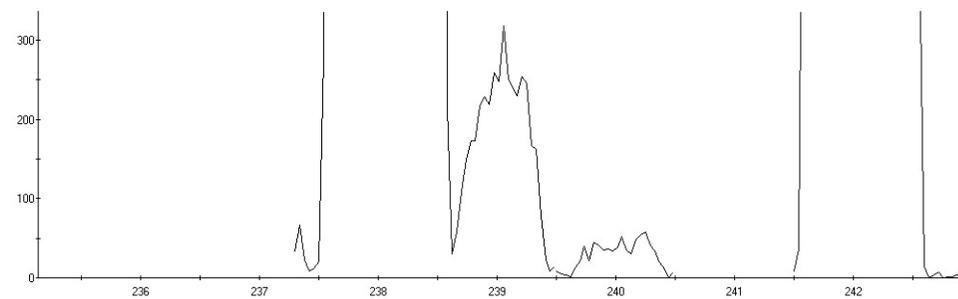


Figure 3.11.7. mass spectrum of plutonium solutions.

(5) Caesium analysis

AMP(Cs) was transferred into a beaker, decanted and the supernatant was siphoned. The AMP(Cs) was finally centrifuged. The separated AMP was dissolved in a minimum amount of 10 M NaOH. As some fine-particle suspension of MnO_2 was carried over in the supernatant solution from the first pre-concentration step (MnO_2 precipitation for Pu) and subsequently scavenged by the AMP, the insoluble fraction was separated by centrifugation. The AMP(Cs) solution in NaOH was transferred to a beaker, heated and boiled to drive off ammonia in order to minimize precipitation of AMP when the solution is re-acidified.

The boiled Cs-AMP-NaOH solution was cooled and diluted to about 500 mL with water. Concentrated HCl was added to adjust the solution to pH 2. Then, 1 g of fresh AMP was added and stirred to collect the Cs (2nd AMP-Cs precipitation). After settling and decantation, the 2nd AMP-Cs was separated by centrifugation and washed. It was again dissolved in a minimum amount of 10 M NaOH, and any eventual insoluble fraction was discarded by centrifugation. The solution was introduced into a standard geometry for gamma-ray counting. (Figure 3.11.8)

The recovery of this process was finally estimated by AAS from a small aliquot of the final solution.

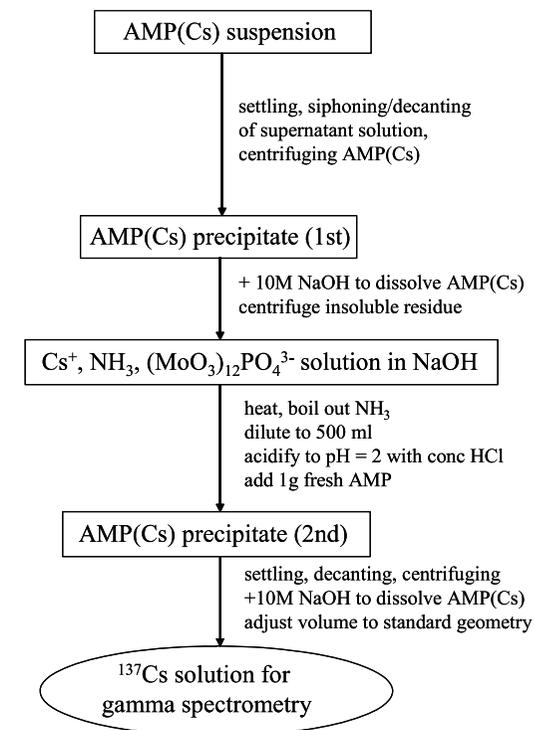


Figure 3.11.8. Caesium separation for gamma-spectrometry.

Gamma-spectrometry at IAEA-MEL

The AMP(Cs) samples were analyzed with high-purity well-type germanium detectors in the underground laboratory at IAEA-MEL. Ultra-low background is achieved by using very old lead and an antic cosmic shield (Figure 3.11.9, Povinec et al., 2005). The detectors used had relative efficiencies ranging from 100 to 200 %, and ^{40}K background count rates ranging from $1 - 5 \cdot 10^{-4} \text{ s}^{-1}$. A typical spectrum from a sample taken at 1000 m water depth is shown in Figure 3.11.10.

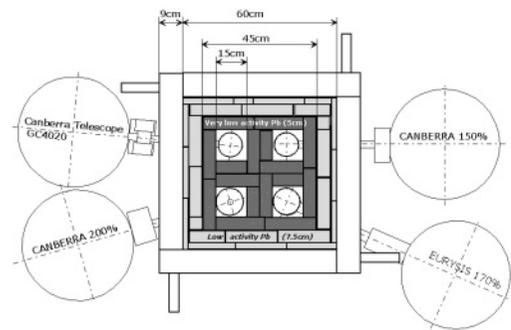


Figure 3.11.9. Schematic diagram of the IAEA-MEL underground (CAVE) facility (Povinec et al., 2005).

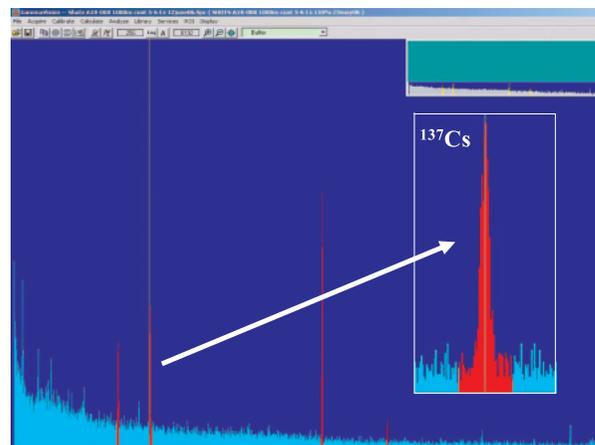


Figure 3.11.10. Gamma-ray spectrum of a seawater sample collected at 1000 m water depth in the Atlantic Ocean.

^{137}Cs gamma-ray spectrometry of seawater samples from the Indian Ocean carried out at the Comenius University of Bratislava, Slovakia

Indian Ocean seawater samples prepared in IAEA-MEL as AMP(Cs) samples were analyzed in the Comenius University of Bratislava, Slovakia. Two shields for low background gamma-ray spectrometers located at about 10 m of water equivalent were built in the Department of Nuclear Physics of the Comenius University of Bratislava, Slovakia (Figure 3.11.11; Sykora et al., 1992; Sykora et al. 2006). The larger one has the outer dimensions of $2 \times 1.5 \times 1.5 \text{ m}$. It is composed of the following layers (from the outside to the inside): 10 cm of lead, 10 cm of electrolytic copper, 10 cm of polyethylene with boric acid, 0.1 cm of electrolytic copper, 0.1 cm of cadmium and 1 cm of perspex. On the top, a layer of 12 cm of iron is added. The inner dimensions of the shield are $80 \times 90 \times 172 \text{ cm}$. To further reduce the detector background, and to decrease the radon contribution and stabilize its content in the shield (by flushing the detector chamber with nitrogen evaporated from a cooling Dewar), an extra copper shield ($12 \times 20 \times 30 \text{ cm}$) has been inserted inside the large shield (Figure 3.11.11).



Figure 3.11.11. Small (left) and large (centre and right) shields for low-level gamma-ray spectrometry constructed in the Department of Nuclear Physics of the Comenius University of Bratislava, Slovakia.

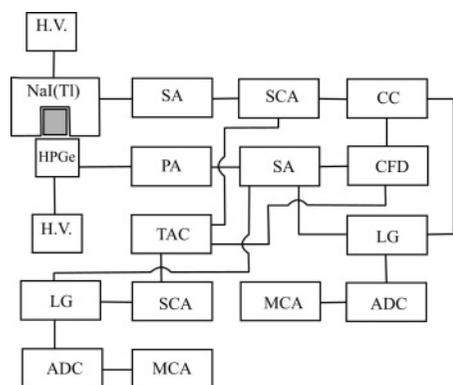


Figure 3.11.12. Schematic diagram of electronic circuits of the coincidence-anticoincidence spectrometer.

The copper has been used because of its low radioactive contamination by uranium and thorium and their decay products. A HPGe coaxial detector produced by PGT (USA) with 70 % relative efficiency (for 1332.5 keV and relative to 75×75 mm NaI(Tl) crystal) and of 270 cm³ sensitive volume operates in this shield. The smaller shield (Figure 3.11.11) has a similar composition of layers to the large shield, however, its inner dimensions are 38×38×62 cm only.

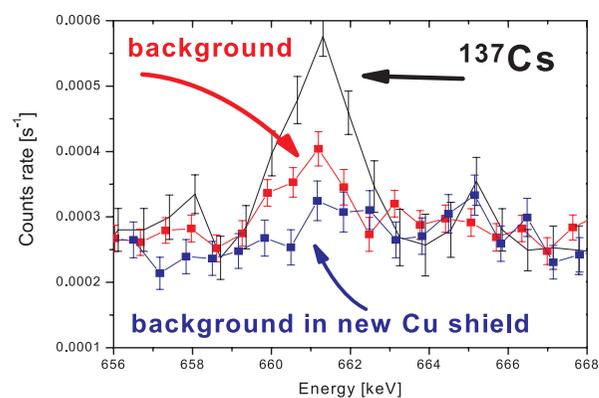


Figure 3.11.13. Comparison of background and sample counting rates in the old and in the additional Cu shield under the 661.6 keV peak of ¹³⁷Cs.

A HPGe coaxial detector of 50 % relative efficiency produced by Canberra (USA), or a HPGe detector of 6 % relative efficiency with Be window produced by ORTEC (USA), operates in this shield. A block scheme of electronics used for coincidence-anticoincidence measurements, anti-Compton (with NaI(Tl) well detector) and/or with anti-cosmic shielding (with plastic scintillation detector) is shown in Figure 3.11.12. A background reduction in the ¹³⁷Cs window after introduction of the additional copper shield into the large shield is shown in Figure 3.11.13.

Typical applications have included non-destructive analysis of natural and anthropogenic radionuclides (mainly cosmogenic ⁷Be, radiogenic ²¹⁰Pb and anthropogenic ¹³⁷Cs) in marine and terrestrial samples.

(6) Strontium analysis

Strontium purification

The calcium oxalate suspension was allowed to settle after transferring into a large beaker. The supernatant solution was siphoned off and the precipitate was centrifuged. It was then dried and ashed at 600 °C to convert the oxalate to carbonate. The ashed sample was weighed to determine the amount of 70 % HNO₃ to be added. A volume of 70 % HNO₃ in mL equal to seven times the ash weight in grams was slowly added to the calcium-strontium carbonate ash in an appropriate beaker. Strontium nitrate (1st) precipitates from this medium while the calcium remains in solution. Barium, radium and lead are expected to accompany the strontium nitrate.

The 1st strontium nitrate precipitate was separated from the mother solution containing the dissolved calcium-strontium ash by decanting the supernatant solution after settling. Heating the strontium nitrate suspension for some hours before allowing it to settle improves the separation by producing a Sr(NO₃)₂ precipitate of larger crystal size. This 1st Sr(NO₃)₂ precipitate was transferred to a pre-weighed 150 ml beaker, then washed with three 30 - 50 mL portions of acetone to remove HNO₃ and more soluble calcium nitrate. The washed Sr(NO₃)₂ was dried under a heat lamp and weighed. A volume of water in ml equal to 1.5 times the weight of dried precipitate in grams was added. This precipitate of Sr(NO₃)₂ will easily dissolve to give a clear solution.

After the salt was dissolved, a second $\text{Sr}(\text{NO}_3)_2$ precipitate was obtained by adding a volume of 70 % HNO_3 equal to ten times the volume of water used to dissolve the salt. This 2nd $\text{Sr}(\text{NO}_3)_2$ was separated by decantation of the supernatant liquid and washed again with small portions of acetone. After drying and weighing, the dissolution, concentrated nitric acid addition and acetone washings steps were repeated to give a 3rd $\text{Sr}(\text{NO}_3)_2$ precipitate.

Further purification of the Sr from barium, radium and lead contaminants was performed by a Ba chromate precipitation from an acetate-buffered solution at pH 5. A final clean-up of the Sr from ingrown Y-90 and some other possible beta-emitting radionuclides (e.g., Bi-210) was made by an iron hydroxide scavenge using 10 - 50 mg of Fe(III) and concentrated ammonia to pH 9. The iron hydroxide precipitate was centrifuged off and the Sr-acetate-chromate solution was acidified with concentrated HCl to pH 1. The purified Sr fraction was diluted with 0.1 M HCl. The chemical recovery of the Sr was determined by X-Ray fluorescence on a sample aliquot.

Milking of ^{90}Y from the purified strontium fraction

This step consists in the separation of the produced ^{90}Y from the ^{90}Sr contained in the solution. For that reason, an ingrowth period of 2 - 3 weeks was allowed before separation of the ^{90}Y . Then, the Sr solution was transferred to a beaker. An accurately known amount of yttrium carrier (10 mg) was added and the solution was evaporated down to 20 ml. The solution was transferred to a centrifuge tube, 1 g of NH_4Cl was dissolved in it and concentrated NH_4OH was added to pH 9 to precipitate yttrium hydroxide. The supernatant solution was decanted away from the Y hydroxide precipitate. The time at which the decantation occurred was noted as the Y-Sr separation time.

After the Y hydroxide dissolution with concentrated HCl, the solution was diluted to 25 mL, and 1 g of NH_4Cl was dissolved in it. Ten mg of stable Sr holdback carrier were added and a second mixed Y hydroxide was precipitated with NH_4OH . The flocculated precipitate was centrifuged and the supernatant solution was decanted. This 2nd Y hydroxide was dissolved in concentrated HCl, diluted and filtered through a membrane filter to remove any insoluble material.

To the Y solution, 0.5 g of oxalic acid was added, the solution was heated and a white yttrium oxalate was precipitated by the addition of NH_4OH to pH 1.5 - 2. This preliminary yttrium oxalate is separated from the solution by filtration through a membrane filter. Then it was dissolved by treatment with concentrated HCl and passed through the filter with rinses into a 100 ml beaker. The final yttrium oxalate precipitate was obtained from 40 - 50 mL of hot solution by dissolving 0.1 g of oxalic acid and adding concentrated ammonia until pH 1.5 - 2. The yttrium oxalate was digested for about 30 minutes to obtain a crystalline form. Then it was filtered onto a pre-washed, pre-weighed 0.2 μm polysulfone membrane filter (22 mm diameter, Gellman Sciences, Inc.). The yttrium oxalate was washed with 0.5 % ammonium oxalate solution and 80 % ethanol.

The final filtered yttrium oxalate was dried in a 70 °C oven for ca. 30 minutes and weighed to determine the yttrium chemical recovery from the stable weighing form of $\text{Y}_2(\text{C}_2\text{O}_4)_3 \cdot 9 \text{H}_2\text{O}$ (10 mg of Y gives 34 mg of yttrium oxalate). Then, the yttrium oxalate-loaded filter was mounted to fit in a Risoe GM-25-5 Beta Multicounter System (Riso National Laboratory, Roskilde, Denmark), a gas-flow proportional counter with anti-coincidence background reduction. Counting generally starts 6 to 8 hours after the Y-Sr separation time. The measured beta-activity decay curve must be consistent with the known 64 hour half-life of ^{90}Y which indicates the high radiochemical purity of the yttrium sources.

(7) Tritium analysis

One liter seawater samples were collected in plastic bottles, tightly sealed and transferred to MEL for storage before analysis. Samples were then sent to Dr. Jurgen Sültenfuß, , University of Bremen, for analysis in the Bremen Mass Spectrometric Facility for tritium analysis using the He-3 ingrowth method (Figure 3.11.14, Sültenfuß et al., 2005). For ingrowth of tritiogenic ^3He in the laboratory, typically 500 mL are sucked into an evacuated 1-L soda-glass bulb. The contained helium is removed (to $< 10^{-6}$ of solubility equilibrium concentration) by flushing the head space with water vapour under heavy shaking for 30 min, where after the bulb is flame sealed. The shaking ensures timely escape of dissolved helium into the head space. The flushing (50 mL/s) is enforced by pumping through a capillary connection that regulates the flow, and, together with a

narrowing in the bulb's head tubing, prevents any diffusion back into the bulb; the resulting water loss amounts to about 2 g, so that isotopic tritium fractionation remains negligible. Beforehand, the bulb's walls are made helium-free by heating the bulb in vacuo to 400 °C for 24 hours. After typically a six-month storage, enough tritiogenic ^3He has been generated to obtain a tritium detection limit of 10 mTU. Any ^3He other than tritiogenic is corrected for using a concurrent measurement of ^4He (the $^3\text{He} / ^4\text{He}$ ratio is approximately the atmospheric one). That correction is a prerequisite for precise measurement of the minute amounts of tritiogenic ^3He produced.

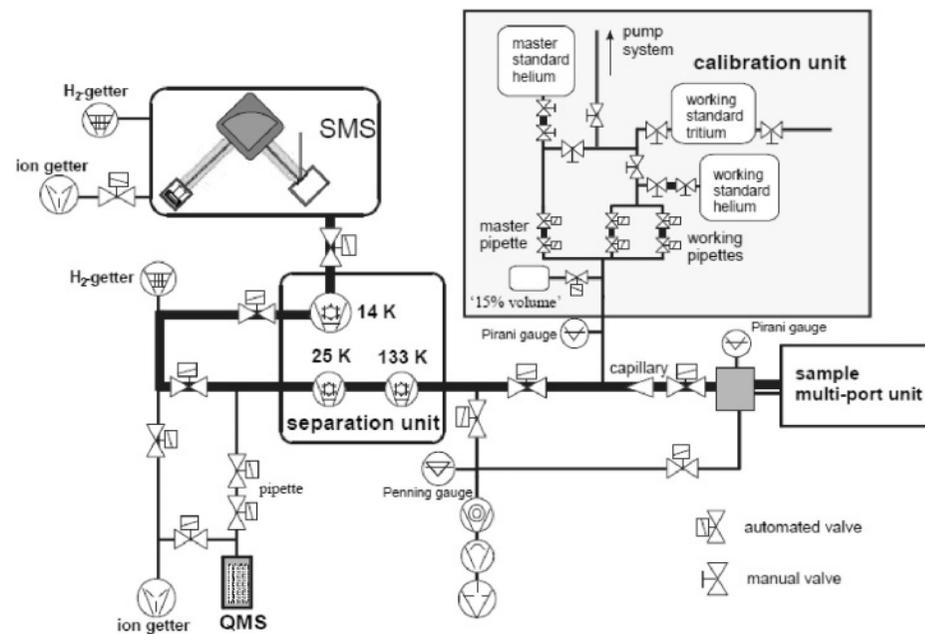


Figure 3.11.14. Scheme of the mass spectrometry system used for tritium analysis (Sültenfuß et al., 2005).

3.11.4 Analyses at Korean Institute of Nuclear Safety (KINS) in South Korea

C. S. Kim (KINS)

(1) Personnel

C. S. Kim: Korean Institute of Nuclear Safety (KINS)

(2) Sample preparation

Iron hydroxide precipitation

Weight of the acidified and filtered seawater was determined and poured into the seawater treatment cistern, and then 30 mg of Fe^{3+} carrier added. After stirring for 1 hour, Pu was co-precipitated with $\text{Fe}(\text{OH})_3$ by addition of NH_4OH up to pH 8-9. $\text{Fe}(\text{OH})_3$ precipitate was collected with 5 L beaker and then heated until boiling on a hot plate. With heating, the pH of suspension was re-adjusted to pH 8 with HCl. After cooling, supernatant was discarded by decantation and the $\text{Fe}(\text{OH})_3$ was recovered on a glass fiber filter by suction filtration, and then the precipitate was dissolved with conc. HCl. The dissolved solution was dried on a hot plate and then dissolved with 12 mL 5 M HNO_3 . The solution was filtered with a membrane filter (0.45 μm) and then the oxidation state of Pu was adjusted according to next procedure prior to loading to an on-line automated separation system.

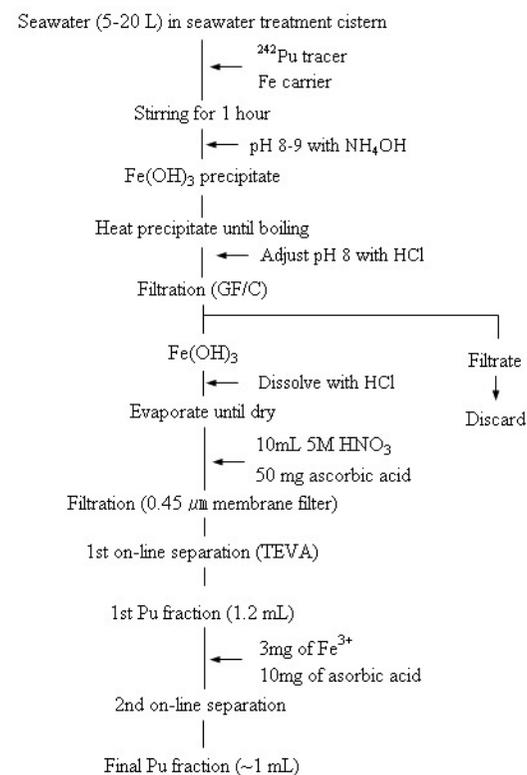


Figure 3.11.15. Pre-treatment of seawater for Pu chemical purification.

Adjustment of oxidation state of plutonium

The oxidation state of Pu in the loading solution was kept to +4 oxidation state by dissolving with 5 M HNO₃ and extra high oxidation state (VI) was reduced to (IV) by the treatment of ascorbic acid. The loading solution was treated with ascorbic acid for at least 20 minutes before loading to on-line separation system.

(3) Chemical purification

Plutonium purification by on-line separation

Chemical separation was carried out by on-line automated purification system as shown schematically in Figure 3.11.15, which is developed by Kim *et al.* (2002). The on-line automated purification process consist of 10 purification steps including the sample loading, rinsing and elution, which is described in Table 3.11.6. The 5 M HNO₃, 1 M HNO₃ and 9 M HCl solutions were used to remove U, Th and bulk matrix elements in sample solution, which were injected into TEVA-Spec resin by two peristaltic tubing pumps. Separation column (3 mm i.d. × 25 mm long) of borosilicate column (Omnifit, Cambridge, England) packed with TEVA resin (Eichrom Industries, Inc., Darien, IL, USA) was installed in the on-line purification system.

To minimize the interference effect of ²³⁸U on 239 m/z, the 1st purified Pu fraction was treated once more by the 2nd on-line purification procedure. The 2nd separation is the same as that of the 1st separation process. To adjust matrix and oxidation state of Pu, 3 mg of Fe³⁺ carrier, 1.2 mL 10 M HNO₃, 10 mg of ascorbic acid and 2.6 mL 5 M HNO₃ were sequentially added to the 1st Pu fraction. Approximately 5 mL 5 M HNO₃ was injected into the 2nd on-line purification system.

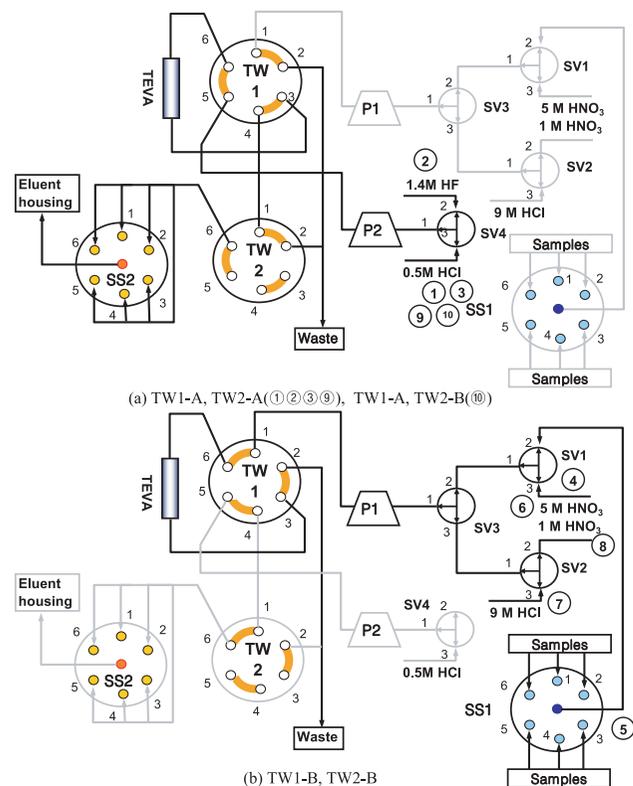


Figure 3.11.16. Schematic diagram of the on-line separation system for Pu isotopes. P1 and P2, peristaltic pump; SS1 and SS2, six-port solvent selector; TW, two-way valve; SV1 ~ SV4, isolation valve. The circled numbers indicate the procedure order, as described in Table 3.11.6.

Table 3.11.6. Description of sequential separation steps in on-line automated purification for Pu.

Step	Pumped medium	two-way 6 port valve 1	two-way 6 port valve 2	Flow rate/ ml min ⁻¹		SV1	SV2	SV3	SV4	Time/s
				Pump1	Pump2					
1	0.5 M HCl	2	1	0	0.83	-	-	-	Bottom	40
2	1.4 M HF	2	1	0	0.83	-	-	-	Top	90
3	5 M HNO ₃	1	2	1.6	0	-	-	-	Bottom	50
4	5 M HNO ₃	1	2	1.6	0	Bottom	-	Top	-	240
5	5 M HNO ₃	1	1	1.6	0	Top	-	Top	-	700
6	5 M HNO ₃	1	2	1.6	0	Bottom	-	Top	-	240
7	9 M HCl	2	1	0	0.83	-	Bottom	Bottom	-	100
8	1 M HNO ₃	1	1	1.6	0	-	Top	Bottom	-	160
9	0.5 M HCl	2	1	0	0.83	-	-	-	Bottom	6
10	0.5 M HCl	2	2	0	0.83	-	-	-	Bottom	75

Description of step

- 1 0.5 M HCl is pumped through resin to rinse residual elements.
- 2 1.4 M HF is pumped through resin to rinse residual elements.
- 3 0.5 M HCl is pumped through resin to fill the eluent line and exchange HF solution
- 4 5 M HNO₃ is pumped through column to pre-treat resin at 1.6 ml min⁻¹.
- 5 Sample is loaded to TEVA-Spec at 1.6 ml min⁻¹.
- 6 5 M HNO₃ is pumped to rinse residual sample and interference materials.
- 7 9 M HCl is pumped through resin to clean Th in resin.
- 8 1 M HNO₃ is pumped to rinse residual U.
- 9 0.5 M HCl is pumped through TEVA-Spec to elute Np at 0.83 ml min⁻¹ for 6 seconds until 0.5 M HCl reach the two-way valve.
- 10 About 1.1 ml 0.5 M HCl is pumped to elute Np and Pu on TEVA-Spec.

(4) ICP-MS analysis

Sample was measured by ICP-SF-MS, a PlasmaTrace 2 (Micromass, Manchester, UK), under the optimum sensitivity and stability. Approximately 1 mL of final Pu fraction was injected into plasma by an Aridus desolvating introduction system (Cetac Technologies, Omaha, NE, USA) involving a T1-H microconcentric nebulizer. The Pu isotopes (^{239}Pu , ^{240}Pu , ^{242}Pu) and ^{238}U were measured three times in peak hopping mode. The details of operation condition used for ICP-SFMS and the sample introduction system are described in Table 3.11.7. To increase integrated count, eluent completely used up and sample was measured three runs to get relative standard deviation. Sample blank was positioned in the first row before samples and ^{242}Pu standard solutions were finally measured to check the chemical recovery. An example of the mass spectrum for Pu isotopes and ^{238}U obtained by ICP-SF-MS is shown in Figure 3.11.17. The concentration of Pu isotopes was calculated base on the isotope dilution analysis (IDA) using following equation.

$$C \pm \sigma_c = \left[(R_s - R_t) \pm \sqrt{(\sigma_{R_s})^2 + (\sigma_{R_t})^2} \right] \frac{T}{W}$$

C : Concentration of ^{239}Pu or ^{240}Pu (pg/g)

R_s : $([^{239}\text{Pu}]_s - [^{239}\text{Pu}]_b) / ([^{242}\text{Pu}]_s - [^{242}\text{Pu}]_b)$ or

$([^{240}\text{Pu}]_s - [^{240}\text{Pu}]_b) / ([^{242}\text{Pu}]_s - [^{242}\text{Pu}]_b)$

R_t : $([^{239}\text{Pu}]_t - [^{239}\text{Pu}]_b) / ([^{242}\text{Pu}]_t - [^{242}\text{Pu}]_b)$ or

$([^{240}\text{Pu}]_t - [^{240}\text{Pu}]_b) / ([^{242}\text{Pu}]_t - [^{242}\text{Pu}]_b)$

s ; sample, b ; blank sample, t ; tracer (^{242}Pu)

$[^{239}\text{Pu}]$, $[^{240}\text{Pu}]$, $[^{242}\text{Pu}]$: ^{239}Pu , ^{240}Pu , ^{242}Pu count rate (cps)

T : Amounts of tracer added (^{242}Pu) (pg)

W : Sample amounts (g)

σ_c : ^{239}Pu or ^{240}Pu standard deviation (pg/g)

σ_{R_s} : $[^{239}\text{Pu}]_s / [^{242}\text{Pu}]_s$ or $[^{240}\text{Pu}]_s / [^{242}\text{Pu}]_s$ standard deviation of sample

σ_{R_t} : $[^{239}\text{Pu}]_t / [^{242}\text{Pu}]_t$ or $[^{240}\text{Pu}]_t / [^{242}\text{Pu}]_t$ standard deviation of tracer

Table 3.11.7. Operation condition of ICP-SF-MS (PT2).

ICP and interface				
RF power, W	1350			
Coolant gas flow, L/min	14			
Auxiliary gas flow, L/min	2.2			
Carrier gas flow, L/min	1.1			
Expansion chamber pressure, mbar	1.6			
Aridus				
Sweeping gas flow, L/min	2.4			
Spray chamber temp., °C	80			
Membrane desolvator temp., °C	160			
Sample uptake rate, mL/min	0.1			
Type of nebulizer	T1			
date acquisition				
Element	^{238}U	^{239}Pu	^{240}Pu	^{242}Pu
Mass range, amu	237.8 - 238.6	238.4 - 239.6	239.4 - 240.6	241.4 - 242.6
Dwell time, ms	7	60	120	15
Width Points	100	100	100	100
Peak widths	1.7	1.6	1.6	1.8
Sweep no.			3	
Runs			3	
Resolving Power			430	
Total analysis time, s/sample	3.57	28.8	57.6	8.1

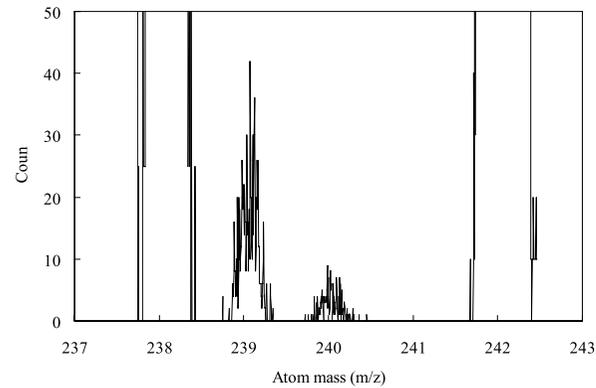


Figure 3.11.17. Mass spectrum of plutonium isotopes and ^{238}U in deep (600 meter) seawater.

3.11.5 Preliminary results of ^{137}Cs and Pu isotopes in the surface layers

M. Aoyama (MRI), M. Eriksson (IAEA-MEL), J. Gastaud (IAEA-MEL), K. Hirose (MRI, LLRL), Y. Hamajima (LLRL), C. S. Kim (KINS), K. Komura (LLRL), I. Levy-Palomo (IAEA-MEL), P. P. Povinec (Comenius Univ. of Bratislava), S. Rezzoug (IAEA-MEL), P. Ross (RNL), J. A. Sanchez-Cabeza (IAEA-MEL), and I. Sykora (Comenius Univ. of Bratislava)

(1) Personnel

M. Aoyama: MRI
M. Eriksson: IAEA-MEL
J. Gastaud: IAEA-MEL
K. Hirose: MRI, LLRL
Y. Hamajima : LLRL
C. S. Kim: KINS
K. Komura: LLRL
I. Levy-Palomo: IAEA-MEL

P. P. Povinec: Comenius University of Bratislava

S. Rezzoug: IAEA-MEL

P. Ross: RNL

J. A. Sanchez-Cabeza: IAEA-MEL

I. Sukora: Comenius University of Bratislava

(2) Preliminary results of ^{137}Cs along the BEAGLE lines

^{137}Cs concentrations in surface waters in the mid latitude region of the Southern Ocean along P06, A10 and I03/4 lines are shown in Figure 3.11.18. Those were in the range from 0.1 to 2.3 Bq m^{-3} , which is no significant difference with that in the North Pacific mid-latitude region (Aoyama et al., 2004, 2006; Povinec et al., 2003). Large ^{137}Cs concentration gradients, with high values in the North Pacific mid-latitude region, and low ones in the South Pacific were observed in the 1970s and 1980s (Bowen et al., 1980; Hirose and Aoyama, 2003).

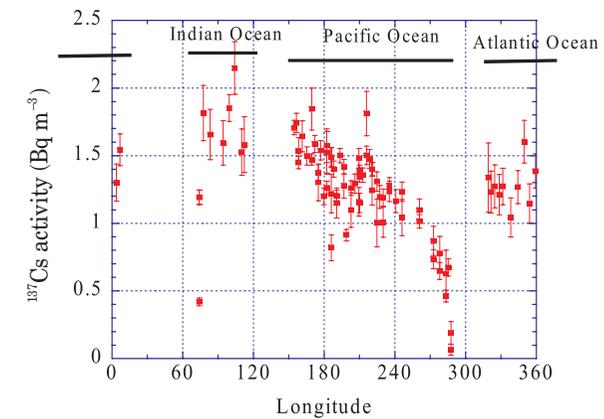


Figure 3.11.18. ^{137}Cs concentration in the surface layers, surface and 100 m depth, along BEAGLE lines in 2003/2004.

The high density ^{137}Cs data revealed a typical longitudinal distribution as shown in Fig. 3.11.18, which depends on sea areas. In the Pacific Ocean, the ^{137}Cs concentrations in the Tasman Sea, 155 deg. E to 180 deg. E, ranged from 1.37 to 1.74 Bq m^{-3} , showing higher values compared with that in the subtropical gyre in the South Pacific. In the Tasman Sea, the ^{137}Cs concentrations gradually decreased from west to east, which corresponds from upstream and downstream of East Australian Current System (EAC), respectively. The surface ^{137}Cs concentration was high in the upstream of EAC and low in the downstream of EAC. In the subtropical gyre, there was no longitudinal gradient of the surface ^{137}Cs concentrations, which ranged from 0.91 to 1.53 Bq m^{-3} , although the surface ^{137}Cs levels varied spatially. In the Eastern South Pacific, the ^{137}Cs concentrations, ranged from 0.07 to 1.14 Bq m^{-3} , showing lower values than that in the Tasman Sea and subtropical gyre.

In the Indian Ocean, the ^{137}Cs concentrations ranged from 1.5 to 2.2 Bq m^{-3} , showing higher values compared with that in the Southern Hemisphere. The ^{137}Cs concentrations in the Mozambique Channel ranged from 0.4 to 1.2 Bq m^{-3} , showing lower values than those in the Indian Ocean and Tasman Sea.

In the Atlantic Ocean, the ^{137}Cs concentrations ranged from 1.1 to 1.6 Bq m^{-3} , showing similar with that in the subtropical gyre in the Pacific Ocean.

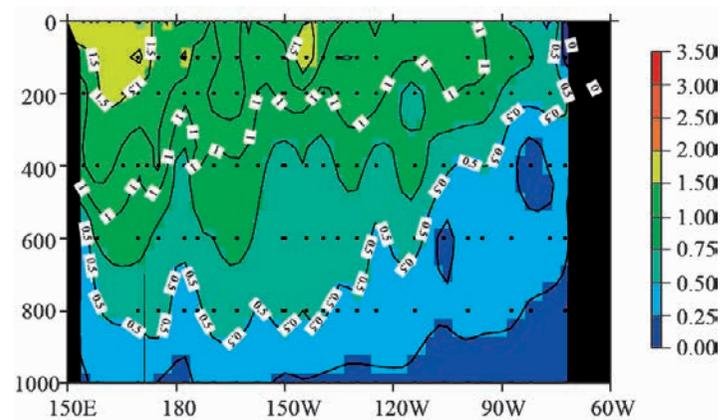


Figure 3.11.19. ^{137}Cs section in the surface layers, surface - 1000 m depth, along P6 line.

The ^{137}Cs concentrations in the layers between the surface to 1000 m depth are shown in Figure 3.11.19.

As well as the general trend of ^{137}Cs concentration in the surface layers (Figure 3.11.18), the ^{137}Cs concentrations in the Tasman Sea was higher than 1.5 Bq m^{-3} between surface to 200 m depth, showing higher values than those in the subtropical gyre and the Eastern South Pacific. The ^{137}Cs concentrations in the layers between surface to 200 m depth ranged from 1.0 to 1.5 Bq m^{-3} in the subtropical gyre and it decreased rapidly in the Eastern South Pacific. This tendency that ^{137}Cs decreased from west to east in general is observed for the depths between the surface to 1000 m depth throughout the Pacific sector.

(3) Preliminary results of Pu isotopes along the BEAGLE lines

$^{239,240}\text{Pu}$ concentrations in surface water in the mid-latitudes of the South Pacific were in the range of 0.5 to 4.1 mBq m^{-3} . The surface $^{239,240}\text{Pu}$ in the South Pacific was the same order of magnitude as that in the subtropical gyre in the North Pacific (1.5 to 9.2 mBq m^{-3}) (Hirose et al., 2001, 2006; Povinec et al., 2003; Yamada et al., 2006). The observation of the current surface $^{239,240}\text{Pu}$ concentrations suggests that there has not been a marked inter-hemisphere distribution in the Pacific, although rather large spatial variation of surface $^{239,240}\text{Pu}$ concentration has been observed.

Close sampling spacing revealed that the surface $^{239,240}\text{Pu}$ concentration shows a different longitudinal distribution from that of ^{137}Cs (seen in Fig. 3.11.18). The $^{239,240}\text{Pu}$ concentrations in the Tasman Sea, ranged from 1.0 to 2.9 mBq m^{-3} , showed a similar longitudinal distribution as did ^{137}Cs . In the subtropical gyre, there was no longitudinal gradient of the surface $^{239,240}\text{Pu}$ concentrations, which ranged from 0.8 to 4.1 mBq m^{-3} , although peaks of the higher $^{239,240}\text{Pu}$ concentrations were observed near 165 °W and 135 °W. In the Eastern South Pacific, the surface $^{239,240}\text{Pu}$ concentrations which ranged from 0.5 to 3.2 mBq m^{-3} , showed a larger variation than that in the Tasman Sea and subtropical gyre. The surface $^{239,240}\text{Pu}$ concentrations in the mid-latitude region of the South Pacific broadly decreased from west to east.

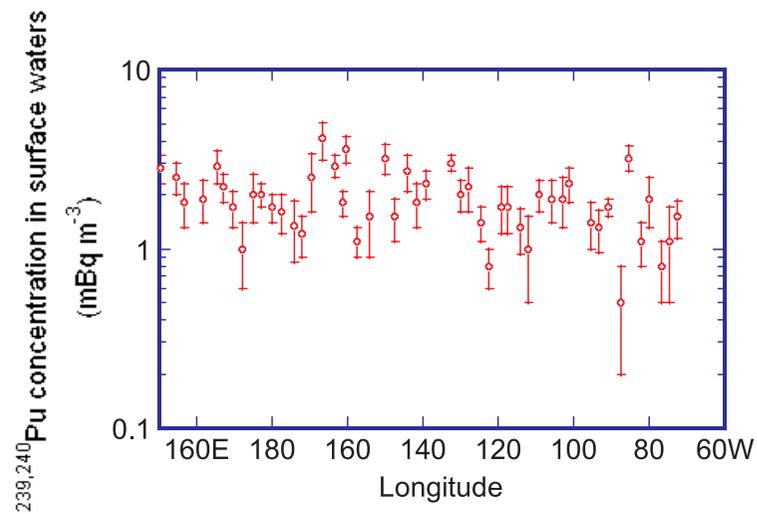


Figure 3.11.20. $^{239,240}\text{Pu}$ concentration in the surface layers along P6 line.

References

- Aoyama, M., K. Hirose, T. Miyao, Y. Igarashi, 2000, Low level ^{137}Cs measurements in deep seawater samples, *Appl. Radiat. Isot.* 53: 159-162.
- Aoyama, M., Hirose, K., Komura, K., & Nemoto, K., 2004. Temporal variation of ^{137}Cs Distribution and Inventory along 165 deg. E in the North Pacific since 1960s to the Present, *International Conference on Isotopes in Environmental Studies - Aquatic Forum 2004, BOOK OF EXTENDED SYNOPSES. IAEA-CN-118*, 256-257.
- Aoyama, M., Fukasawa, M., Hirose, K., Mantoura, R. F. C., Povinec, P. P., Kim, C. S., & Komura, K., 2006. Southern Hemisphere Ocean Tracer Study (SHOTS): An overview and preliminary results, *INTERNATIONAL CONFERENCE ON ISOTOPES AND ENVIRONMENTAL STUDIES, Radionuclides in the Environment, Vol.8*, Ed., P. P. Povinec and J.A. Sanchez-Cabeza, Elsevier, London, pp 53-66.
- Bojanowski, R. and D. Knapinska-Skiba, 1990, Determination of low-level Sr-90 in environmental materials: a novel approach to the classical method, *J. Radioanal. Nuclear Chem.*, 138: 207-218.
- Bowen, V. T., Noshkin, V. E., Livingston, H. D., & Volchok, H. L., 1980. Fallout radionuclides in the Pacific Ocean: Vertical and horizontal distributions, largely from GEOSECS stations. *Earth Planet. Sci. Lett.*, 49, 411-434.
- Folsom T. R. and C. Sreekumaran, 1966, Some reference methods for determining radioactive and natural cesium for marine studies. In: *Reference methods for marine radioactivity studies, Annex IV, IAEA, Vienna.*
- Hirose, K., Aoyama, M., Miyao T. & Igarashi Y., 2001. Plutonium in seawaters of the western North Pacific. *J. Radioanal. Nucl. Chem. Articles* 248, 771-776.
- Hirose, K., & Aoyama, M., 2003. Analysis of ^{137}Cs and $^{239,240}\text{Pu}$ concentrations in surface waters of the Pacific Ocean. *Deep Sea Res. II*, 50, 2675-2700.
- Hirose, K., M. Aoyama, Y. Igarashi, K. Komura, 2005, Extremely low background measurements of ^{137}Cs in seawater samples using an underground facility (Ogoya), *J. Radioanal. Nucl. Chem.*, 263: 349-353.
- Hirose, K., Aoyama, M., Kim, C. S., Kim, C. K., & Povinec, P. P., 2006. Plutonium isotopes in seawater of the North Pacific: effect of close-in fallout. *Radionuclides in the Environment, Vol. 8*, Ed., P. P. Povinec and J. A. Sanchez-Cabeza, pp.67-82.
- Hirose, K., M. Aoyama, Y. Igarashi, K. Komura, 2007, Oceanic ^{137}Cs : Improvement of ^{137}Cs Analysis in Small Volumes Seawater Samples Using The Underground Facility (Ogoya), *J. Radioanal. Nucl. Chem.* (in press).
- Kim, C. S., C. K. Kim, K. J. Lee, 2002, Determination of Pu Isotopes in Seawater by an On-Line Sequential Injection Technique with Sector Field Inductively Coupled Plasma Mass Spectrometry, *Anal. Chem.* 74(15): 3824-3832.
- Komura, K., Y. Hamajima, 2004, Ogoya Underground Laboratory for the measurement of extremely low levels of environmental radioactivity: Review of recent projects carried out at OUL, *Appl. Radiat. Isot.* 61: 164-189.
- La Rosa, J. J., W. Burnett, S-H. Lee, I. Levy, J. Gastaud, P. P. Povinec, 2001, Separation of actinides, cesium and strontium from marine samples using extraction chromatography and sorbents. *J. Radioanal. Nucl. Chem.* 248: 765-770.
- Povinec, P. P., Livingston, H. D., Shima, S., Aoyama, M. Gastaud, J., Goroncy, I., Hirose, K., Hynh-Ngoc, L.,

- Ikeuchi, Y., Ito, T., LaRosa, J., Kwong, L. L. W., Lee, S.-H., Moriya, H., Mulsow, S., Oregioni, B., Pettersson H. & Togawa, T. 2003. IAEA '97 expedition to the NW Pacific Ocean-results of oceanographic and radionuclide investigations of the water column. *Deep-Sea Res. Part II*, 50, 2607-2637.
- Povinec, P. P., J-F. Commanducci, I. Levy-Palomo, 2005, IAEA-MEL's underground counting laboratory (CAVE) for the analysis of radionuclides in the environment at very low-levels. *J. Radioanal. Nucl. Chem.*, 263/2: 441-445.
- Sültenfuß, J., W. Roether, M. Rhein, 2005, The Bremen Mass Spectrometric Facility for the Measurement of Helium Isotopes, Neon, and Tritium in Water, IAEA-CN-119/7.
- Sykora, I., Durcik M., Stanicek J., Povinec P., 1992, Radon problem in low-level gamma-ray spectrometry. In: *Rare Nuclear Processes* (Ed.P. Povinec), World Sci., Singapore, p. 321-326.
- Sykora, I., M. R. Jeskovsky, R. Janik, K. Holý, M. Chudý, P. P. Povinec, 2006, Low-level single and coincidence gamma-ray spectrometry. *J. Radioanal. Nucl. Chem.* (in press).
- Van R. Smit, J., W. Robb, J. J. Jacobs, 1959, AMP-Effective ion exchanger for treating fission waste. *Nucleonics* 17, 116-123.
- Yamada, M., Zheng, J., & Wang, Z.-L., 2006. ^{137}Cs , $^{239+240}\text{Pu}$ and $^{240}\text{Pu} / ^{239}\text{Pu}$ atom ratios in the surface waters of the western North Pacific Ocean, eastern Indian Ocean and their adjacent seas. *Sci. Total Environ.*, 366, 242-252.

4. Errata and Updated Data of the Data Books Volume 1 and 2

4.1 Errata in the documents

Coefficients of Note 2 in Figure caption of Volume 2 (p. 91) should be corrected as follows.

$$a_0 = 6.4409, b_0 = -3.9577e-4, a_1 = 4.3830, b_1 = 6.3317e-4$$

4.2 Mistakes in the figures

In Figures 14, 15 and 16 in Volume 2 (vertical sections for dissolved inorganic carbon, total alkalinity and pH), data with quality flags of 6 (mean of replicate measurements) were not included.

4.3 Updates in the data files

(1) FLUOR in the CTD data

Flags for FLUOR in the CTD exchange format files were wrong (flags for CTDOXV were set by mistake) and corrected.

(2) pH

Reporting precision for pH increased from F7.3 to F7.4 (FORTRAN format).

(3) Total alkalinity and dissolved inorganic carbon

Following flags and a value for carbon related parameters were revised.

EXPCODE	STNNBR	CASTNO	SAMPNO	PARAMETER: Change
49MR03K04_1	172	1	4	ALKALI_FLAG_W: 2 -> 3
49MR03K04_1	172	1	1	ALKALI_FLAG_W: 2 -> 3
49MR03K04_1	X15	1	6	ALKALI_FLAG_W: 2 -> 3
49MR03K04_1	150	1	16	ALKALI_FLAG_W: 2 -> 3

49MR03K04_1	137	1	1	ALKALI_FLAG_W: 2 -> 3
49MR03K04_2	95	1	1	ALKALI: 2291.3 -> 2381.2
49MR03K04_2	59	1	33	ALKALI_FLAG_W: 2 -> 3
49MR03K04_2	59	1	14	ALKALI_FLAG_W: 2 -> 3
49MR03K04_2	47	1	27	ALKALI_FLAG_W: 2 -> 4
49MR03K04_2	11	1	9	TCARBON_FLAG_W: 2 -> 3
49MR03K04_4	7	1	17	ALKALI_FLAG_W: 2 -> 3
49MR03K04_4	9	1	19	ALKALI_FLAG_W: 2 -> 3
49MR03K04_4	11	1	19	ALKALI_FLAG_W: 2 -> 3
49MR03K04_4	11	1	15	ALKALI_FLAG_W: 6 -> 3
49MR03K04_4	X17	1	13	ALKALI_FLAG_W: 2 -> 4
49MR03K04_4	18	1	16	TCARBON_FLAG_W: 2 -> 3
49MR03K04_4	27	1	32	TCARBON_FLAG_W: 2 -> 3
49MR03K04_4	27	1	12	ALKALI_FLAG_W: 2 -> 3
49MR03K04_4	33	1	1	ALKALI_FLAG_W: 2 -> 3
49MR03K04_4	38	1	22	ALKALI_FLAG_W: 2 -> 3
49MR03K04_4	38	1	15	ALKALI_FLAG_W: 6 -> 3
49MR03K04_4	38	1	3	ALKALI_FLAG_W: 2 -> 4

4.4 Planned updates

In the future, data of total organic carbon (TOC) will be available through our web site: <http://www.jamstec.go.jp/iorgc/ocorp/data/beagle2003/index.html>. In addition, data of the artificial radionuclides will be updated.

Figure captions

Figure 1 Observation lines for WHP P6, A10 and I3/I4 revisit in Blue Earth Global Expedition 2003 (BEAGLE2003) with bottom topography based on ETOPO5 (Data announcement 88-MGG-02,1988).

Figure 2 Station locations for WHP P6, A10 and I3/I4 revisit in BEAGLE2003 with bottom topography based on Smith and Sandwell (1997).

Figure 3 CFC-11 (CCl_3F ; pmol kg^{-1}) cross section. Data with quality flags of 2 and 6 were plotted. Vertical exaggeration of the 0-6,500 m section is 1000:1. Expanded section of the upper 1000 m is made with a vertical exaggeration of 2500:1.

Figure 4 Same as Figure 3 but for CFC-12 (CCl_2F_2 ; pmol kg^{-1})

Figure 5 Same as Figure 3 but for $\Delta^{14}\text{C}$ of dissolved inorganic carbon (‰).

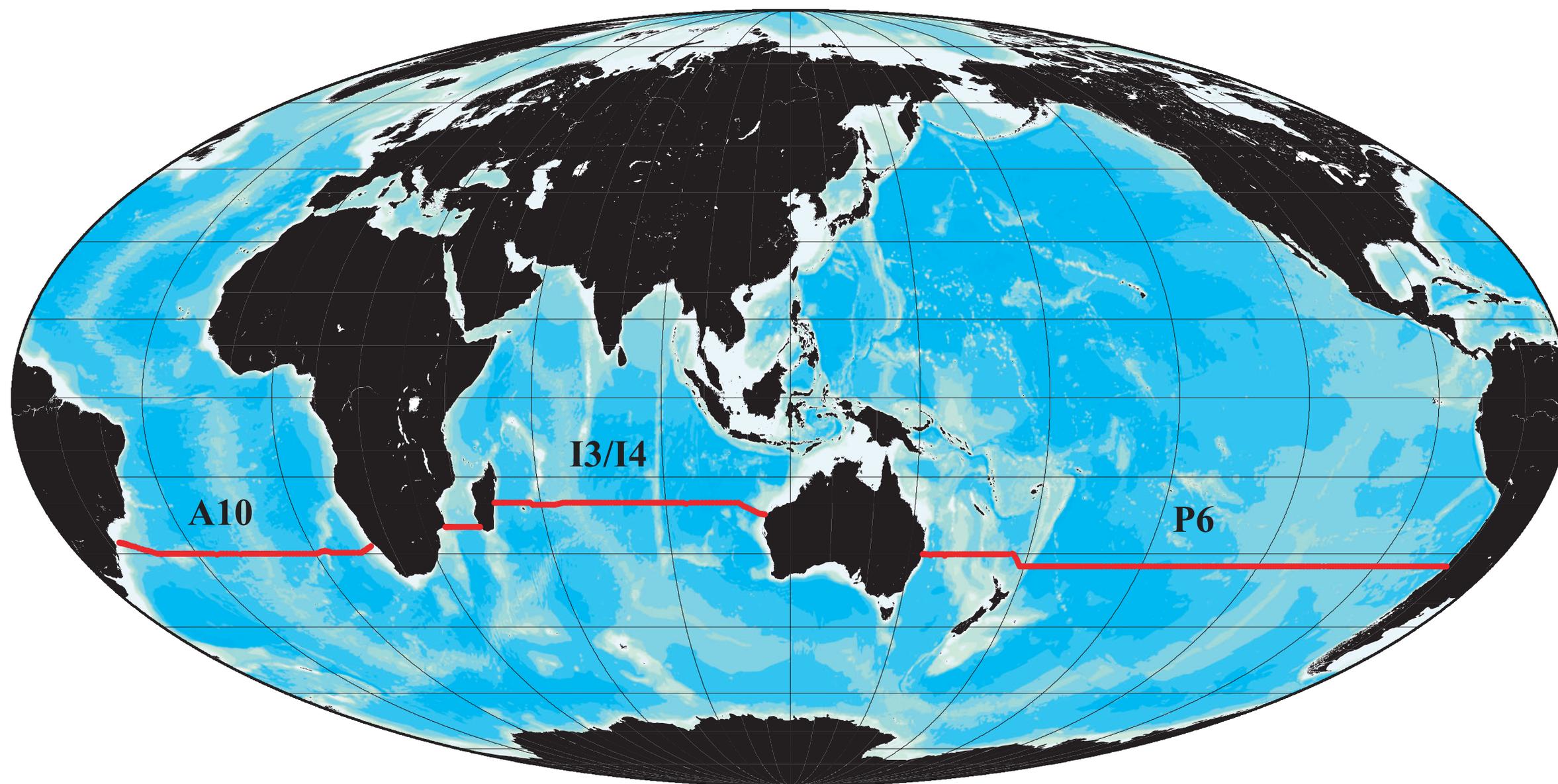
Figure 6 Same as Figure 3 but for $\delta^{13}\text{C}$ of dissolved inorganic carbon (‰).

References

Data Announcement 88-MGG-02 (1988): Digital relief of the Surface of the Earth, NOAA, National Geophysical Data Center, Boulder, Colorado.

Smith, W. H. F. and D. T. Sandwell (1997): Global seafloor topography from satellite altimetry and ship depth soundings, *Science*, 277, 1956-1962.

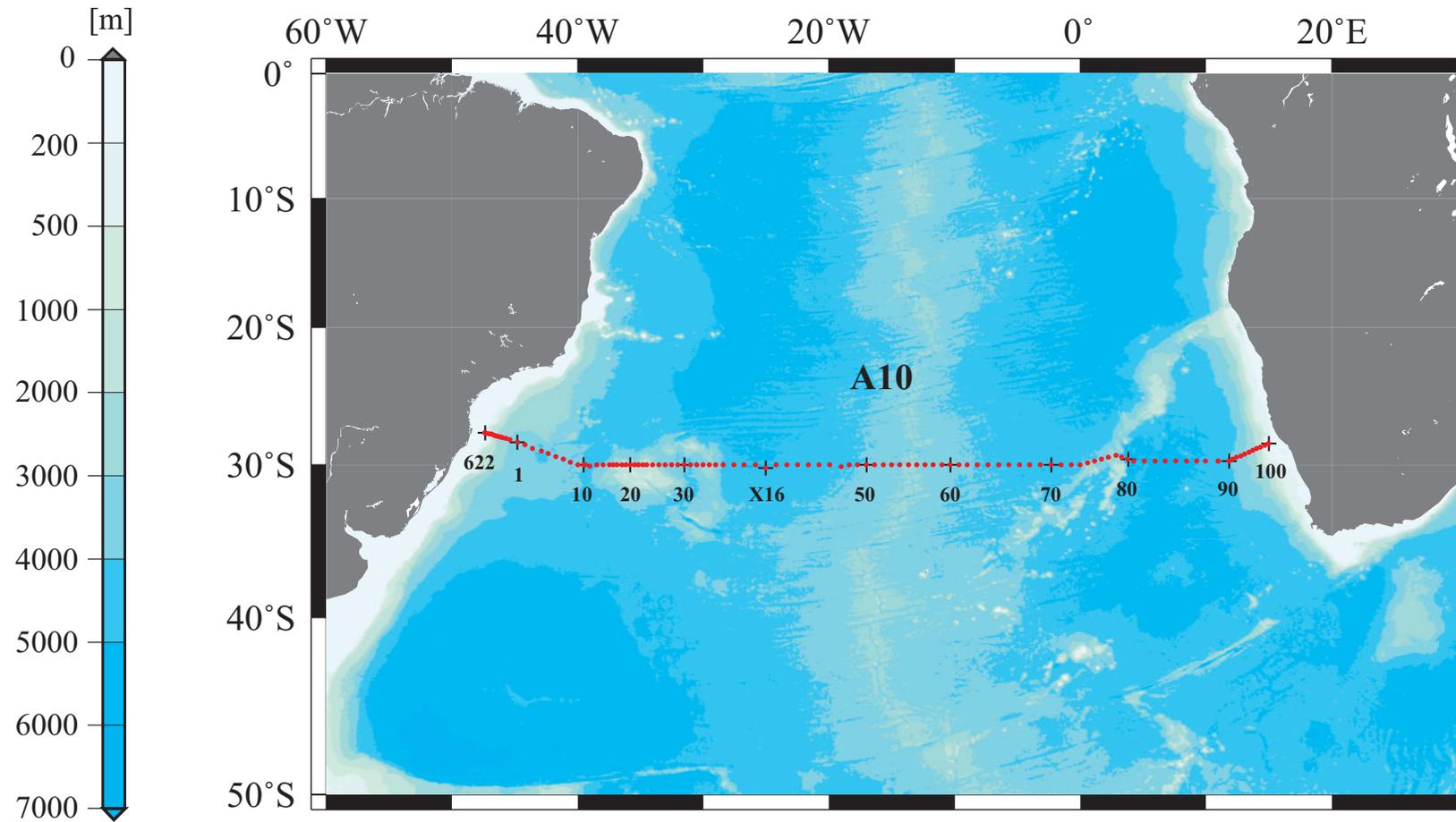
Figure 1

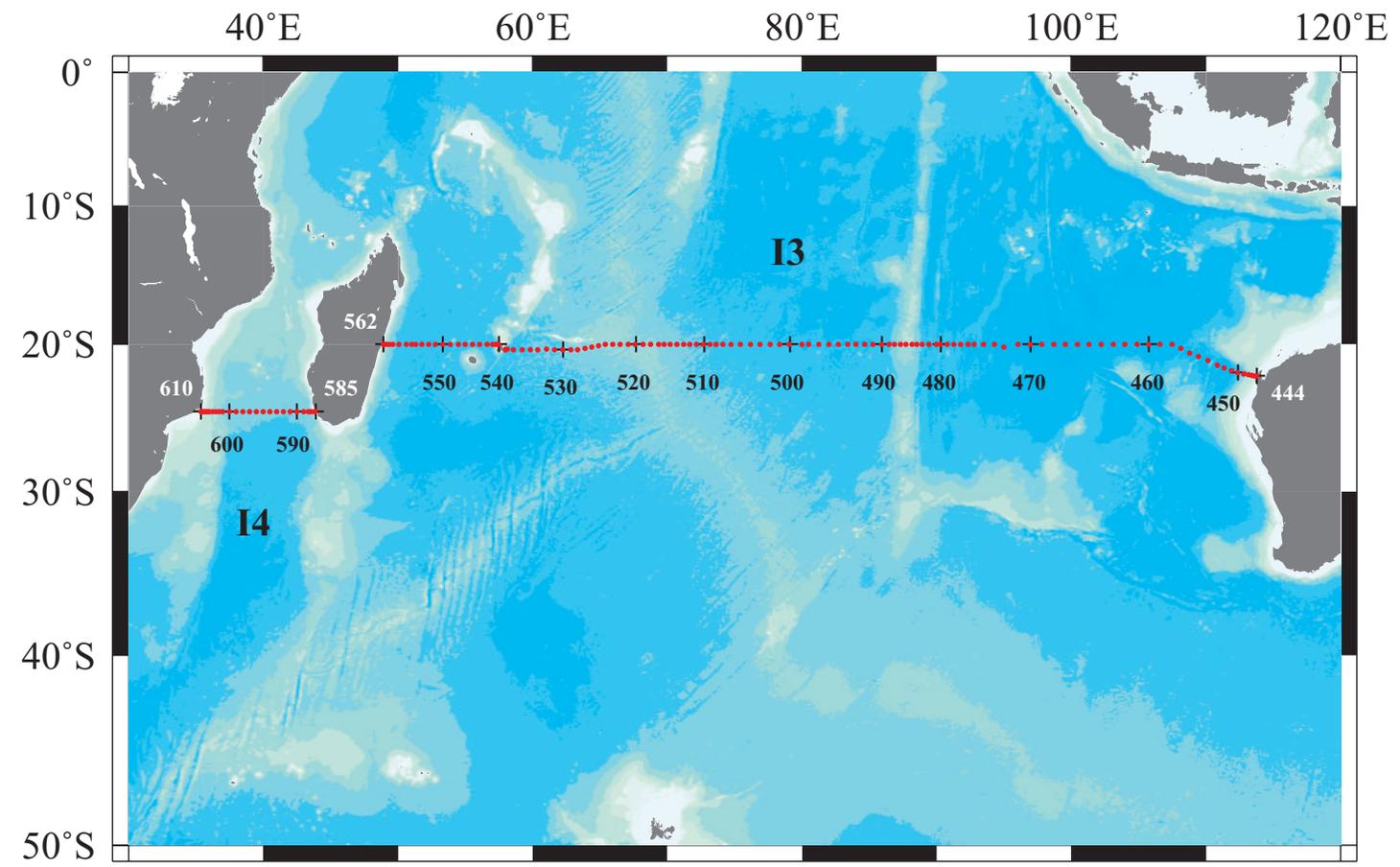


OBSERVATION LINES FOR WHP P6, A10, I3/I4 REVISIT IN 2003

Figure 2

**STATION LOCATIONS
FOR WHP P6, A10, I3/I4
REVISIT IN 2003**





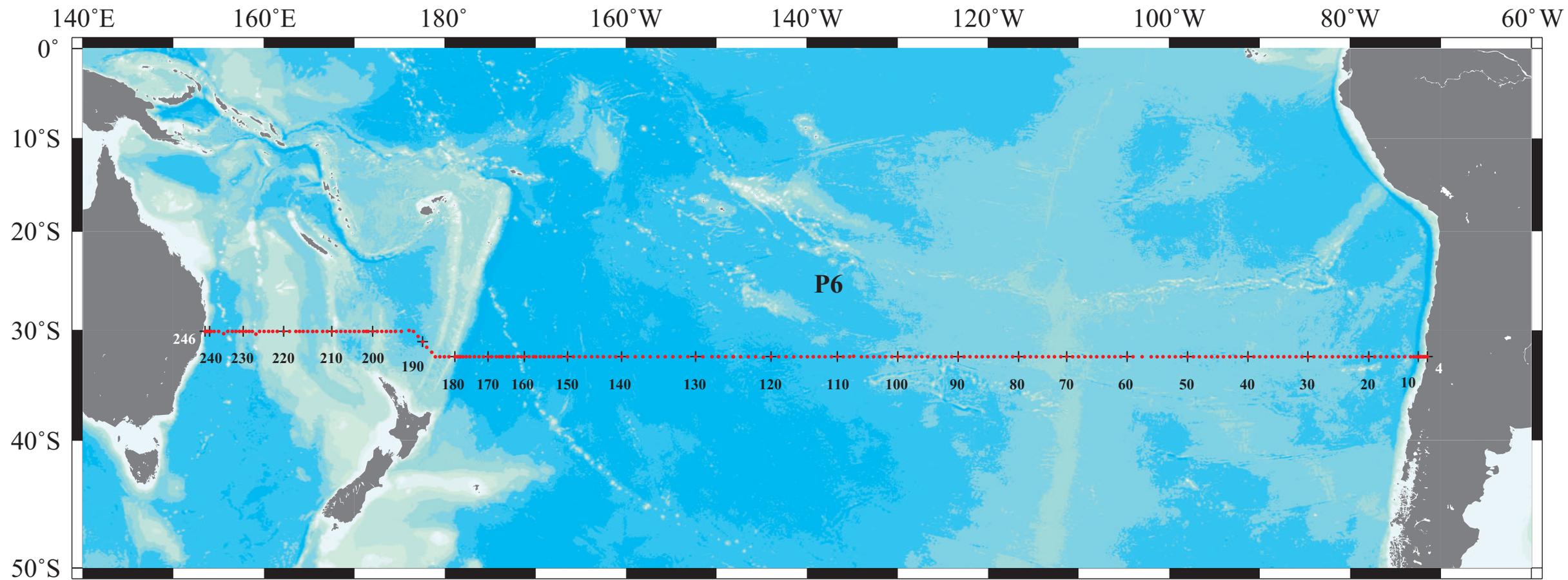
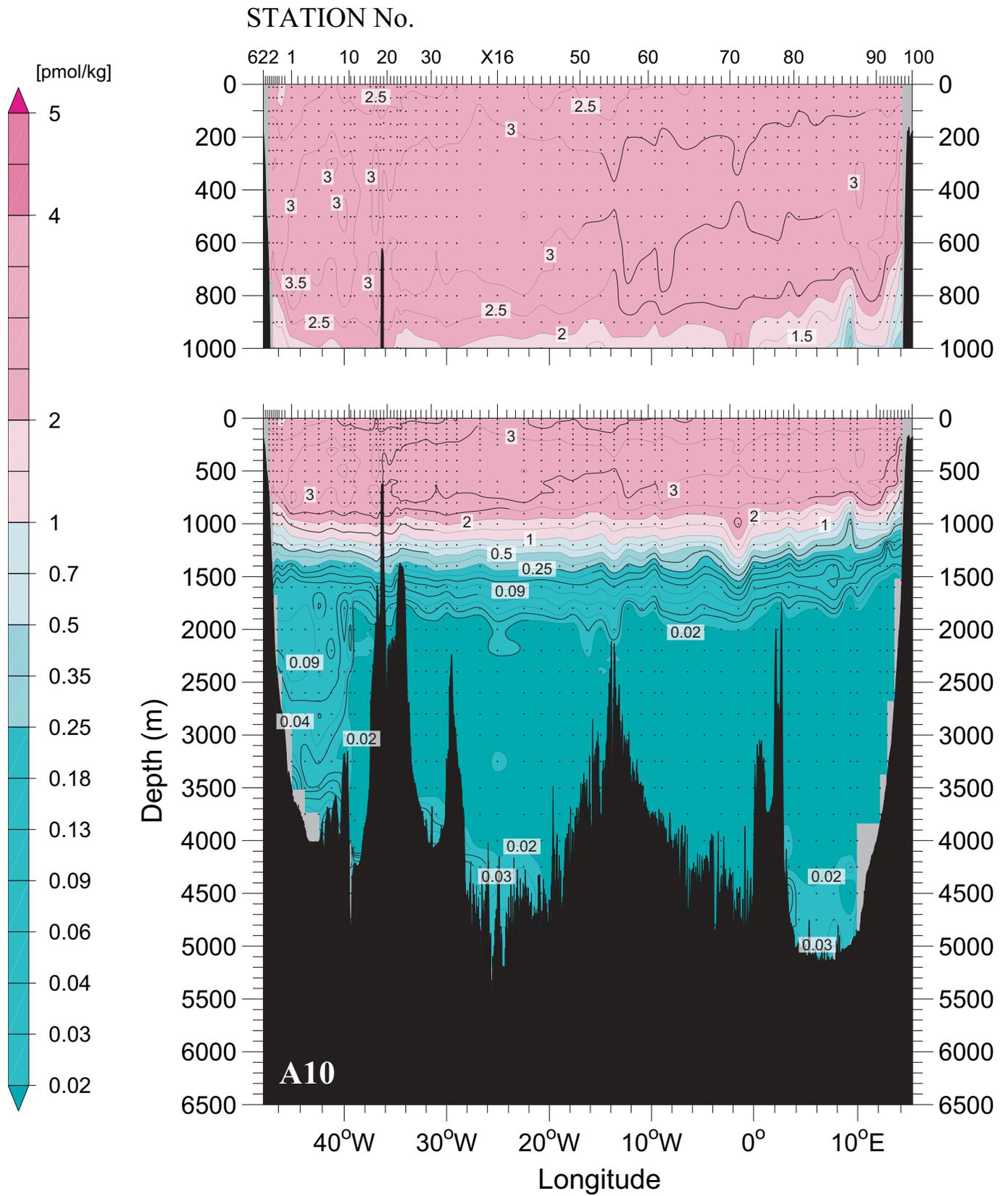
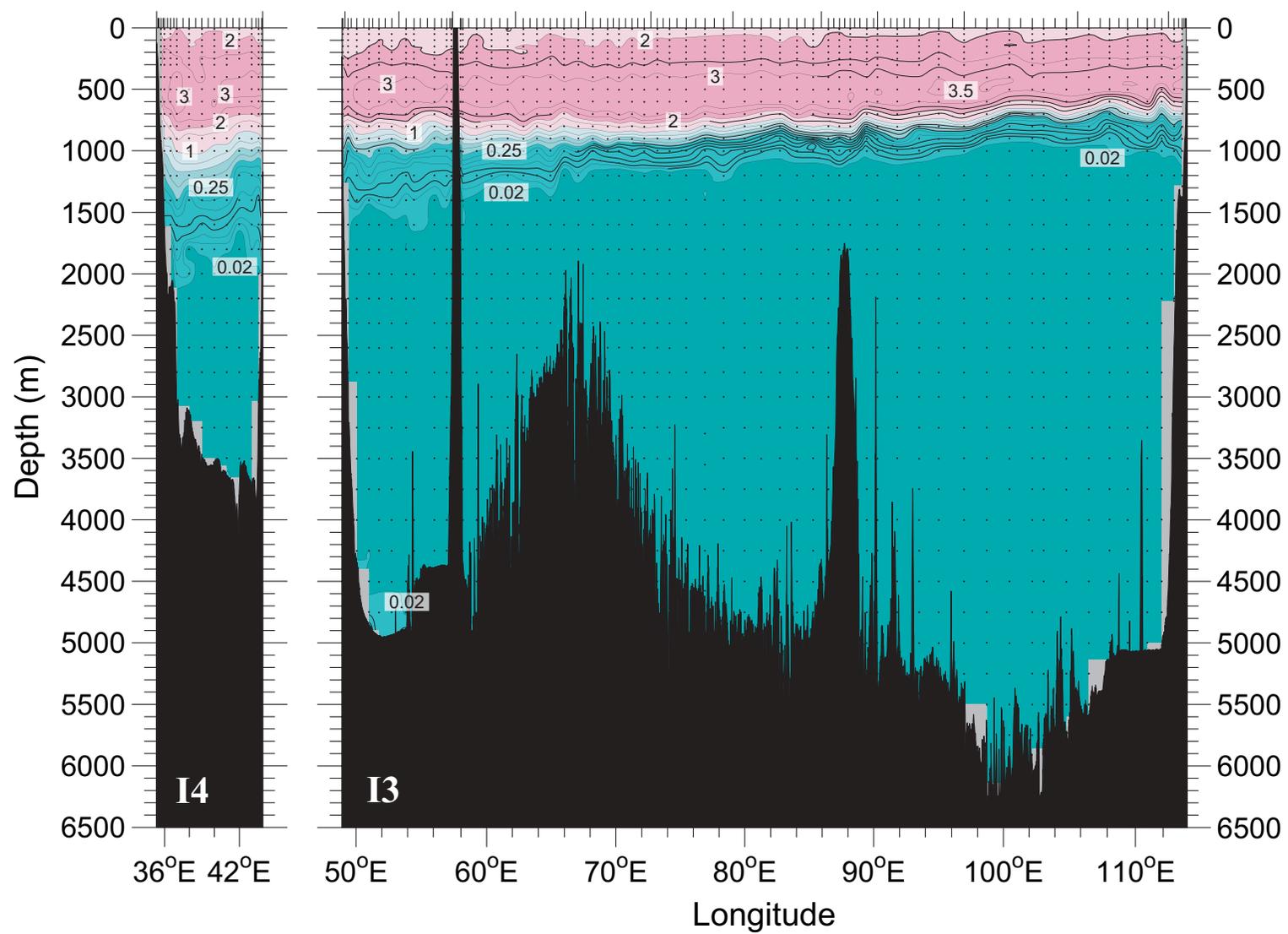
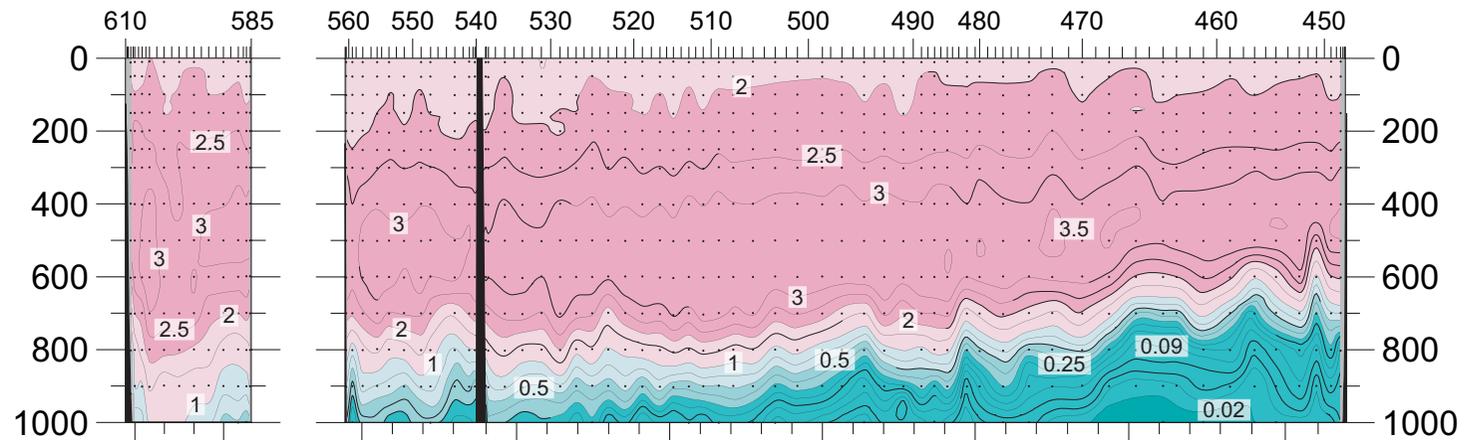


Figure 3

CFC-11 [pmol kg^{-1}]



STATION No.



STATION No.

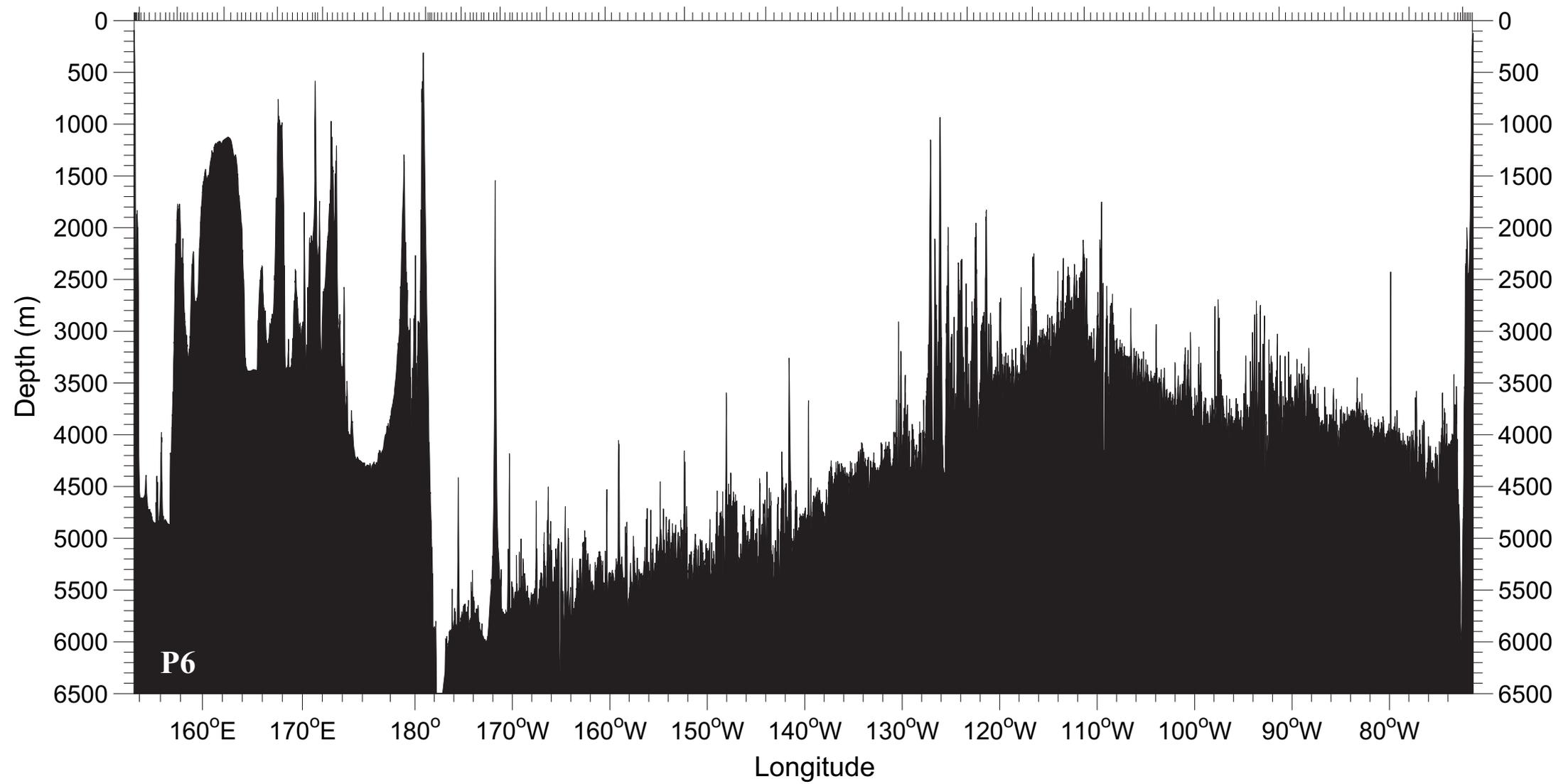
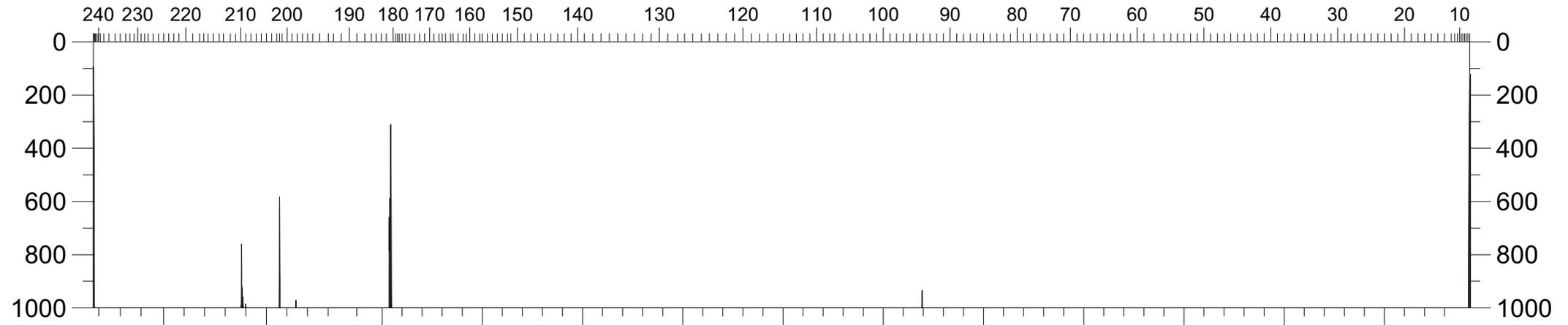
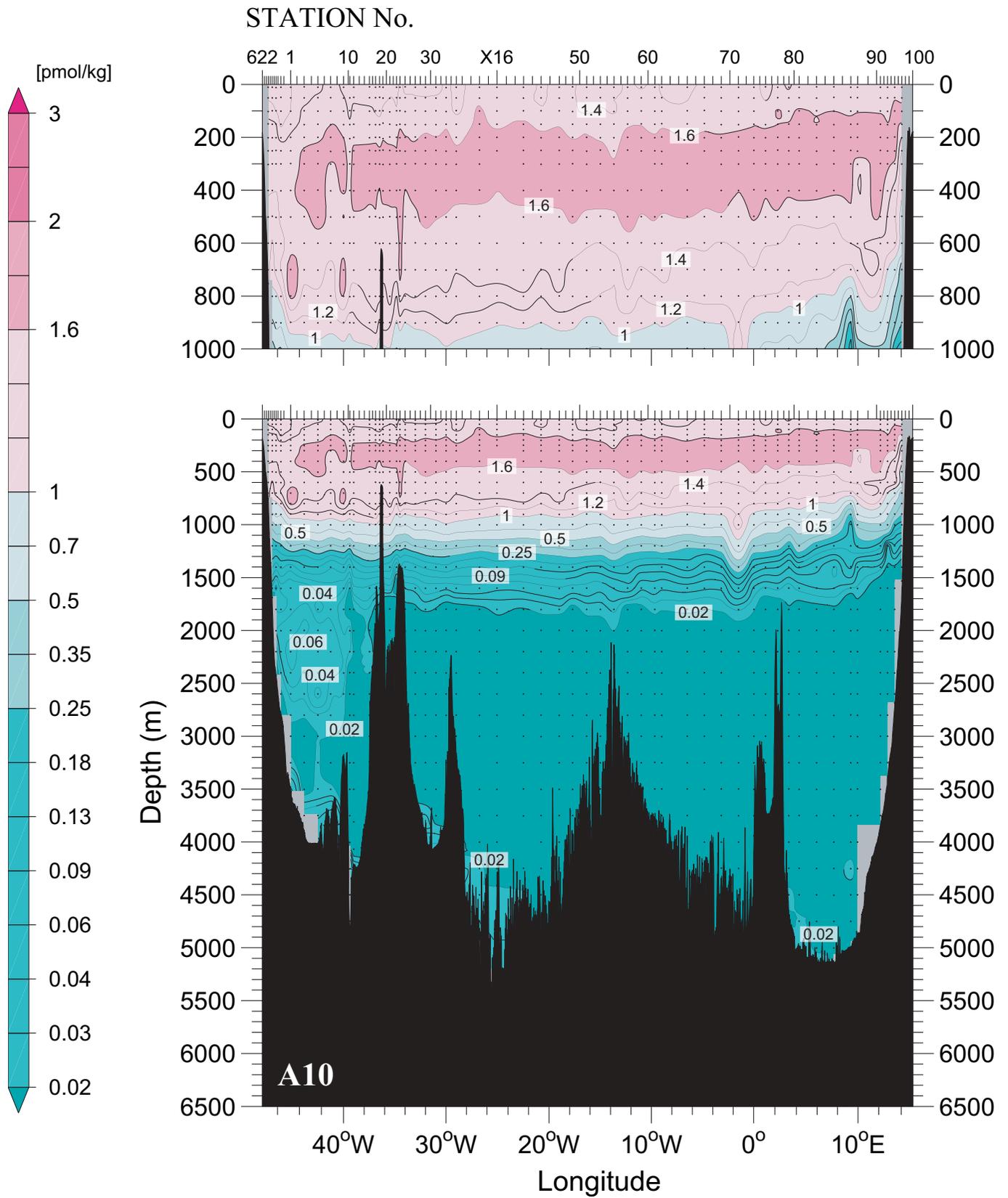
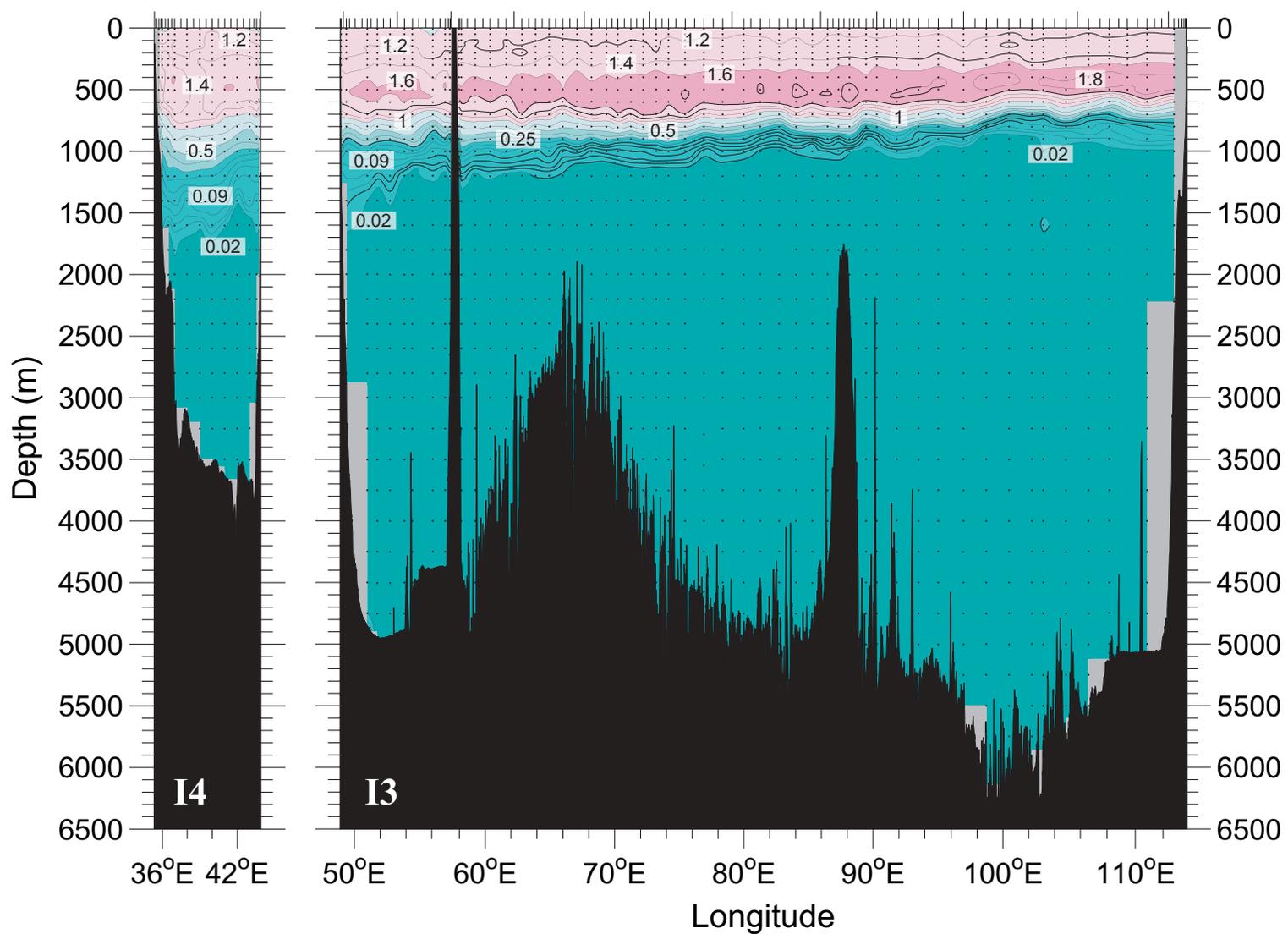
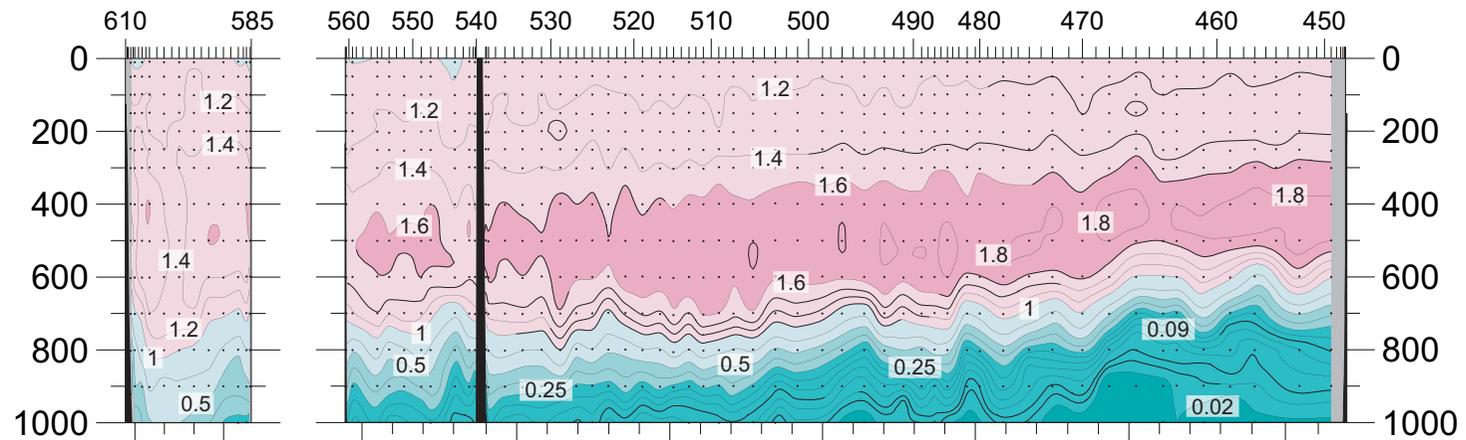


Figure 4

CFC-12 [pmol kg⁻¹]



STATION No.



STATION No.

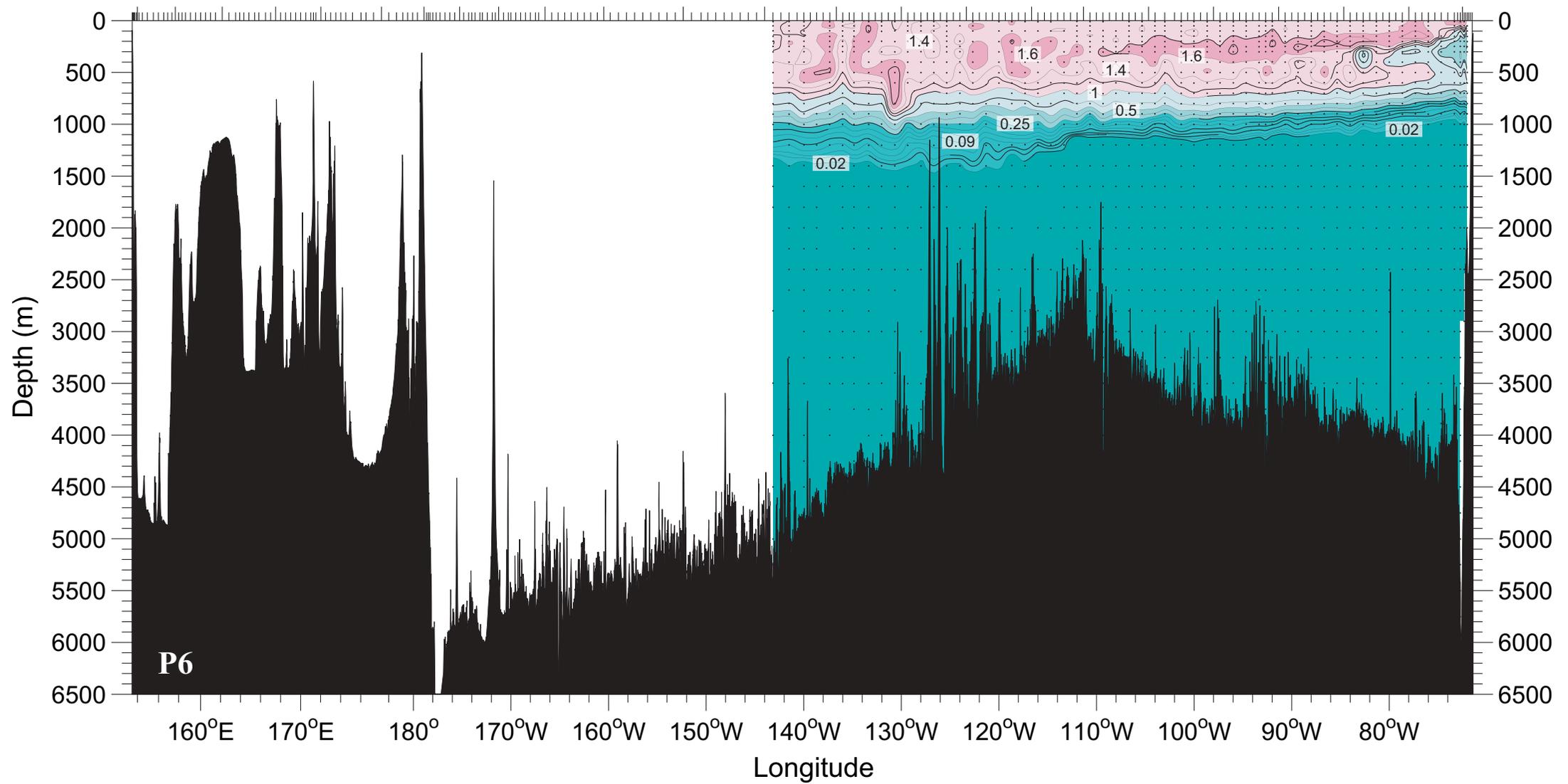
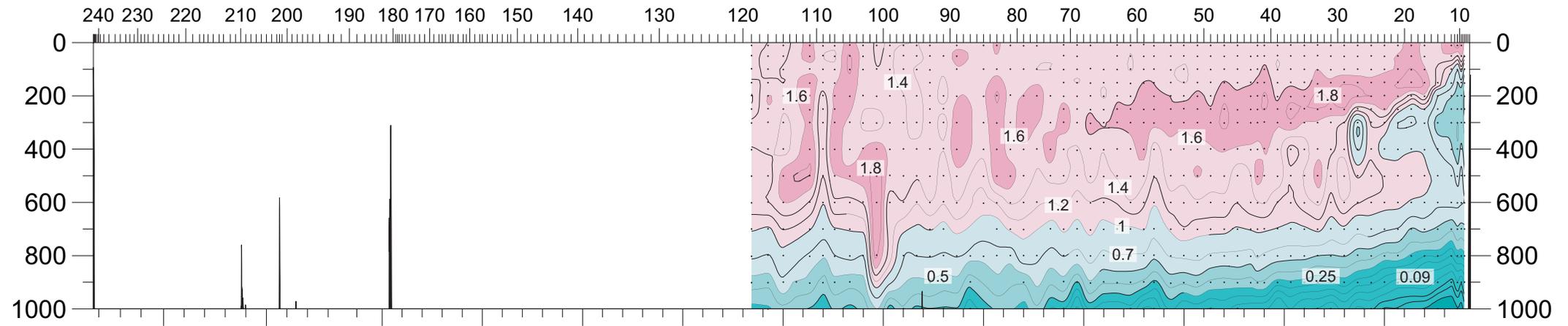
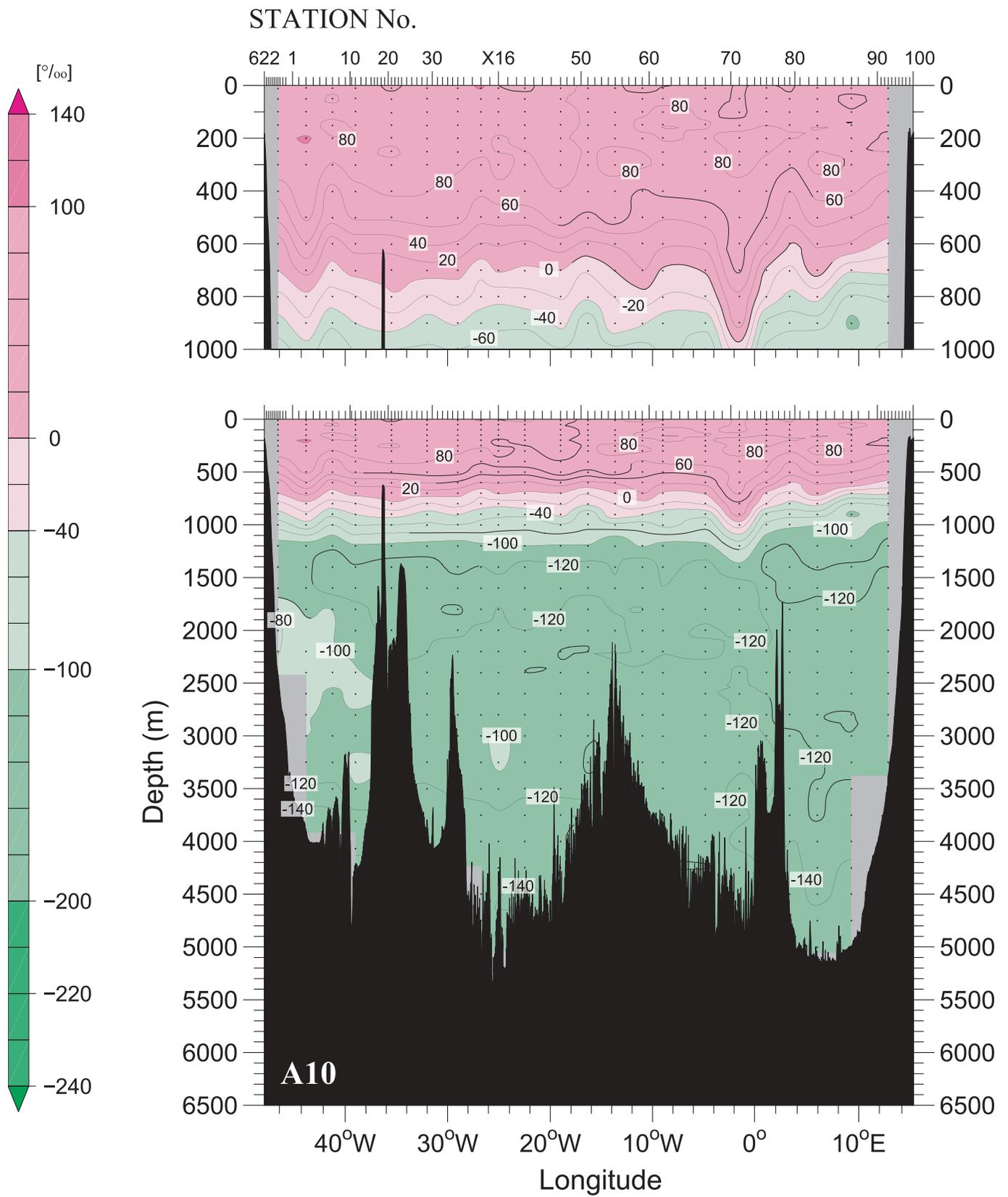
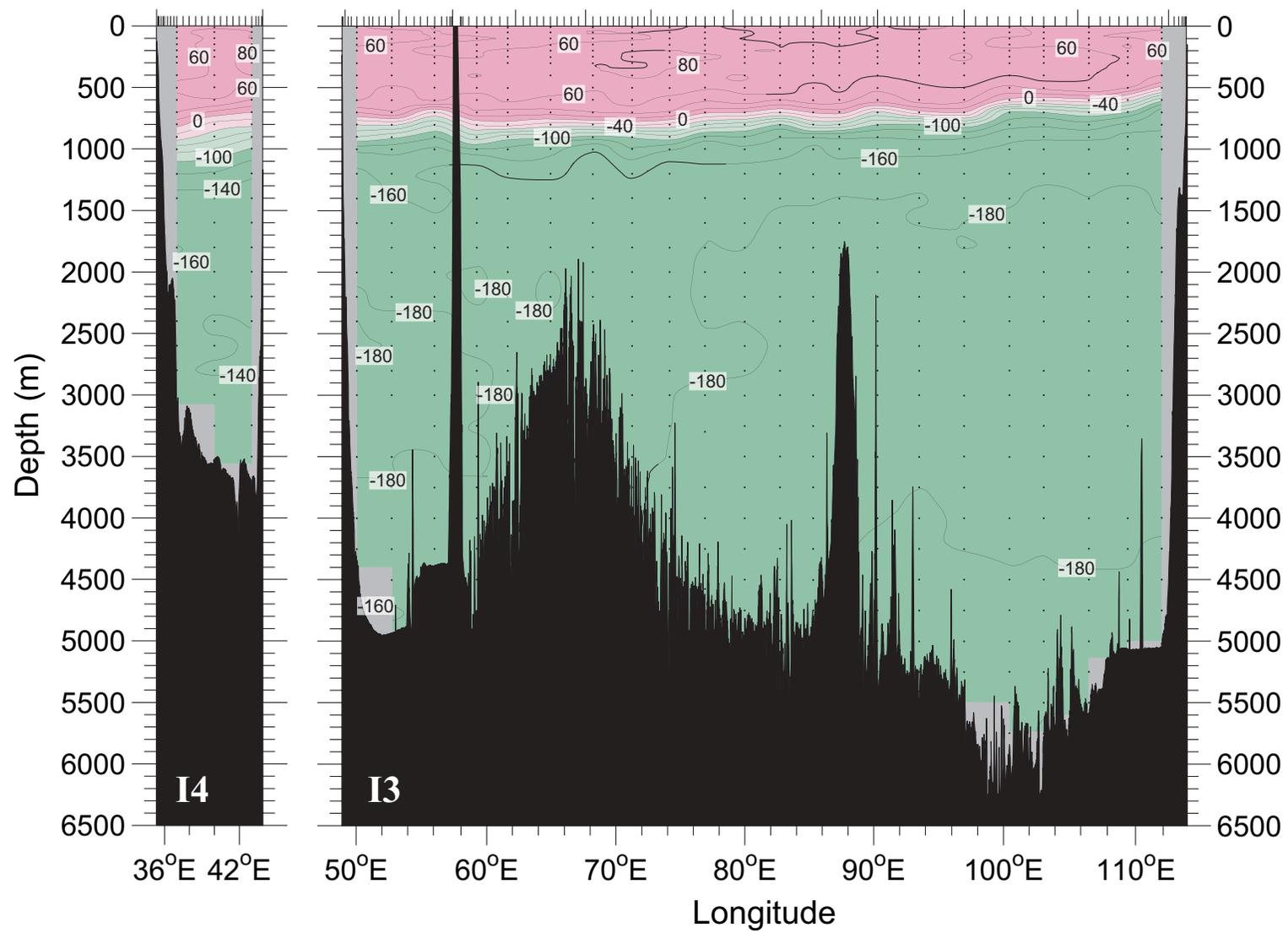
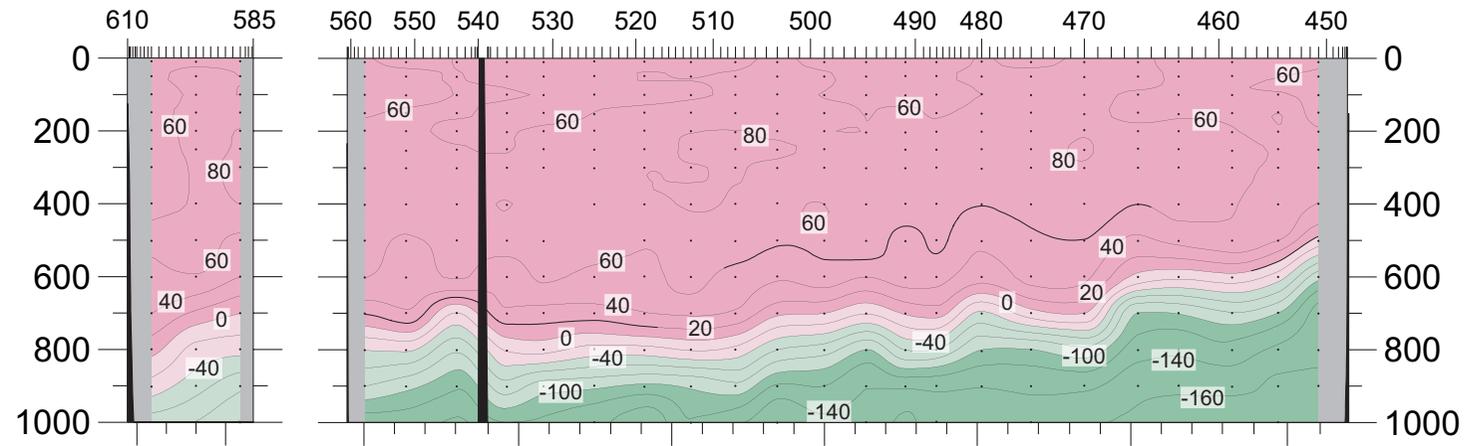


Figure 5

$\Delta^{14}\text{C}$ [‰]



STATION No.



STATION No.

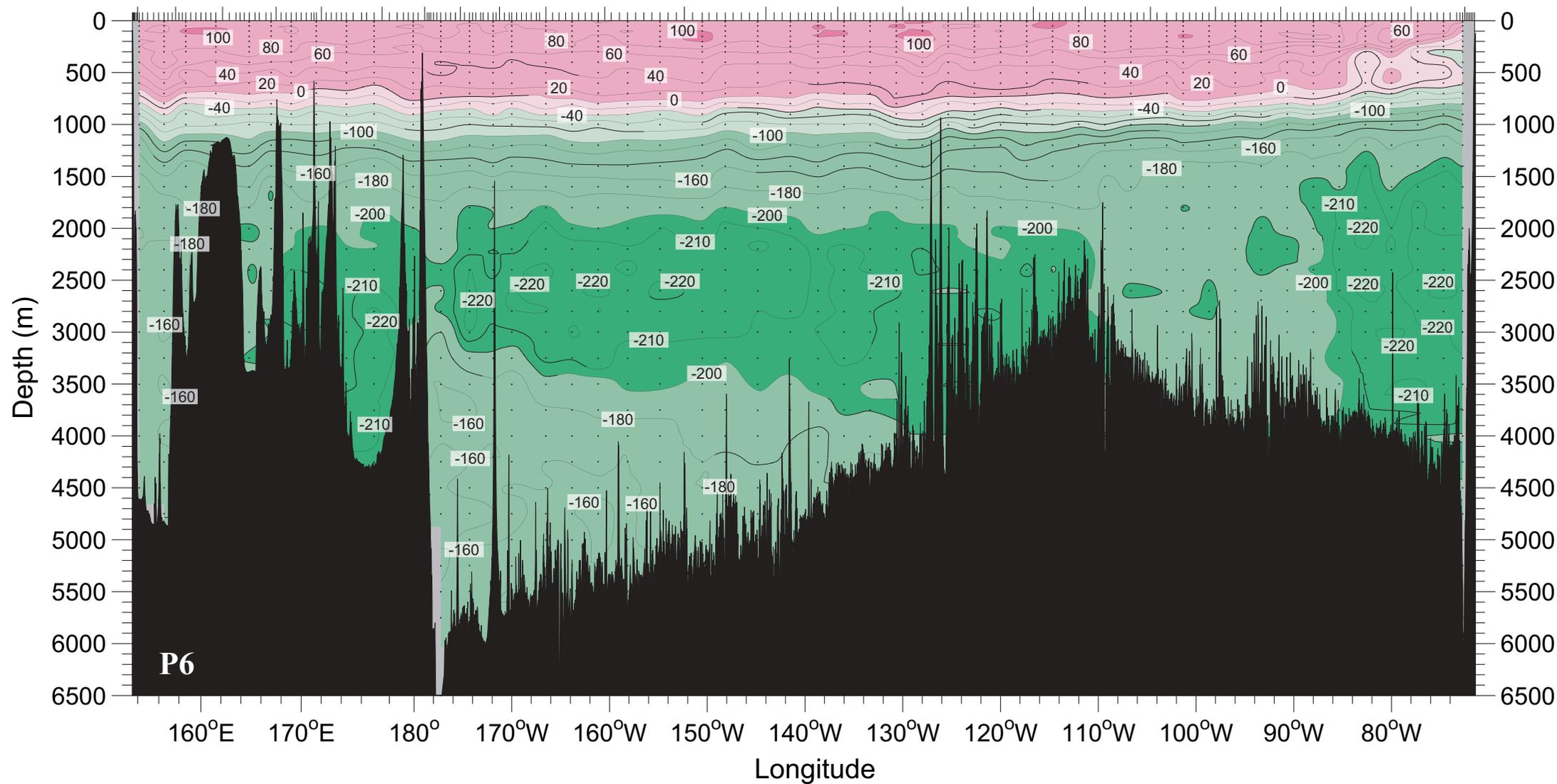
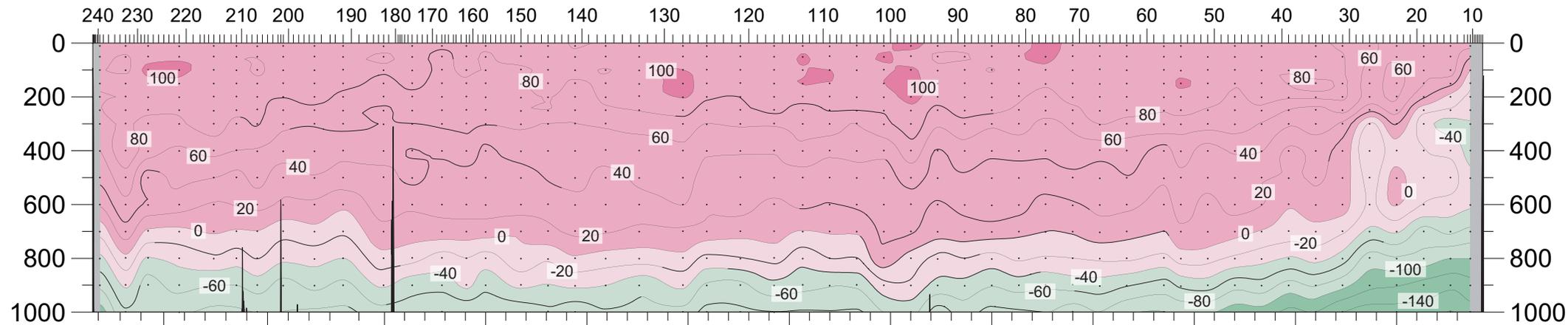
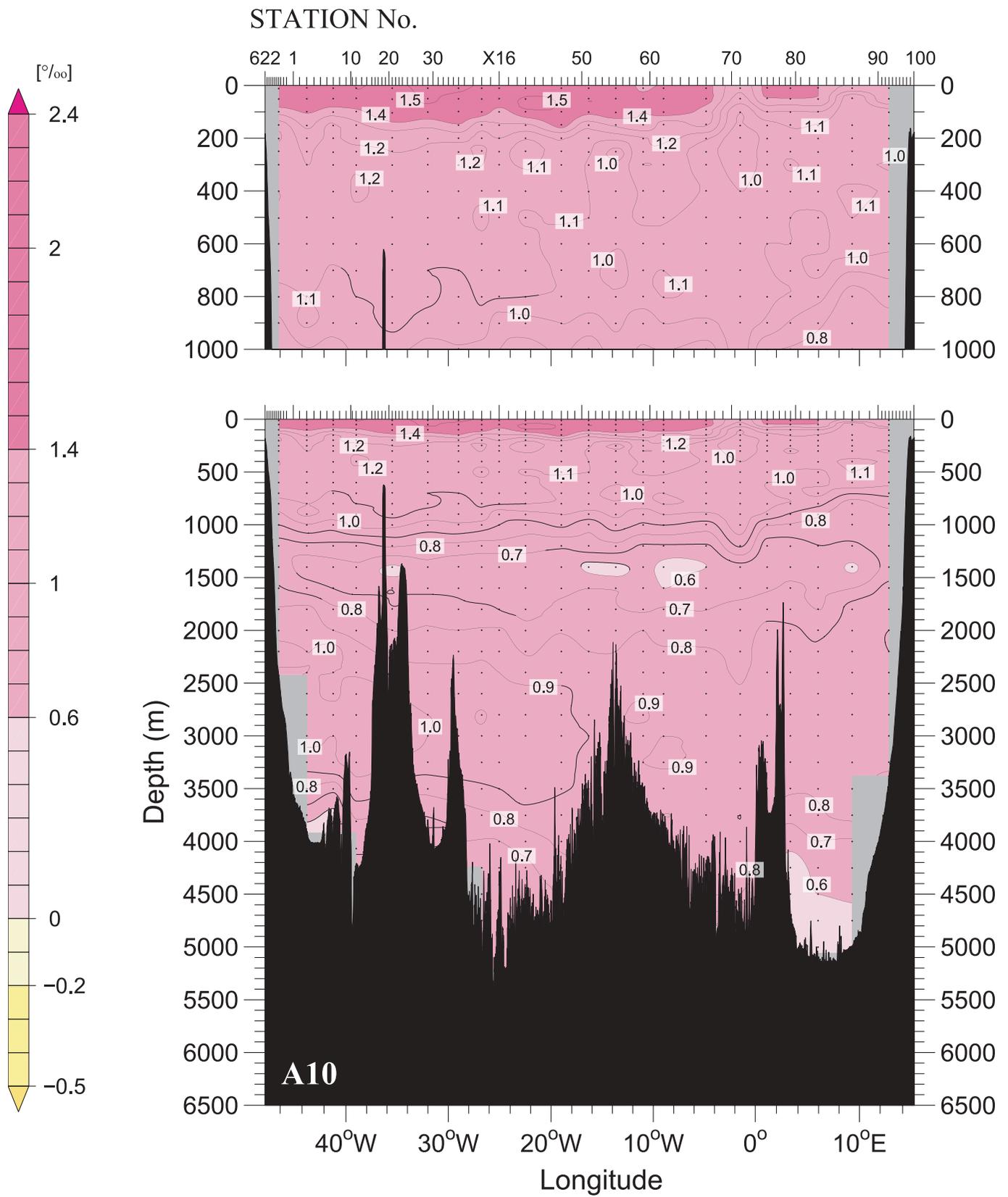
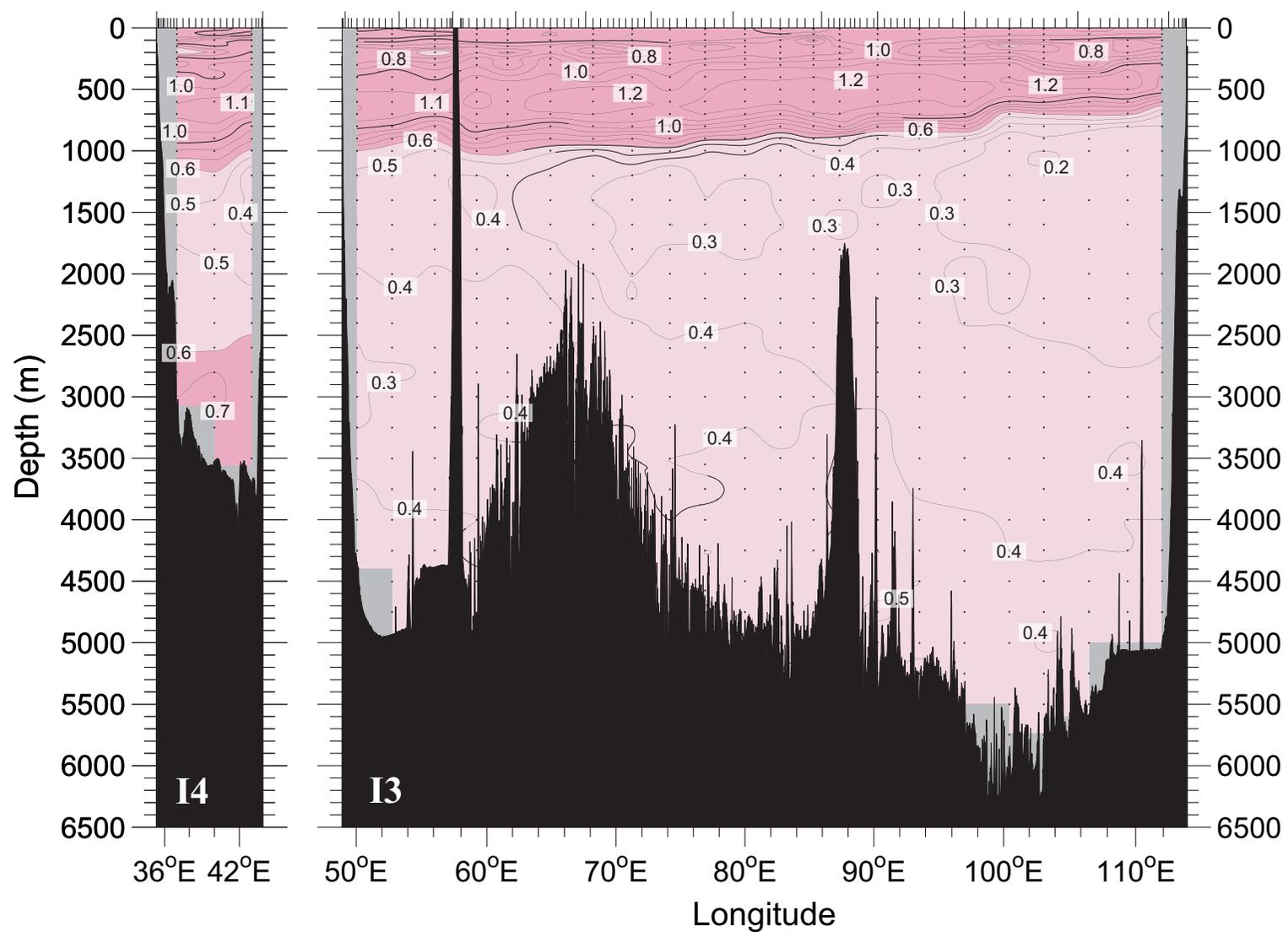
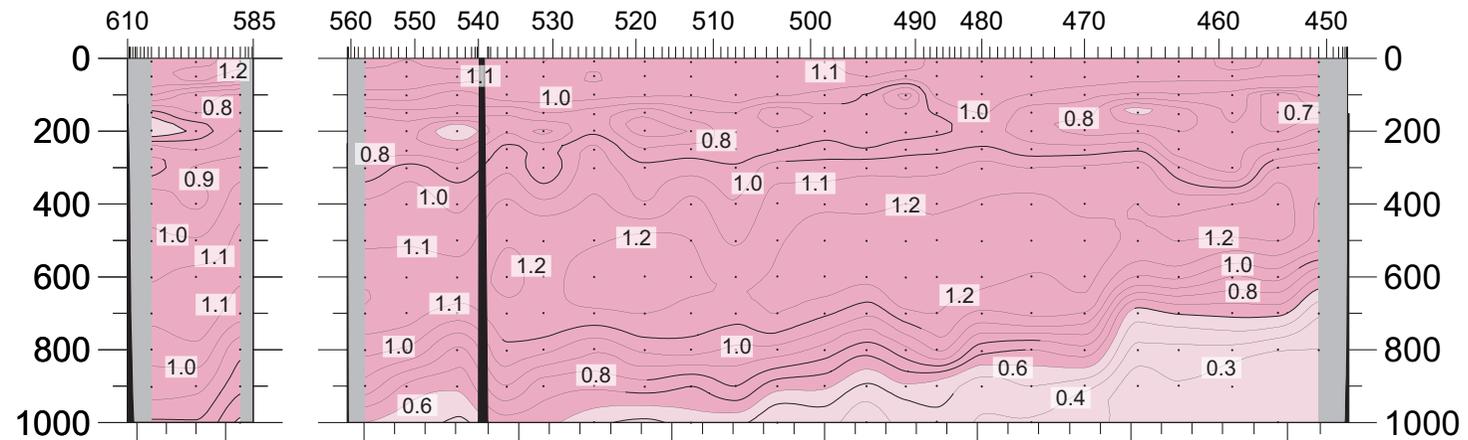


Figure 6

$\Delta^{13}\text{C}$ [‰]



STATION No.



STATION No.

